

PONTIFICIA UNIVERSIDAD CATÓLICA DEL PERÚ
ESCUELA DE POSGRADO



PUCP

**CONTRIBUTIONS TO IDA-PBC WITH ADAPTIVE CONTROL FOR
UNDERACTUATED MECHANICAL SYSTEMS**

**TESIS PARA OPTAR EL GRADO ACADÉMICO DE MAGISTER EN LA MAESTRÍA EN
INGENIERÍA DE CONTROL Y AUTOMATIZACIÓN**

AUTOR

Jhossep Augusto Popayán Avila

ASESORES

Prof. Dr.-Ing. Johann Reger (TU ILMENAU)
Prof. Dr. Antonio Morán Cárdenas

Septiembre, 2018



PONTIFICIA
**UNIVERSIDAD
CATÓLICA**
DEL PERÚ


TECHNISCHE UNIVERSITÄT
ILMENAU

Contributions to IDA-PBC with Adaptive Control for Underactuated Mechanical Systems

Master Thesis in Technische Kybernetik und Systemtheorie / Ingeniería de
Control y Automatización

submitted by

Jhossep Popayán

born in Ancash - Perú

in the

Control Engineering Group

**Department of Computer Science and Automation
Technische Universität Ilmenau**

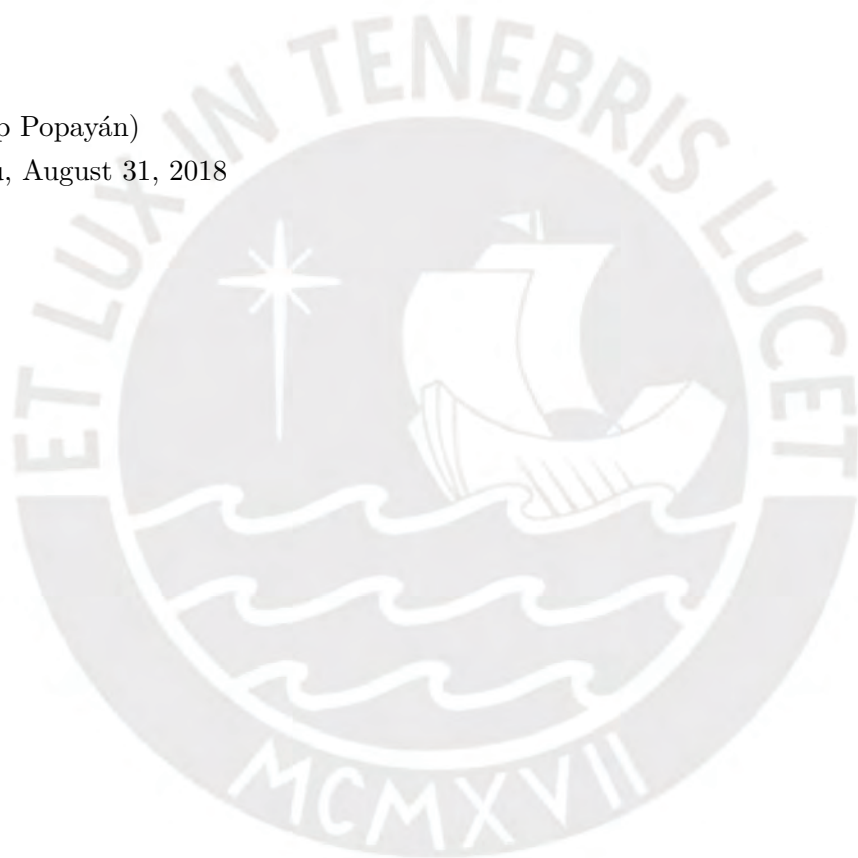
Responsible Professor at TU Ilmenau: **Prof. Dr.-Ing. Johann Reger**
Responsible Professor at PUCP: **Prof. Dr. Antonio Morán Cárdenas**
Assistant Advisor at TU Ilmenau: **M.Sc. Oscar B. Cieza Aguirre**
Submission Date: **August 31, 2018**

Declaration

I declare that the work is entirely my own and was produced with no assistance from third parties.

I certify that the work has not been submitted in the same or any similar form for assessment to any other examining body and all references, direct and indirect, are indicated as such and have been cited accordingly.

(Jhossep Popayán)
Ilmenau, August 31, 2018



To my beloved parents Rosa Avila and
Belaunde Bustamante.



Abstract

This master thesis is devoted to developing an adaptive control scheme for the well-known Interconnection and Damping Assignment Passivity-Based Control (IDA-PBC) technique. The main objective of this adaptive scheme is to asymptotically stabilize a class of Underactuated Mechanical Systems (UMSs) in the presence of uncertainties (not necessarily matched). This class of UMSs is characterized by the solvability of the Partial Differential Equation (PDE) resulting from the IDA-PBC technique. Two propositions are stated in this work to design the adaptive IDA-PBC. One of the main properties of these propositions is that even though the parameter estimation convergence is not guaranteed, the adaptive IDA-PBC achieves asymptotic stabilization. To illustrate the effectiveness of these propositions, this work performs simulations of the Inertia Wheel Inverted Pendulum (IWIP) system, considering a time-dependent input disturbance, a type of physical damping, i.e., friction (not considered in the standard IDA-PBC methodology), and parameter uncertainties in the system (e.g., inertia).

Kurzfassung

Diese Masterarbeit ist der Entwicklung eines adaptiven Regelverfahrens für einschlägig bekannte IDA-PBC-Methodik gewidmet. Das Hauptziel dieses adaptiven Verfahrens ist die asymptotische Stabilisierung einer Klasse von unteraktuierten mechanischen Systemen (UMSs) unter Unsicherheiten, die nicht notwendigerweise in einem Eingangskanal auftreten (englisch: *matched*) sind. Diese Klasse von UMSs zeichnet sich durch die Lösbarkeit einer PDE aus, die sich aus der IDA-PBC-Methodik ergibt. In dieser Arbeit werden zwei Ansätze zur Entwicklung von adaptivem IDA-PBC gemacht. Eine Haupteigenschaft dieser Ansätze ist, dass, obwohl die Konvergenz der Parameterschätzung nicht gewährleistet ist, adaptives IDA-PBC eine asymptotische Stabilisierung erreicht. Um die Wirksamkeit dieser Ansätze zu veranschaulichen, führt diese Arbeit Simulationen an einem invertierten Schwungradpendel (IWIP) durch, wobei eine zeitabhängige Eingangsstörung, eine Art der physikalischen Dämpfung, d.h. Reibung (nicht in der Standard IDA-PBC-Methodik enthalten), und die Parameterunsicherheiten des Systems (z.B. Trägheit) berücksichtigt werden.

Acknowledgment

I would like to thank my thesis advisor M.Sc. Oscar Cieza at TU Ilmenau. His office door was always open whenever I ran into a trouble spot or had a question about my research or writing. He consistently allowed this thesis to be my own work, but steered me in the right the direction whenever he thought I needed it.



Contents

1. Introduction	1
1.1. Motivation	1
1.2. Literature Review	2
1.2.1. Underactuated Mechanical Systems	2
1.2.2. Control of UMSs	3
1.2.3. Remarks on Passivity-Based Control for UMSs	5
1.2.4. Adaptive Control for UMSs	7
1.3. Contributions of this Thesis	8
1.4. Outline of the Thesis	9
2. Mathematical Preliminaries	10
2.1. Stability of Nonlinear Systems	10
2.1.1. Autonomous Systems	10
2.1.2. Nonautonomous Systems	13
2.2. Passivity-Based Control: Interconnection and Damping Assignment	16
2.2.1. Passivity	16
2.2.2. Port-Hamiltonian Systems	18
2.2.3. Port-Hamiltonian Modeling of a Mechanical System	19
2.2.4. Interconnection and Damping Assignment Passivity-Based Control	19
2.3. Adaptive control	23
2.3.1. Adaptive Dynamic Inversion	24
2.3.2. Adaptive Approach Applied to IDA-PBC	25
3. Adaptive IDA-PBC	27
3.1. Input Disturbance	27
3.2. Parameter Uncertainty	29
4. Adaptive IDA-PBC Application: Inertia Wheel Inverted Pendulum	38
4.1. Inertia Wheel Inverted Pendulum (IWIP) Model	38

4.2. Standard IDA- PBC	40
4.2.1. Energy Shaping	40
4.2.2. Damping Injection	42
4.2.3. Zero-State Detectability	43
4.3. Simulation for Input Uncertainty	46
4.3.1. Zero-State Detectability	46
4.3.2. Simulation Results	48
4.4. Simulation for Friction Compensation	50
4.4.1. Zero-State Detectability	51
4.4.2. Simulation Results	52
4.5. Simulation Subject to Parameter Uncertainty	57
4.5.1. Zero-State Detectability	59
4.5.2. Simulation Results	60
 5. Conclusion and Future Work	 72
 Appendices	 74
A. Additional Calculations	75
A.1. Matching Condition and Equivalent Formulation	75
A.2. Calculation of the Inverse Transformation Matrix	75
 Abbreviations	 77
 References	 86

Chapter 1

Introduction

1.1 Motivation

In recent decades, special attention has been paid to a special class of mechanical systems, namely, Underactuated Mechanical Systems (UMSs), i.e., systems that have fewer control inputs than Degrees of Freedom (DOF). This is mainly because of its broad application field and the fact that classical control techniques are very often not applicable to this class of systems [1]. The control theory regarding fully actuated systems is quite vast and its control design is relatively straightforward; however, they lack the efficiency, agility, and robustness that UMSs can provide. The reason for it is that fully actuated systems are forced to follow a desired trajectory, while UMSs could take advantage of its natural dynamics [2].

A fair amount of control techniques has been developed to control UMSs (e.g., stabilization and tracking). A generalization of these systems has been attempted by many authors with the aim to propose a systematic control design method for UMSs; however, it has been difficult to find structural properties of UMSs in a sufficiently general form to treat this class of systems in a unified way [1].

A well-established control technique for physical systems is the so-called Passivity-Based Control (PBC) introduced in [3]. This technique has been proven to be very powerful to control physical systems described by the Euler-Lagrange (EL) motion equations (e.g., mechanical, electrical and electromechanical systems). Stabilization by this technique is achieved by passivation of the system with a storage function that has a minimum at the desired equilibrium point. The desired closed-loop system is still an EL system as long as it was stabilized shaping only the potential energy. However, this property is lost when the shaping of the total energy is required to stabilize the system [4, 5]. To overcome this drawback, a new PBC theory called Interconnection

and Damping Assignment (IDA)-PBC was developed in [5] where the shaping of the total energy is allowed while the previously mentioned properties hold; that is, i) the closed-loop system has still a Hamiltonian structure, and ii) the closed-loop storage function is the total energy. An extension of this theory applied to the stabilization of UMSs is presented in [6], where they characterize a class of systems for which IDA-PBC yields a smooth stabilizing controller. This class is given by systems whose set of Partial Differential Equations (PDEs), corresponding to the potential and kinetic energy, can be solved.

Uncertainties in a system model, as well as external disturbances among others, can lead to the instability of the closed-loop system. Adaptive control and robust control are two main techniques for uncertainty compensation. Adaptive control is more suitable in dealing with uncertainties in constant or slow-varying parameters while robust control is more appropriate when dealing with unmodeled dynamics and quickly varying parameters [7]. In [8] an adaptive approach combined with the canonical transformation theory is presented for general Port-Hamiltonian (PH) systems. Although the IDA-PBC technique applied to UMSs has a certain range of robustness against uncertainties (discussed in [9]), this work is devoted to developing an adaptive control law based on the IDA-PBC technique in order to extend its application realm. The types of uncertainties, for which the adaptive controller is designed, discussed in this work are input disturbance and parameter uncertainties.

1.2 Literature Review

1.2.1 Underactuated Mechanical Systems

UMSs are defined as systems that have fewer control inputs than DOF. As a consequence of the underactuation, the generalized inputs cannot control the instantaneous acceleration in an arbitrary direction, therefore UMSs cannot follow arbitrary trajectories [1, 2]. The research field to determine suitable control algorithms for UMSs is quite active due to the variety of real-life applications such as swimming and flying robots, walking robots, underactuated manipulators, flexible systems, among others; plus, these systems are usually far more interesting than fully actuated systems.

UMSs can be classified in various ways such as in [1, 10, 11]. One of those classifications focuses on the reasons of underactuation, which, summarized in [10, p. 15], can be stated as: i) Nature of the system dynamics (e.g., aircrafts, underwater vehicles, spacecraft, and helicopters), ii) Imposed by design to reduce costs, weight or another practical purpose (e.g., satellites with two thrusters and flexible-link robots), iii) Actuator failure (e.g., airplanes and surface vessels), iv) Artificially imposed to generate

low-order complex nonlinear systems in order to gain insight into controlling high-order UMSs (e.g., IWIP and beam and ball system).¹

As was previously mentioned, a countless number of UMSs can be found in real life, some of them have practical applications such as airplanes, surface vessels, magnetic suspension, etc. and some others are mainly used for academic purposes (standards for nonlinear control where it is not feasible to apply classical control algorithms [1]) such as, but not limited to, the beam and ball system, the Translational Oscillator Rotational Actuator (TORA) system, the IWIP system, the Acrobot system and the Cart-Pole system.

When it comes to UMSs it is common to find that some of them are subject to nonholonomic constraints, either first- or second-order nonholonomic constraints (velocity or acceleration constraints). Velocity constraints occur mainly in wheeled mobile robots and wheeled vehicles (e.g., the pure rolling conditions of wheels) while acceleration constraints occur mainly in surface vessels, underwater vehicles, spacecraft and robot manipulators [12]. The underactuation property of UMSs is sometimes considered as a second-order constraint [1]. However, this work will consider neither nonholonomic nor holonomic constraints; that is, constraints that depend only on the generalized coordinates and time. Useful information regarding nonholonomic systems can be found in [13].

1.2.2 Control of UMSs

Unlike the class of fully actuated systems, where some control techniques such as feedback linearization and passivity based adaptive control can be applied to the entire class, there are only few control techniques such as collocated Partial Feedback Linearization (PFL) that can be applied to the entire class of UMSs [14]. Addressing the developments regarding each of the most popular control techniques applied to UMSs is too broad to survey in a single chapter and since it is not the main topic of this work, only the main idea and some of their applications will be presented. Table 1.1 shows the most popular control techniques to stabilize UMSs summarized from [11].

In a nonlinear UMS, the fact that there are more DOF than control inputs makes it impossible to completely linearize this system by a change of coordinates. However, a partial linearization of this systems can be achieved [1].

Collocated PFL refers to the global linearization of the active (actuated) configuration variables using an invertible change of control [15]. The control law in the resulting system appears in both subsystems (actuated and underactuated). Even though the collocated PFL offers a structural simplification of the control problem, it was shown

¹The IWIP system is sometimes referred as the Inertia Wheel Pendulum (IWP) system.

Control Techniques for UMSs	
Partial Feedback Linearization	Collocated PFL Non-Collocated PFL
Energy Based methods	Backstepping Controlled Lagrangian (CL) IDA-PBC
Sliding Mode Control (SMC)	
Fuzzy Control	
Optimal Control	

Table 1.1. – Main control techniques for UMSs

in [16] that for some systems, the application of this technique leads to unstable zero dynamics, so the choice of the control input is not trivial. In [10] is presented an appropriate structure for a global change of coordinates that decouples both subsystems with respect to the new control. Some UMSs, where collocated PFL has been used, are: the acrobot system [17], three link gymnast robot [16], and the cart-pole system [18].

Non-collocated PFL linearizes the passive (underactuated) configuration variables. However, to achieve such linearization, the Strong Inertial Coupling condition [15] must hold, i.e., the number of actuated DOF is at least as great as the number of underactuated DOF. This method has been successfully applied to the following UMSs: the flexible one-link robot [10], the surface vessel [19], and the Pendubot [20].

Non-collocated PFL, as well as collocated PFL, is used as an initial step for reduction and control of UMSs [11].

Backstepping is a recursive technique that has been proven to be effective to achieve global stabilization of UMSs. The main idea of this technique is that in each iteration, a "virtual" system is designed, such that it is strictly passive with respect to a "virtual" input and a "virtual" output [21, 22]. This technique is mainly suitable for low-DOF systems because the higher the DOF of the system, the higher the complexity of the procedure. Some UMSs, where backstepping has been applied, are: Unmanned Aerial Vehicles (UAVs) [23], Vertical Take-Off and Landing (VTOL) aircrafts [24, 25], and surface vessels [26].

Sliding Mode Control is a technique insensitive to parameter variation and external perturbations. The reason for this lies in the principle of this technique; that is, the system is forced to reach a given surface, called a switching surface, and remain there. The equations and parameters defining this surface determine the dynamic behavior (sliding mode), which is independent of the structural properties of the system. The procedure is done in two steps. First, a surface is determined in order to achieve a sliding mode with the desired properties, afterward, a discontinuous control law chosen

such that the surface is invariant and attractive [1, 27]. This technique has one major drawback though: the existence of a phenomenon called *chattering*, i.e., high-frequency oscillations of the controlled variables in the surroundings of the surface. Application of this technique to UMSs include: wheeled inverted pendulum [28], the beam and ball system [29], and underactuated satellites [30].

Even though in Table 1.1 CL and IDA-PBC appear as two different control techniques it is shown in [31] that the CL method is contained in the IDA-PBC method.

The main idea of the IDA-PBC technique is to assign a desired Port-Controlled Hamiltonian (PCH) structure to the closed-loop in order to regulate the behavior of non-linear systems. The reason why IDA-PBC is aimed to control physical systems described by PCH models is that these models are natural candidates to describe many physical systems [32]. The design of the IDA-PBC control law can be split into two parts, the first is the so-called energy shaping where the total energy function of the system is modified to assign the desired equilibrium and the second part is the damping injection to achieve asymptotic stability. The main differences between IDA-PBC and CL is that the CL method produces a state feedback that transforms a given EL system into the desired EL system by modifying the generalized inertia matrix and potential energy function while the IDA-PBC method generates a state feedback that transforms a given Hamiltonian system into a desired Hamiltonian system by additionally modifying the interconnection and dissipation matrices [5, 33]. There is one difficulty though when applying the IDA-PBC technique (as well as in CL); that is, since we are interested in UMSs there are some restrictions known as *matching conditions* that have to be satisfied. There are three main approaches to fulfill these matching conditions: non-parameterized, parameterized, and algebraic IDA. Taking advantage of the structure of UMSs, the parameterized IDA approach is usually used for their stabilization. Applying parameterized IDA, the matching conditions yield a PDE that has to be solved, which is usually not an easy task; however, the particular PDE that has to be solved in IDA-PBC is parameterized in terms of the interconnection and damping matrices, which can be chosen by the designer, based on physical considerations, to simplify the solution of the PDE [33]. The math involved in the IDA-PBC methodology and mathematical preliminaries for the right understanding of this work will be further presented in Chapter 2.

1.2.3 Remarks on Passivity-Based Control for UMSs

The IDA-PBC technique is formulated for systems described by PCH models. However, it is not restricted to stabilize only this class of systems, this is due to its universal stabilization property [32].

In [6] it is shown that, for the IDA-PBC technique, if the difference between the DOF and actuators is one, and the open-loop inertia matrix depends only on the underactuated coordinate, then the kinetic shaping energy PDEs can be reduced to a set of Ordinary Differential Equations (ODEs), which are easier to solve. Systems that fulfill the first requirement are common in the control literature, some few examples are the beam and ball system, and the cart and pendulum system. A simplification of the potential energy PDEs for mechanical systems with underactuation degree one is developed in [34], and applied to a rotary inverted pendulum.²

As well as in IDA-PBC, in the Energy Shaping (ES) [36] technique there is often the necessity to solve PDEs. However, in [37] it is proposed a new ES method to stabilize a class of PH systems where there is no need to solve PDEs. A related work is presented in [38].

A generalization of the IDA-PBC technique for mechanical systems is presented in [39] where it is claimed that the introduction of generalized forces, which replaces a sub-matrix of the interconnection matrix, reduces the number of kinetic shaping energy PDEs; however, it is demonstrated in [40] that this affirmation is not correct. Even though the affirmation in [39] was wrong, it was the motivation of an extension of the Simultaneous Interconnection and Damping Assignment (SIDA)-PBC technique [41].

One of the main steps of the standard IDA-PBC technique is splitting the control action into two terms, namely, energy-shaping and damping injection. It was shown in [41] that such partition induces some loss of generality, that is why in their work both terms are calculated simultaneously. In addition, to extend even more the application range of the IDA-PBC technique, motivated by [39], the inclusion of generalized forces is considered in [42, 43].

It would be logical to think that energy dissipation enhances the stability of a system; however, this is not necessarily true since the effect of the combination of gyroscopic and dissipation forces on a mechanical system's stability is unexpected [44]. A related phenomenon is studied in [45] where it is analyzed the effect of the presence of physical damping (e.g., friction) on the closed-loop stability in the IDA-PBC technique. For the case when the closed-loop stability in IDA-PBC with physical damping is lost, their work states the necessary and sufficient conditions in order to guarantee the existence of a control redesign, plus, if those conditions are met, they provide two methods for the redesign.

²An approach to ease the calculation of the matching conditions for linear PCH systems is presented in [35].

1.2.4 Adaptive Control for UMSs

After designing a controller for a specific system, the performance of this controller applied to the real system will not necessarily be the same from the simulations previously performed. This is because in order to design the controller a mathematical model approximation has to be made. However, one can take into account a class of system model uncertainties that are likely to appear in the system and then analyze the properties of the designed controller. These model uncertainties cannot be expressed in mathematical equations, but they may be characterized [46]. Adaptive control is a technique used to compensate the effect of those model uncertainties on a system response. Even though many of the existing control techniques have already shown robustness against a certain range of uncertainties, techniques from adaptive control are being used to improve the performance of such control techniques.

In [47] an interesting work regarding adaptive control of UMSs is done. They extend the adaptive control results for fully actuated systems to the underactuated case using a collocated adaptive control approach. One of the main advantages of their technique, besides local stability and convergence of the collocated variables, is that since they do not use any acceleration measurements, causality issues are avoided.

An adaptive control scheme for general nonautonomous PH systems, where matched uncertainties are considered³, is proposed in [8, 48]. Their work combines the canonical transformation and stabilization of PH systems together with adaptive control in order to asymptotically stabilize such systems in the presence of matched uncertainties (mainly input disturbances). It is also important to remark that, even though their technique theoretically accounts for uncertainties caused by unknown system parameters (e.g., Inertia values) that can be linearly parameterized in the control input, it might not always be feasible due to the fact that one of the main conditions that they require is the matrix of known functions to be non-constant and bounded as time goes to infinity (basically a time-dependent function). They also apply their adaptive control scheme to tracking control of fully actuated mechanical systems. A survey reviewing their work is presented in [49], where learning control methodologies for PH systems are also presented.

In order to compensate for the effect of uncertainties in the IDA-PBC control law for the IWIP system, an adaptive control law is proposed in [50]. Since the efficiency of the IDA-PBC controller depends on the tuning of its gains, the goal of the proposed adaptive law is to adapt some of the IDA-PBC control law gains and so improve the performance of the controller. The adaptive law proposed in their work coincides with the one from [8]. A few remarks about their work are: i) at the beginning of their work,

³An uncertainty is matched if it enters the system through the same channel as the control input.

it is mentioned that they will deal with the asymptotic stability of the IWIP system; however, they only prove stability, ii) Besides the simulations and real-life experiment, there is no analysis about how their adaptive control law does improve the efficiency of the IDA-PBC controller.

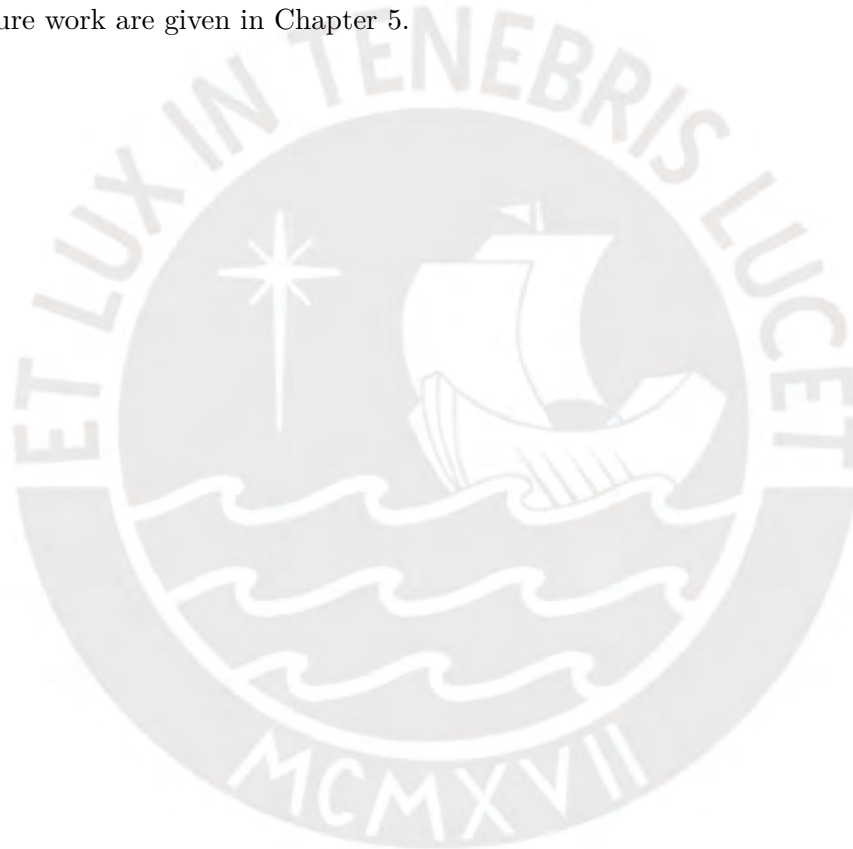
The work done in [51] presents an interesting approach to deal with external disturbances and parametric uncertainties for a set of nonlinear PCH systems with a common control input. Their work first presents theorems for the simultaneous stabilization of two nonlinear PCH systems. For the case when there simultaneously exist parametric uncertainties in two PCH system, a theorem is stated to achieve an adaptive simultaneous stabilization of those systems. Additionally, if besides parametric uncertainties, there are external disturbances, another theorem is stated in order to obtain a robust adaptive simultaneous stabilization. Finally, they study the case for more than two PCH systems and provide a theorem for the simultaneous stabilization of those systems.

1.3 Contributions of this Thesis

This thesis focuses on the asymptotic stabilization of a special class of mechanical systems, namely, UMSs (represented as PH systems) whose PDEs in the IDA-PBC technique can be solved, and are affected by parameter uncertainties (not necessarily matched) and input disturbances. To achieve that, a couple of propositions are stated based on the standard IDA-PBC technique and adaptive control in order to extend its application realm. The first proposition deals with input disturbances while the second one deals with parameter uncertainties including friction, which is obviated in the standard IDA-PBC procedure. Stability in the first proposition is demonstrated using nonautonomous systems' stability theory because the external disturbance is considered as a time-dependent function, while stability theory for autonomous systems is used for the second proposition because the parameter uncertainties are considered time-independent. Asymptotic stability is established under the condition of zero state detectability with respect to the passive output. Both propositions could have been stated in a single one. However, to convey the main idea behind the adaptive approach in a clearer way for each case, it was decided to keep them apart. In order to prove the validity of the preceding propositions, some simulations are carried out on the well-known IWIP system and then compared to the standard IDA-PBC technique.

1.4 Outline of the Thesis

The remainder of this thesis is organized as follows: In Chapter 2 mathematical preliminaries that will help to improve the understanding of the proposed propositions are presented. In Chapter 3, as a base controller the one resulting from the IDA-PBC technique is used and, two propositions, that add an adaptive part to the standard IDA-PBC, are presented to compensate the effect of parameter uncertainties and input disturbance on the response of UMSs expressed as PH systems. The well-known IWIP system is used in Chapter 4 to carry out a variety of simulations in order to verify the validity of the adaptive IDA-PBC control approach. Finally, some concluding remarks and future work are given in Chapter 5.



Chapter 2

Mathematical Preliminaries

This chapter is devoted to presenting the necessary mathematical foundations for the right understanding of the adaptive IDA-PBC approach discussed in Chapter 3. In Section 2.1, the theory to study the stability of nonlinear autonomous and nonautonomous systems is discussed. The basis of PBC, the definition and properties of PH systems, and the IDA-PBC technique are reviewed in Section 2.2. Finally, The main idea of the adaptive approach taken in this work is stated in Section 2.3.

2.1 Stability of Nonlinear Systems

In this section, the stability of equilibrium points in nonlinear systems is studied. Since the analytical solutions of nonlinear differential equations generally cannot be obtained, it is necessary to employ other mathematical tools in order to establish the stability of these systems. Stability in the sense of Lyapunov is presented and then concepts to extend Lyapunov's stability theory are stated. Lyapunov's work, *The Problem of Motion Stability*, includes two methods for stability analysis: linearization method and the direct method. This work will focus on the latter one. In the case of nonlinear systems, the terms time-varying or time-invariant, used in linear systems, are typically replaced by the terms nonautonomous and autonomous respectively. All the concepts stated in this section, together with the proofs of theorems and lemmas, can be found in [52, 53].

2.1.1 Autonomous Systems

Let's consider the autonomous system

$$\dot{x} = f(x), \tag{2.1}$$

where $f : D \rightarrow \mathbb{R}^n$ is a locally Lipschitz map from a domain $D \subset \mathbb{R}^n$ into \mathbb{R}^n . Without loss of generality, the equilibrium point $x^* \in D$ of (2.1), which obeys

$$f(x^*) = 0,$$

can be considered to be the origin of \mathbb{R}^n , that is, $x^* = 0$. This can be done because any equilibrium point can be shifted to the origin via a change of variables. Therefore, it will be assumed that $f(x)$ satisfies $f(0) = 0$. Let $x(t)$ be the solution of (2.1), i.e., the state trajectory, corresponding to the initial condition $x(0) = x_0$.

Definition 2.1 (Lyapunov Stability) *The equilibrium point $x^* = 0$ of (2.1) is*

- *stable, if for each $\varepsilon > 0$ there is $\delta = \delta(\varepsilon) > 0$ such that $\forall x_0 \in \mathbb{R}^n$ with*

$$\|x_0\| < \delta \implies \|x(t)\| < \varepsilon, \forall t \geq 0;$$

- *unstable, if it is not stable;*
- *asymptotically stable, if it is stable and δ can be chosen such that $\forall x_0 \in \mathbb{R}^n$ with*

$$\|x_0\| < \delta \implies \lim_{t \rightarrow \infty} x(t) = 0;$$

- *exponentially stable, if it is asymptotically stable and there exist two strictly positive numbers α and λ such that $\forall x_0 \in \mathbb{R}^n$ with*

$$\|x_0\| < \delta \implies \|x(t)\| \leq \alpha \|x_0\| e^{-\lambda t}, \forall t \geq 0.$$

□

Having defined the stability concepts, we now have to define a way to determine the stability of an equilibrium. Lyapunov's direct method is based on a physical observation: "if the total energy of a mechanical (or electrical) system is continuously dissipated, then the system, whether linear or nonlinear, must eventually settle down to an equilibrium point" [53, p. 57]

Definition 2.2 (Positive/Negative (semi-)definite) *Let $\mathcal{X} \subseteq \mathbb{R}^n$ be an open set containing $x = 0$. A function $V = V(x)$ with $V : \mathcal{X} \rightarrow \mathbb{R}$ is called positive (negative) definite if*

- 1) *V is continuously differentiable with respect to x ,*
- 2) *$V(0) = 0$, and*

$$3) V(x) > 0 \quad (V(x) < 0) \quad \forall x \in \mathcal{X} \setminus \{0\}.$$

However, if instead of 3) the following is satisfied

$$3') V(x) \geq 0 \quad (V(x) \leq 0) \quad \forall x \in \mathcal{X} \setminus \{0\},$$

then V is called positive (negative) semidefinite. □

Theorem 2.1 (Lyapunov's direct method) Let $x^* = 0$ be an equilibrium point of (2.1) and $\mathcal{X} \subseteq \mathbb{R}^n$ be an open set containing x^* . If there exists a function $V = V(x)$ with $V : \mathcal{X} \rightarrow \mathbb{R}$ such that

1) V is positive definite and

$$2) \dot{V} \text{ is negative semidefinite, i.e., } \dot{V}(x) = \frac{\partial V(x)}{\partial x} f(x) \leq 0 \quad \forall x \in \mathcal{X},$$

then the equilibrium point $x^* = 0$ is stable. Moreover, if

2') \dot{V} is negative definite,

then $x^* = 0$ is asymptotically stable. □

Functions that initially satisfy 1) in Theorem 2.1 are called Lyapunov function candidates, while functions satisfying 1)-2) and 1)-2') are called Lyapunov functions and strict Lyapunov functions respectively.

The sign definiteness of functions of the quadratic form, i.e., $V(x) = x^\top P x$, where P is a real symmetric matrix, can be easily verified. $V(x)$ is positive definite (positive semidefinite) if and only if P is positive definite (positive semidefinite), i.e., $P \succ 0$ ($P \succeq 0$). Even though there is no general systematic way to find Lyapunov functions, there are some approaches that can help to find them, e.g., consider the total energy of a mechanical or electrical system as natural Lyapunov candidates; or apply the *variable gradient method*.

Remark The Lyapunov stability criterion is only sufficient. Therefore, if the conditions stated in Theorem 2.1 are not fulfilled, it does not imply that the equilibrium is not stable or asymptotically stable.

Although the sufficient conditions for asymptotic stability have been introduced in the Theorem 2.1, it is not always possible or at least easy to find a strict Lyapunov function. Therefore, Lyapunov's theory needs to be expanded appealing to the concept of invariance principle, which is stated in the next theorem.

Theorem 2.2 (LaSalle's invariance principle) *Let $\Omega \subset \mathcal{X}$ be a compact set that is positively invariant with respect to (2.1). Let $V : \mathcal{X} \rightarrow \mathbb{R}$ be a continuously differentiable function such that $\dot{V}(x) \leq 0$ in Ω . Let $\mathcal{S} = \{x \in \Omega | \dot{V}(x) = 0\}$ and ϵ be the largest positively invariant set in \mathcal{S} . Then every solution $x(t)$ starting in Ω approaches ϵ as $t \rightarrow \infty$. \square*

One important remark of Theorem 2.2 is that the function $V(x)$ is not required to be positive definite as it was in Lyapunov's theorem 2.1. Since the main interest of this work is to show that $\lim_{t \rightarrow \infty} x(t) = 0$, it has to be established that ϵ is the origin. This is accomplished by showing that no solution, other than the trivial solution $x \equiv 0$, can stay identically in \mathcal{S} . In order to extend Theorem 2.1, Theorem 2.2 is specialized, which results in the following theorem, also known as the Barbashin-Krasovskii theorem.

Theorem 2.3 *Let $x^* = 0$ be an equilibrium point of (2.1) and $V : \mathcal{X} \rightarrow \mathbb{R}$ be a continuously differentiable positive definite function on a domain $\mathcal{X} \subseteq \mathbb{R}^n$ containing the origin, such that $\dot{V}(x) \leq 0$ in \mathcal{X} . Let $\mathcal{S} = \{x \in \mathcal{X} | \dot{V}(x) = 0\}$ and suppose that no solution, other than the trivial solution $x \equiv 0$, can stay identically in \mathcal{S} . Then the origin is asymptotically stable. \square*

Remark Theorem 2.3 is equivalent to Theorem 2.1 when $\dot{V}(x)$ is negative definite.

2.1.2 Nonautonomous Systems

Let's consider the nonautonomous system

$$\dot{x} = f(x, t), \quad x_0 = x(t_0), \quad (2.2)$$

where $f : \mathcal{X} \times [t_0, \infty) \rightarrow \mathbb{R}^n$ is piecewise continuous in t and Locally Lipschitz in x on $\mathcal{X} \times [t_0, \infty)$, with an open set $\mathcal{X} \subseteq \mathbb{R}^n$ containing $x = 0$. The equilibrium points x^* of (3.22) at $t = t_0$ are defined by

$$f(x^*, t) \equiv 0, \quad \forall t \geq t_0 \geq 0.$$

Similar to autonomous systems, without loss of generality, the equilibrium points x^* of (3.22) can be assumed to be at the origin of \mathbb{R}^n , that is, $x^* = 0$. Unlike autonomous systems, the stability behavior of the equilibrium points in nonautonomous systems will, in general, depend on t_0 . Therefore, a redefinition of Definition 2.1 must be done for nonautonomous systems.

Definition 2.3 (Lyapunov stability for nonautonomous systems)

The equilibrium point $x^ = 0$ of (3.22) is*

- stable, if for each $\varepsilon > 0$ there is $\delta = \delta(\varepsilon, t_0) > 0$ such that $\forall x_0 \in \mathbb{R}^n$ with

$$\|x_0\| < \delta \implies \|x(t)\| < \varepsilon, \forall t \geq t_0 \geq 0; \quad (2.3)$$

- uniformly stable, if for each $\varepsilon > 0$ there is $\delta = \delta(\varepsilon) > 0$, independent of t_0 , such that (2.3) is satisfied;
- unstable, if it is not stable;
- asymptotically stable, if it is stable and there is a positive constant $c = c(t_0)$ such that $\lim_{t \rightarrow \infty} x(t) = 0$, for all $x_0 \in \mathbb{R}^n$ with $\|x_0\| < c$;
- uniformly asymptotically stable, if it is uniformly stable and there is a positive constant c , independent of t_0 , such that for all $x_0 \in \mathbb{R}^n$ with $\|x_0\| < c$, $\lim_{t \rightarrow \infty} x(t) = 0$, uniformly in t_0 ; that is, for each $\eta > 0$, there is $T = T(\eta) > 0$ such that

$$\|x(t)\| < \eta, \forall t \geq t_0 + T(\eta), \forall x_0 \in \mathbb{R}^n \text{ with } \|x_0\| < c.$$

□

In order to study the stability of nonautonomous systems, Lyapunov's stability theory for autonomous systems is extended. The following theorem will state the sufficient conditions to prove uniform stability and uniform asymptotic stability.

Theorem 2.4 (Uniform Stability/Asymptotic Stability) *Let $x^* = 0$ be an equilibrium of (3.22). If there exists a function $V = V(x, t)$ with $V : \mathcal{X} \times [t_0, \infty) \rightarrow \mathbb{R}$, continuously differentiable such that $\forall t \geq 0$ and $\forall x \in \mathcal{X}$*

$$W_1(x) \leq V(x, t) \leq W_2(x),$$

$$\frac{\partial V(x)}{\partial t} + \frac{\partial V(x)}{\partial x} f(x, t) \leq 0,$$

where $W_1(x)$ and $W_2(x)$ are continuous positive definite functions on \mathcal{X} , then $x^* = 0$ is uniformly stable. Moreover, if

$$\frac{\partial V(x)}{\partial t} + \frac{\partial V(x)}{\partial x} f(x, t) \leq -W_3(x),$$

where $W_3(x)$ is a continuous positive definite function on \mathcal{X} . Then $x^* = 0$ is uniformly asymptotically stable. □

Let us note that LaSalle's invariance principle, used to prove asymptotic stability for autonomous systems when $\dot{V}(x)$ is negative semidefinite, can no longer be applied to

the case of nonautonomous systems. However, a similar, but a weaker statement can be presented using the following lemma.⁴

Lemma 2.1 (Barbălat) *Let $f(t)$ be a differentiable function. If the following conditions are satisfied*

- 1) $\lim_{t \rightarrow \infty} f(t) = c, |c| < \infty$
- 2) $\dot{f}(t)$ is uniformly continuous

then $\lim_{t \rightarrow \infty} \dot{f}(t) = 0$. □

Uniform continuity of a function is usually not easy to prove using its definition (not mentioned here). However, a sufficient condition to prove it indirectly is to demonstrate that $\dot{f}(t)$ is Lipschitz-continuous or $\ddot{f}(t)$ is bounded.

Now, an extension of Lemma 2.1 is presented for the analysis of dynamic systems. This extension looks similar to the invariance set theorem in the Lyapunov analysis, hence its name.

Lemma 2.2 (Lyapunov-Like Lemma) *if there exists a scalar function $V(x, t) : \mathbb{R}^n \times [t_0, \infty) \rightarrow \mathbb{R}$ differentiable in x such that*

- 1) $V(x, t)$ is lower bounded,
- 2) $\dot{V}(x, t)$ is negative semidefinite, and
- 3) $\dot{V}(x, t)$ is uniformly continuous in time,

then $\lim_{t \rightarrow \infty} \dot{V}(x, t) = 0$. □

Uniform continuity of $\dot{V}(x, t)$ is typically verified, similar to Lemma 2.1, by proving that $\ddot{V}(x, t)$ is bounded. Note that, $V(x, t)$ then approaches a finite limiting value V_∞ , such that $V_\infty \leq V(x(t_0), t_0)$.

Some important differences between the Lyapunov-like and Lyapunov analysis are:
 i) The function V is required to be only lower bounded in x and t instead of being positive definite, ii) The function \dot{V} , besides being negative semidefinite, also has to be uniformly continuous.

⁴Weaker in the sense that unlike LaSalle's invariance principle, the Lyapunov-like lemma does not give any information about the domain of attraction.

2.2 Passivity-Based Control: Interconnection and Damping Assignment

2.2.1 Passivity

This section focuses on establishing the mathematical basis for the so-called passivity-based control, i.e., dissipativity and passivity properties. Dissipativity is a property of physical systems, that is closely related to the notion of energy dissipation (e.g., dissipation as heat in resistors for electrical systems and dissipation due to friction in mechanical systems). To mathematically define the concept of dissipativity, two functions must be defined: storage function, which measures how much energy is stored in the system; and the supply rate, which measures how fast external energy is being injected in the system. The main idea behind the dissipativity property is that a system cannot have, at a certain time, more energy than what was injected into it. The main sources of the mathematical concepts, here presented, were borrowed from [4, 52, 54–57].

Assumption The system

$$\Sigma : \begin{cases} \dot{x} = f(x, u), & x \in \mathcal{X} \subseteq \mathbb{R}^n, u \in \mathcal{U} \subseteq \mathbb{R}^m \\ y = h(x, u), & y \in \mathcal{Y} \subseteq \mathbb{R}^p \end{cases} \quad (2.4)$$

with $u = 0$ has an equilibrium at $x^* = 0$, that is, $f(0, 0) = 0$ and $h(0, 0) = 0$. For all initial conditions $x(0) = x_0$ and input functions $u = u(t)$, the solution $x(t) = \varphi(x_0, u(t), t), \forall t \geq 0$ is unique. Let $s : \mathcal{U} \times \mathcal{Y} \rightarrow \mathbb{R}$ be the supply rate of Σ . The supply rate s satisfies $\forall x_0 \in \mathcal{X}$ and $\forall u(t) \in \mathcal{U}$ the following relationship

$$\int_0^t |s(u(\tau), y(\tau))| d\tau < \infty, \forall t \geq 0.$$

Definition 2.4 (Dissipativity) *The system Σ is said to be dissipative with respect to the supply rate s , if there exists a non-negative storage function $V(x) \geq 0, V : \mathcal{X} \rightarrow \mathbb{R}^+$, such that $\forall x_0 \in \mathcal{X}$ and $\forall u(t) \in \mathcal{U}$ (that result in the solution trajectory $x = x(t)$), the following inequality (integral dissipativity inequality) holds*

$$V(x(t)) \leq V(x_0) + \int_0^t s(u(\tau), y(\tau)) d\tau. \quad (2.5)$$

□

In case (2.5) holds with equality $\forall x_0, t \geq 0, u(t)$, then the system Σ is conservative with respect to s . The physical interpretation of (2.5) is that there cannot be internal "creation of energy"; that is, the stored energy $V(x(t))$ at any time $t \geq t_0 \geq 0$ is at most equal to the initial stored energy $V(x(t_0))$, plus the supplied energy $\int_{t_0}^t s(u(\tau), y(\tau)) d\tau$. Therefore, there can only be internal dissipation of energy.

Inequality (2.5) can be equivalently rewritten (assuming $V(x(t))$ is continuously differentiable) as

$$\frac{\partial V(x(t))}{\partial x} f(x, u) \leq s(u(t), y(t)), \quad \forall t \geq 0 \quad (\text{differential dissipativity inequality})$$

Definition 2.5 (Passivity) *The system Σ with $\mathcal{U} = \mathcal{Y} = \mathbb{R}^m$ is said to be passive if it is dissipative with respect to the supply rate $s(u(t), y(t)) = u^\top y$ and the storage function satisfies $V(0) = 0$. \square*

Definition 2.6 (Zero-State Observability) *Σ is zero-state observable if $u(t) = 0, y(t) = 0, \forall t \geq 0$, implies $x(t) = 0, \forall t \geq 0$. \square*

A weaker version of the observability property, used to prove asymptotic stability, is presented in the next definition.

Definition 2.7 (Zero-State Detectability) *Σ is zero-state detectable if $u(t) = 0, y(t) = 0, \forall t \geq 0$, implies $\lim_{t \rightarrow \infty} x(t) = 0$. \square*

Even though the zero-state observability and detectability properties are defined for autonomous systems, they can be used for non-autonomous systems.

Theorem 2.5 (Passivity and Stability) *Let the system Σ be passive with a C^1 storage function V and y be C^1 in u for all x . Then the following properties hold:*

- (i) *if V is positive definite, then the equilibrium $x = 0$ of Σ with $u = 0$ is stable.*
- (ii) *if Σ is Zero-State detectable (ZSD), then the equilibrium $x = 0$ of Σ with $u = 0$ is stable.*
- (iii) *When there is no throughput, i.e., $y = h(x)$, then the feedback $u = -y$ achieves asymptotic stability of $x = 0$ if and only if Σ is ZSD. \square*

Assumption From now on, it is assumed that Σ has no feedthrough terms, i.e., $y = h(x)$.

2.2.2 Port-Hamiltonian Systems

PH systems are generalizations of the Hamiltonian representation of systems stemming from different physical domains. They are defined in terms of a Hamiltonian function and two geometric structures: power-conserving interconnection and energy dissipation. These structures are such that, the Hamiltonian function satisfies the dissipation inequality. The literature regarding PH systems is quite vast. In this work, we are going to focus on a special case of PH systems, that is, input-state-output PH systems. The mathematical concepts, here presented, are mainly borrowed from [54, 58, 59].

A generalized time-invariant PH system in the standard input-state-output representation is given by⁵

$$\begin{aligned} \dot{x} &= (J(x) - R(x)) \frac{\partial H(x)}{\partial x} + g(x)u, \\ y &= g^\top(x) \frac{\partial H(x)}{\partial x}, \end{aligned} \quad (2.6)$$

where $x \in \mathbb{R}^n$, $u, y \in \mathbb{R}^m$, $J(x) = -J^\top(x) \in \mathbb{R}^{n \times n}$ is the power-conserving internal interconnection structure (generally known as the natural interconnection matrix), $R(x) = R^\top(x) \succeq 0 \in \mathbb{R}^{n \times n}$ is the resistive structure (generally known as the damping matrix) and $g(x) \in \mathbb{R}^{n \times m}$ is the input matrix and determines how the control signal enter into the system. The Hamiltonian $H(x) \in \mathbb{R}$ is the total stored energy of the system. Since the structures $J(x)$ and $R(x)$ are skew-symmetric and positive semidefinite, respectively, the passivity inequality holds

$$\frac{\partial H(x(t))}{\partial t} = \left(\frac{\partial H}{\partial x} \right)^\top \dot{x} = - \left(\frac{\partial H}{\partial x} \right)^\top R \left(\frac{\partial H}{\partial x} \right) + \overbrace{\left(\frac{\partial H}{\partial x} \right)^\top g}^{y^\top} u \leq u^\top y.$$

Notice that, if

- 1) $u = 0 \implies \dot{H}(x) \leq 0$ and
- 2) the equilibrium $x^* = \arg \min H(x) \implies H(x) > 0, \forall x \in \mathcal{X} \subseteq \mathbb{R}^n \setminus \{0\}$,

then H is a (weak) Lyapunov function.

⁵From now on, the gradients are considered as column vectors.

2.2.3 Port-Hamiltonian Modeling of a Mechanical System

Mechanical systems have a the following natural PH system representation

$$\overbrace{\begin{bmatrix} \dot{q} \\ \dot{p} \end{bmatrix}}^{\dot{x}} = \left(\overbrace{\begin{bmatrix} 0 & I_n \\ -I_n & 0 \end{bmatrix}}^J - \overbrace{\begin{bmatrix} 0 & 0 \\ 0 & R(q) \end{bmatrix}}^R \right) \begin{bmatrix} \frac{\partial H}{\partial q} \\ \frac{\partial H}{\partial p} \end{bmatrix} + \overbrace{\begin{bmatrix} 0 \\ G(q) \end{bmatrix}}^g u, \quad (2.7)$$

where $q \in \mathbb{R}^n$ and $p \in \mathbb{R}^n$ are the generalized positions and momenta, respectively, and form the system's state $x = [q^\top, p^\top]^\top$. For fully actuated systems $G(q) = I_n$. We will focus on underactuated mechanical systems, so the matrix $G(q) \in \mathbb{R}^{n \times m}$ is not invertible i.e., $\text{rank}(G) = m < n$. If we were to consider natural damping we would have to meet the conditions stated in [45]. To avoid these conditions, we assume the system has no natural damping (at least for the IDA-PBC technique), so the system (2.7) becomes

$$\begin{bmatrix} \dot{q} \\ \dot{p} \end{bmatrix} = \begin{bmatrix} 0 & I_n \\ -I_n & 0 \end{bmatrix} \begin{bmatrix} \frac{\partial H}{\partial q} \\ \frac{\partial H}{\partial p} \end{bmatrix} + \begin{bmatrix} 0 \\ G(q) \end{bmatrix} u. \quad (2.8)$$

2.2.4 Interconnection and Damping Assignment Passivity-Based Control

The main goal of the so-called IDA-PBC technique is to modify the total energy function of the system (2.8) into a desired closed-loop energy function in order to obtain the desired equilibrium $(q^*, 0)$. Additionally, damping is added to achieve asymptotic stability. The closed-loop system is a PH system, whose energy function will be determined via the solution of a PDE. This method was introduced in [5] to control physical systems described by PCH models to exploit its properties (mentioned in Section 2.2.2). However, it was showed in [32] that it can be applied to a more general class of systems, namely, nonlinear affine systems. This work will be based on the application of this method to UMS. The concepts here presented are mainly borrowed from [33, 44]. The references [5, 32, 45, 59] are also taken into consideration.

First, a general idea of the IDA-PBC technique for general nonlinear systems is presented, then a more specific approach for UMSs is introduced.

Consider the following nonlinear affine system

$$\dot{x} = f(x) + g(x)u. \quad (2.9)$$

As stated before, the closed-loop function is a PH system, which is obtained via a state feedback $u = u(x)$, that is,

$$f(x) + g(x)u = (J_d(x) - R_d(x)) \frac{\partial H_d(x)}{\partial x}. \quad (2.10)$$

From the properties mentioned in Section 2.2.2, the (asymptotic) stability of the equilibrium x^* can be achieved using Theorem 2.1, which can be applied if the following requirements are satisfied

$$R_d(x) (\succ) \succeq 0, \quad (2.11)$$

$$x^* = \arg \min H_d(x). \quad (2.12)$$

The equality (2.10), for UMSs (i.e., $g(q) \in \mathbb{R}^{n \times m}$), can equivalently be rewritten as

$$u = (g^\top g)^{-1} g^\top \left((J_d(x) - R_d(x)) \frac{\partial H_d(x)}{\partial x} - f \right), \quad (2.13a)$$

$$0 = g^\perp \left((J_d(x) - R_d(x)) \frac{\partial H_d(x)}{\partial x} - f \right), \quad (2.13b)$$

where $g^\perp \in \mathbb{R}^{(n-m) \times n}$ is a full rank left annihilator of $g(x)$, i.e., $g^\perp g = 0$ (Lemma 2 in [60]). Equation (2.13b) is usually referred as the matching equation, which can be difficult to solve. Solving this matching condition is the key step when applying the IDA-PBC technique.

Apart from the previous conditions imposed on J_d and R_d , that is, $J_d = -J_d^\top$ and $R_d = R_d^\top \succeq 0$, they are free parameters. H_d can be totally, or partially, fixed so that (2.12) is satisfied. g^\perp has an additional degree of freedom, since it is not unique for a given $g(x)$. There are mainly three ways to solve the matching equation, these are:

Non-Parameterized IDA Here, the interconnection J_d and damping R_d matrices are fixed, which was the original idea of IDA in [5], hence its name. Additionally, g^\perp is fixed. This yields a PDE whose solutions define the energy functions. A suitable solution that satisfies (2.12) has to be selected.

Algebraic IDA The desired energy function is fixed, then (2.13b) becomes an algebraic equation in J_d , R_d and g^\perp .

Parameterized IDA The structure of the desired energy function is physically motivated, for instance, for mechanical systems the energy function is its total energy, i.e., the sum of kinetic and potential energy. Fixing the structure of H_d results in a new PDE to define its unknown parameters. It also imposes some constraints in J_d and R_d .

This work will focus on the application of the parameterized IDA applied to a class of mechanical systems, namely, underactuated mechanical systems whose PDE (2.13b) can be solved. Therefore, we now present the calculations to determine a suitable control law u_{ida} for such an approach. The structure of the nominal mechanical system's (2.8) energy function is described by⁶

$$H(q, p) = \frac{1}{2} p^\top M^{-1}(q) p + V(q), \quad (2.14)$$

where $M(q) = M^\top(q) \succ \alpha I_n \in \mathbb{R}^n$, for some $\alpha \in \mathbb{R}^+$ is the inertia matrix and $V(q)$ is the potential energy. The structure of the desired energy function is

$$H_d(q, p) = \frac{1}{2} p^\top M_d^{-1}(q) p + V_d(q), \quad (2.15)$$

where $M_d(q) = M_d^\top(q) \succ \alpha I_n \in \mathbb{R}^n$, for some $\alpha \in \mathbb{R}^+$ and $V_d(q)$ represent the closed-loop inertia matrix and potential energy function, respectively.

The desired equilibrium x^* has to belong to an admissible set.

Definition 2.8 (Admissible equilibrium) *The equilibrium point $(q^*, 0)$ of the nominal system (2.8) is said to be admissible if the following equality is satisfied*

$$G^\perp \left. \frac{\partial V(q)}{\partial q} \right|_{q^*} = 0. \quad (2.16)$$

$V_d(q)$ is required to have an isolated minimum at the desired equilibrium q^* , i.e.,

$$q^* = \arg \min V_d(q). \quad (2.17)$$

The closed-loop PH system is

$$\begin{bmatrix} \dot{q} \\ \dot{p} \end{bmatrix} = \left(\begin{array}{c|c} \overbrace{\begin{bmatrix} 0 & J_1 \\ -J_1^\top & J_2 \end{bmatrix}}^{J_d} & \overbrace{\begin{bmatrix} 0 & 0 \\ 0 & R_2 \end{bmatrix}}^{R_d} \\ \hline & \end{array} \right) \begin{bmatrix} \frac{\partial H_d}{\partial q} \\ \frac{\partial H_d}{\partial p} \end{bmatrix}. \quad (2.18)$$

Now, the equality (2.10) becomes

$$\begin{bmatrix} 0 & I_n \\ -I_n & 0 \end{bmatrix} \begin{bmatrix} \frac{\partial H}{\partial q} \\ \frac{\partial H}{\partial p} \end{bmatrix} + \begin{bmatrix} 0 \\ G \end{bmatrix} u_{ida} = \begin{bmatrix} 0 & J_1 \\ -J_1^\top & J_2 - R_2 \end{bmatrix} \begin{bmatrix} \frac{\partial H_d}{\partial q} \\ \frac{\partial H_d}{\partial p} \end{bmatrix}. \quad (2.19)$$

⁶Even though it was mentioned that IDA is not restricted to control PH systems, it is considered here that the nominal system is PH.

From (2.19) it is clear that $\dot{q} = M^{-1}p$ must hold in both, the nominal and closed-loop systems. Therefore, $J_1 = M^{-1}M_d$.

The control law that satisfies (2.19), taken from (2.13a), is

$$u_{ida} = \left(G^\top G\right)^{-1} G^\top \left(\frac{\partial H}{\partial q} - M_d M^{-1} \frac{\partial H_d}{\partial q} + (J_2 - R_2) M_d^{-1} p \right), \quad (2.20)$$

only if the following PDE can be solved

$$G^\perp \left(\frac{\partial H}{\partial q} - M_d M^{-1} \frac{\partial H_d}{\partial q} + (J_2 - R_2) M_d^{-1} p \right) = 0. \quad (2.21)$$

Assuming $R_2 = R_2(q)$ and $J_2 = J_{20}(q) + J_{21}(q, p)$, with J_{21} linear in p , the matching condition (2.21) can be naturally separated in dependency of p ; that is, independent of p (corresponding to potential energy), linear in p (corresponding to dissipation) and quadratic in p (corresponding to kinetic energy). Thus, the matching condition (2.21) can be rewritten as the following set of PDEs

$$G^\perp \left(\frac{\partial p^\top M^{-1} p}{\partial q} - M_d M^{-1} \frac{\partial p^\top M_d^{-1} p}{\partial q} + 2J_{21} M_d^{-1} p \right) = 0, \quad (2.22a)$$

$$G^\perp \left(\frac{\partial V}{\partial q} - M_d M^{-1} \frac{\partial V_d}{\partial q} \right) = 0, \quad (2.22b)$$

$$G^\perp (J_{20} - R_2) M_d^{-1} p = 0. \quad (2.22c)$$

The first equation in (2.22) is a non-homogeneous, first-order quasilinear PDE that has to be solved to determine the elements of the closed-loop inertia matrix M_d . For a given inertia matrix M_d , (2.22b) is a simple linear PDE for the desired potential energy V_d . The third equation is an algebraic solve by choosing

$$J_{20} - R_2 = G(K_j - K_v)G^\top, \quad (2.23)$$

where $K_j = -K_j^\top \in \mathbb{R}^{m \times m}$ and $K_v = K_v^\top \succ 0$. From (2.23) it is clear that $R_2 = GK_v G^\top$. Therefore, the closed-loop system can be finally rewritten as

$$\begin{bmatrix} \dot{q} \\ \dot{p} \end{bmatrix} = \begin{bmatrix} 0 & M^{-1}M_d \\ -M_d M^{-1} & \underbrace{J_2 - GK_v G^\top}_{R_2} \end{bmatrix} \begin{bmatrix} \frac{\partial H_d}{\partial q} \\ \frac{\partial H_d}{\partial p} \end{bmatrix}. \quad (2.24)$$

The control law can be decomposed into two terms, which are energy shaping and damping injection

$$u_{ida} = u_{es}(q, p) + u_{di}(q, p). \quad (2.25)$$

The term R_2 in (2.24) can be obtained by defining

$$u_{di} = -K_v G^\top \frac{\partial H_d}{\partial p}. \quad (2.26)$$

Now, combining (4.14) together with (2.20) and (2.26) we get

$$u_{es} = \left(G^\top G\right)^{-1} G^\top \left(\frac{\partial H}{\partial q} - M_d M^{-1} \frac{\partial H_d}{\partial q} + J_2 M_d^{-1} p\right). \quad (2.27)$$

The so-called passive output of the closed-loop system (2.24) is defined by

$$y_d = G^\top \frac{\partial H_d}{\partial p}. \quad (2.28)$$

Proposition 2.1 ([33]) *The system (2.24) with (2.15) and (2.17) has a stable equilibrium point at $(q^*, 0)$. This equilibrium is asymptotically stable if (2.24) is zero-state detectable from the output y_d .*

Proof

$$\begin{aligned} \dot{H}_d &= \left(\frac{\partial H_d}{\partial q}\right)^\top \dot{q} + \left(\frac{\partial H_d}{\partial p}\right)^\top \dot{p} \\ &= -\underbrace{\left(\frac{\partial H_d}{\partial p}\right)^\top G K_v}_{y_d^\top} \underbrace{G^\top \left(\frac{\partial H_d}{\partial p}\right)}_{y_d} \leq -\lambda_{\min}\{K_v\} \|y_d\|^2 \leq 0. \end{aligned}$$

Asymptotic stability, under the zero-state detectability condition, is established invoking Barbashin-Krasovskii Theorem 2.3.

2.3 Adaptive control

When the time comes to apply a designed controller to the mechanical system itself, it can be noticed that the performance of the controller does not exactly match the one from the simulations. This variation is usually directly connected to the fact that to obtain the control law, some mathematical simplifications were made. Additionally, it can be the result of the noise in the sensors' readings, input disturbance, parameter uncertainties, malfunction of some elements of the system, etc. Some control techniques can already handle such uncertainties up to a certain range, however, their application realm could be extended if the effect of those uncertainties was compensated⁷. Adap-

⁷The robustness of IDA-PBC against external disturbances is analyzed in [9].

tive control arises to compensate for the effect of those unknown factors and ensure a desired performance (e.g., ensure the stability of an uncertain system). This section shortly explains the approach taken in order to extend the application realm of the so-called IDA-PBC technique (applied to UMSs), adding an adaptive term to compensate input disturbances and parameter uncertainties. The reader may refer to the following literature regarding adaptive control [7, 46]

The approach taken to add and design the, previously mentioned, adaptive term is based mainly on the idea of the Adaptive Dynamic Inversion (ADI) control presented in [7]. However, it has to be remarked that such a control technique was presented for tracking, not stabilization (which is what we focus on in this work).

2.3.1 Adaptive Dynamic Inversion

A short review of this technique, applied to a first-order systems, is presented in this section.

Consider the first-order autonomous system

$$\dot{x} = ax + bu + f(x), \quad (2.29)$$

where a , b are constant unknown parameters, $f(x)$ is an uncertain nonlinear function that can be expressed as $f(x) = \theta^\top \Phi(x)$, where $\theta \in \mathbb{R}^n$ is a vector of constant unknown parameters and $\Phi(x) \in \mathbb{R}^n$ is a vector of known basis functions.

The desired stable reference system is

$$\dot{x}_m = a_m x_m + b_m r, \quad (a_m < 0). \quad (2.30)$$

The control goal is to achieve trajectory tracking, i.e., $\lim_{t \rightarrow \infty} (x(t) - x_m(t)) = 0$.

Rewriting the dynamics of the system (2.29) leads to

$$\dot{x} = \hat{a}x + \hat{b}u + \hat{f}(x) - \overbrace{(\hat{a} - a)}^{\Delta_a} x - \overbrace{(\hat{b} - b)}^{\Delta_b} u - \overbrace{(\hat{f}(x) - f(x))}^{\Delta_{f(x)}} \quad (2.31)$$

$$= \hat{a}x + \hat{b}u + \hat{f}(x) - \Delta_a x - \Delta_b u - \underbrace{(\hat{\theta} - \theta)^\top}_{\Delta_\theta} \Phi(x). \quad (2.32)$$

The chosen ADI control feedback is

$$u = \frac{1}{\hat{b}}((a_m - \hat{a})x + b_m r) - \hat{\theta}^\top \Phi(x), \quad (2.33)$$

and yields the closed-loop system

$$\dot{x} = a_m x_m + b_m r - \Delta_a x - \Delta_b u - \Delta_\theta \Phi(x).$$

The Lyapunov function candidate is

$$V = e^2 + \gamma_a^{-1} \Delta_a^2 + \gamma_b^{-1} \Delta_b^2 + \Delta_\theta^\top \Gamma_\theta^{-1} \Delta_\theta, \quad (2.34)$$

where $e = x - x_m$ is the tracking error; $\gamma_a \in \mathbb{R}$, $\gamma_b \in \mathbb{R}$ and $\Gamma_\theta \in \mathbb{R}^{n \times n}$ are tunable positive (definite) constant gains, also referred as adaptation rate constants.

Applying Lyapunov stability theory, we get that in order to obtain the energy rate

$$\dot{V} = 2a_m e^2 \leq 0, \quad (2.35)$$

the following adaptation laws have to be selected

$$\begin{aligned} \dot{\hat{a}} &= \gamma_a x e, \\ \dot{\hat{b}} &= \gamma_b u e, \\ \dot{\hat{\theta}} &= \Gamma_\theta \Phi(x) e. \end{aligned}$$

From (2.35), it is clear that the system is stable. Asymptotic stability is demonstrated invoking the Lyapunov-like Lemma 2.2.

A remark about this technique is that the parameter convergence is not guaranteed, however, parameter convergence is not required to achieve a zero tracking error. Additionally, it has to be guaranteed somehow that \hat{b} does not cross zero.

2.3.2 Adaptive Approach Applied to IDA-PBC

Based on the, previously described, ADI technique, the adaptive approach of this work is presented in the following lines.

The concept, here presented, assumes that the nominal system (2.8) has only input disturbance. However, this concept is generalized in Chapter 3 for parameter uncertainty. For simplicity, the nominal PH system (2.8) with input uncertainty will be expressed as follows

$$\dot{x} = f(x) + g(x)(u(x, t) + \delta(x, t)), \quad (2.36)$$

where $\delta(x, t) = \varphi(x, t)\theta$ is the input uncertainty, $\varphi(x, t)$ is a matrix of known basis functions and θ is a vector of unknown constants.⁸ The desired closed-loop system

⁸The dimensions are assumed to be suitable.

(2.24) is

$$\dot{x} = \bar{f}(x) = f(x) + g(x)u_{ida}. \quad (2.37)$$

The choice of the control law

$$u = u_{ida}(x) - \hat{\delta}(x, t) = u_{ida}(x) - \overbrace{\varphi(x, t)\hat{\theta}}^{u_{adap}} \quad (2.38)$$

yields the following closed-loop system

$$\dot{x} = \bar{f}(x) - g(x)\varphi(x, t)\tilde{\theta}, \quad (2.39)$$

where $\tilde{\theta} = \hat{\theta} - \theta$, $\hat{\theta}$ is the estimation of θ . The adaptation law results from the stability analysis of (2.39). Since it is assumed that the input disturbance has an explicit time-dependency, then to prove the stability of (2.39) it is required to use Lyapunov theory for nonautonomous systems, i.e., Theorem 2.4. Additionally, to prove asymptotic stability, it is used the Barbălat-based Lemma 2.2 together with the zero-state detectability condition. If the input disturbance has no explicit time-dependency, then stability can be proved using Lyapunov theory for autonomous systems, i.e., Theorem 2.1. Asymptotic stability is established by invoking Barbashin-Krasovskii Theorem 2.3 or Theorem 2.5 (iii). Figure 2.1 shows a simple diagram of the adaptive control approach.

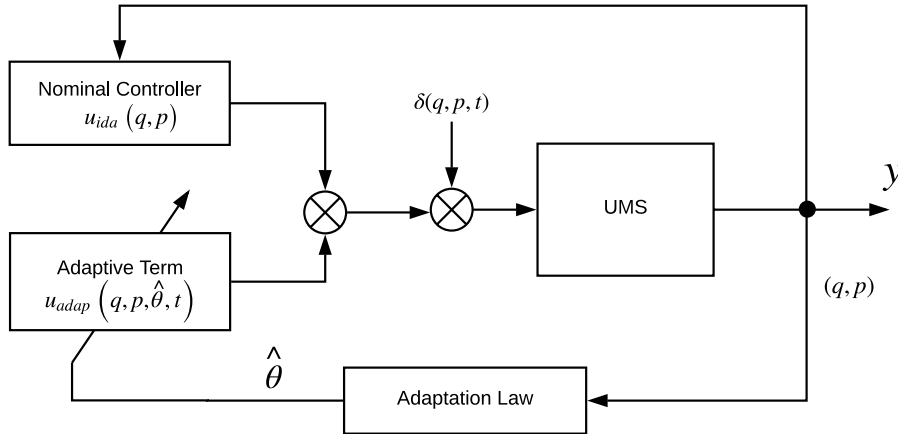


Figure 2.1. – Adaptive control diagram

Chapter 3

Adaptive IDA-PBC

In this chapter, two propositions are going to be established in order to asymptotically stabilize a special class of mechanical systems, namely, UMSs (represented as PH system) whose PDEs in the IDA-PBC technique can be solved, that is under the effect of two types of uncertainties. The first is a disturbance in the control input and the second one is parameter uncertainty of the system's energy. Both propositions were obtained using a similar approach, therefore being similar to each other. In fact, both propositions could be expressed in just one. However, it was decided to state them separately just for clearness purposes, presenting the main idea of the adaptive approach behind all the math involved.

3.1 Input Disturbance

In this section, the nominal system (2.8) affected by an explicitly time-dependent input disturbance $\delta(q, p, t)$ is considered as follows

$$\begin{bmatrix} \dot{q} \\ \dot{p} \end{bmatrix} = \begin{bmatrix} 0 & I_n \\ -I_n & 0 \end{bmatrix} \begin{bmatrix} \frac{\partial H}{\partial q} \\ \frac{\partial H}{\partial p} \end{bmatrix} + \begin{bmatrix} 0 \\ G(q) \end{bmatrix} (u + \overbrace{\Phi(q, p, t)\theta}^{\delta}), \quad (3.1)$$

where $\Phi(q, p, t) \in \mathbb{R}^{m \times l}$ is a matrix of known basis functions and $\theta \in \mathbb{R}^l$ is a column vector of constant unknown parameters. To compensate for the input disturbance, the control law

$$u = u_{ida} - \Phi(q, p, t)\hat{\theta} \quad (3.2)$$

is used, which leads to the system

$$\begin{bmatrix} \dot{q} \\ \dot{p} \end{bmatrix} = \begin{bmatrix} 0 & M^{-1}M_d \\ -M_dM^{-1} & J_2 - R_2 \end{bmatrix} \begin{bmatrix} \frac{\partial H_d}{\partial q} \\ \frac{\partial H_d}{\partial p} \end{bmatrix} - \begin{bmatrix} 0 \\ G(q) \end{bmatrix} \Phi(q, p, t)\tilde{\theta}, \quad (3.3)$$

for $\tilde{\theta} = \hat{\theta} - \theta$, and $\hat{\theta}$ is the estimation of θ . The system (3.3) is composed of two terms, the desired system from IDA-PBC (2.24) and an additional term due to the uncertainty.

Proposition 3.1 (Motivated by [8]) *The system (3.3) with the adaptation law*

$$\dot{\tilde{\theta}} = K\Phi^\top G^\top \left(\frac{\partial H_d}{\partial p} \right), \quad (3.4)$$

with constant $\mathbb{R}^{l \times l} \ni K = K^\top \succ 0$, has a stable equilibrium point at $(q^*, 0)$. Additionally, if the system (3.3)-(3.4) is zero-state detectable from the output $y_d = G^\top \left(\frac{\partial H_d}{\partial p} \right)$, then the equilibrium is asymptotically stable.

Proof

Stability. In this case, since the system (3.3) is nonautonomous, the Theorem 2.4 will be used. We define a new energy function for the closed-loop system (3.3)-(3.4) as

$$\bar{H}_d(q, p, \tilde{\theta}, t) = H_d(q, p) + \frac{1}{2} \tilde{\theta}^\top K^{-1} \tilde{\theta} - H_d(q^*, 0). \quad (3.5)$$

From Theorem 2.4 and (3.5): $W_1 = W_2 = \bar{H}_d$. The term $H_d(q^*, 0)$ is included only to ensure that $\bar{H}_d > 0$, so we can use it as a Lyapunov candidate. Now, the time derivative of the Lyapunov candidate is taken in order to verify if it is a Lyapunov function.

$$\begin{aligned} \dot{\bar{H}}_d &= \dot{H}_d + \tilde{\theta}^\top K^{-1} \dot{\tilde{\theta}} \\ &= \left(\frac{\partial H_d}{\partial q} \right)^\top \dot{q} + \left(\frac{\partial H_d}{\partial p} \right)^\top \dot{p} + \tilde{\theta}^\top K^{-1} \dot{\tilde{\theta}} \\ &= \left(\frac{\partial H_d}{\partial q} \right)^\top M^{-1} M_d \left(\frac{\partial H_d}{\partial p} \right) + \left(\frac{\partial H_d}{\partial p} \right)^\top \left(-M_d M^{-1} \left(\frac{\partial H_d}{\partial q} \right) \right. \\ &\quad \left. + (J_2 - GK_v K^\top) \left(\frac{\partial H_d}{\partial p} \right) - G\Phi \tilde{\theta} \right) + \tilde{\theta}^\top K^{-1} \dot{\tilde{\theta}} \\ &= - \left(\frac{\partial H_d}{\partial p} \right)^\top GK_v G^\top \left(\frac{\partial H_d}{\partial p} \right) - \left(\left(\frac{\partial H_d}{\partial p} \right)^\top G\Phi - \dot{\tilde{\theta}}^\top K^{-1} \right) \tilde{\theta} \end{aligned} \quad (3.6)$$

$$= - \left(\frac{\partial H_d}{\partial p} \right)^\top GK_v G^\top \left(\frac{\partial H_d}{\partial p} \right) \leq -\lambda_{\min}\{K_v\} \|y_d(t)\|^2 \leq 0. \quad (3.7)$$

In (3.6), the term regarding $\tilde{\theta}$ can be canceled using the adaptive law (3.4) and the fact that since θ is constant $\dot{\tilde{\theta}} = \dot{\hat{\theta}}$. From (3.7), it has been proven that \bar{H}_d is a Lyapunov function and hence $(q^*, 0)$ is a stable equilibrium.

Asymptotic stability. Rearrange (3.3) together with (3.4) in order to obtain the following port-Hamiltonian system

$$\begin{bmatrix} \dot{q} \\ \dot{p} \\ \dot{\tilde{\theta}} \end{bmatrix} = \begin{bmatrix} 0 & M^{-1}M_d & 0 \\ -M_dM^{-1} & J_2 - GK_vG^\top & -G\Phi K \\ 0 & K\Phi^\top G^\top & 0 \end{bmatrix} \begin{bmatrix} \frac{\partial \bar{H}_d}{\partial q} \\ \frac{\partial \bar{H}_d}{\partial p} \\ \frac{\partial \bar{H}_d}{\partial \tilde{\theta}} \end{bmatrix}. \quad (3.8)$$

A more general representation of (3.8) is stated in [8]. The rearrangement yields a bigger system whose coordinates are now $(q, p, \tilde{\theta})$.

To prove asymptotic stability, the Lyapunov-like Lemma 2.2 is invoked and from it, under the assumption that a bounded $V_d(q)$ implies a bounded $q(t)$, the following is obtained

$$\dot{\bar{H}}_d \leq 0 \implies q(t), p(t) \text{ and } \tilde{\theta} \text{ bounded.} \quad (3.9)$$

To fulfill all the conditions in Lemma 2.2, it is also required that $\dot{\bar{H}}_d$ is uniformly continuous. A sufficient condition to prove the uniform continuity of $\dot{\bar{H}}_d$ is to verify that $\ddot{\bar{H}}_d$ is bounded. Assuming the total energy function \bar{H}_d is twice differentiable with respect to the time, the second order derivative of the new energy function is

$$\ddot{\bar{H}}_d = -2y_d^\top(q, p, \tilde{\theta})K_v\dot{y}_d(q, p, \tilde{\theta}). \quad (3.10)$$

From (3.9)-(3.10) it is concluded that $\dot{\bar{H}}_d$ is uniformly continuous. Therefore

$$\lim_{t \rightarrow \infty} \dot{\bar{H}}_d \leq -\lambda_{\min}\{K_v\}\|y_d(t)\|^2 = 0 \implies \lim_{t \rightarrow \infty} y_d = 0. \quad (3.11)$$

To achieve asymptotic stability, the zero-state detectability in Definition 2.7 is also called upon, this is

$$y_d = 0 \implies \lim_{t \rightarrow \infty} (q, p, \tilde{\theta}) = (q^*, 0, \tilde{\theta}^*). \quad (3.12)$$

Now, combining (3.11)-(3.12)

$$\lim_{t \rightarrow \infty} \dot{\bar{H}}_d = 0 \implies \lim_{t \rightarrow \infty} (q, p, \tilde{\theta}) = (q^*, 0, \tilde{\theta}^*). \quad (3.13)$$

Therefore, the closed-loop system (3.8) is asymptotically stable. \square

Remark The use of Proposition 3.1 does not necessarily make $\hat{\theta}$ reach its true value.

3.2 Parameter Uncertainty

Now, a system parameter uncertainty in the system's energy is considered, which does not necessarily affect the system in the control signal channel. The effect of the uncer-

tainty is reflected in the system's total energy as follows

$$\begin{aligned} H_R(q, p) &= \frac{1}{2} p^\top \left(M^{-1}(q) + \Delta_M(q) \right) p + (V(q) + \Delta_V(q)) \\ &= \overbrace{\frac{1}{2} p^\top M^{-1} p}^H + V + \overbrace{\frac{1}{2} p^\top \Delta_M p}^{H_\Delta} + \Delta_V. \end{aligned}$$

The structure of the system with parameter uncertainty is

$$\begin{bmatrix} \dot{q} \\ \dot{p} \end{bmatrix} = \begin{bmatrix} 0 & I_n \\ -I_n & -R \end{bmatrix} \begin{bmatrix} \frac{\partial H}{\partial q} \\ \frac{\partial H}{\partial p} \end{bmatrix} + \begin{bmatrix} 0 & I_n \\ -I_n & -R \end{bmatrix} \begin{bmatrix} \frac{\partial H_\Delta}{\partial q} \\ \frac{\partial H_\Delta}{\partial p} \end{bmatrix} + \begin{bmatrix} 0 \\ G(q) \end{bmatrix} u. \quad (3.14)$$

Since $G(q)$ is not invertible we can no longer directly subtract the uncertainty with the estimation like we did before. Consequently, we perform a momentum transformation, see [61], and apply the same approach as in Proposition 3.1.

Remark Notice that in this case, the friction is taken into consideration in order to be compensated by the adaptive law.

Lemma 3.1 Consider the system (2.7) with the momentum transformation

$$s = T(q)p \in \mathbb{R}^n, \quad (3.15)$$

and the following choice of $T(q)$

$$T(q) = \begin{bmatrix} \left(G(q)^\top G(q) \right)^{-1} G^\top(q) \\ G^\perp(q) \end{bmatrix}, \quad (3.16)$$

where $T(q) \in \mathbb{R}^{n \times n}$ is non-singular. Applying the coordinate transformation (3.15) on the system (2.7) results in

$$\begin{bmatrix} \dot{s} \\ \dot{q} \end{bmatrix} = \begin{bmatrix} E - F & -T \\ T^\top & 0 \end{bmatrix} \begin{bmatrix} \frac{\partial \mathcal{H}}{\partial s} \\ \frac{\partial \mathcal{H}}{\partial q} \end{bmatrix} + \begin{bmatrix} I_m \\ 0_{r \times m} \\ 0_{n \times m} \end{bmatrix} u, \quad r = n - m, \quad (3.17)$$

where

$$\begin{aligned} \mathcal{H}(q, s) &= \frac{1}{2} s^\top \mathcal{M}^{-1}(q) s + V(q), \\ \mathcal{M}^{-1}(q) &= T^{-\top} M^{-1} T^{-1}, \\ E &= \left(\frac{\partial T p}{\partial q} \right)^\top T^\top - T \left(\frac{\partial T p}{\partial q} \right), \end{aligned}$$

$$F = TRT^\top.$$

□

Proof The system's total energy in the new coordinates is given by

$$\mathcal{H}(q, s) = H(q, p) \Big|_{p=T^{-1}s} = \frac{1}{2} s^\top \overbrace{T^{-\top} M^{-1} T^{-1}}^{\mathcal{M}^{-1}} s + V(q) = \frac{1}{2} s^\top \mathcal{M}^{-1} s + V(q).$$

Application of the chain rule for $\mathcal{H}(q, s)$ results in

$$\begin{aligned} \frac{\partial H}{\partial q} &= \frac{\partial \mathcal{H}}{\partial q} + \frac{\partial s}{\partial q} \frac{\partial \mathcal{H}}{\partial s}, \\ \frac{\partial H}{\partial p} &= \frac{\partial q}{\partial p} \frac{\partial \mathcal{H}}{\partial q} + \frac{\partial s}{\partial p} \frac{\partial \mathcal{H}}{\partial s} = T^\top \frac{\partial \mathcal{H}}{\partial s}, \end{aligned}$$

and the system dynamics in the new coordinates

$$\begin{aligned} \dot{q} &= \frac{\partial H}{\partial p} = T^\top \left(\frac{\partial \mathcal{H}}{\partial s} \right), \\ \dot{s} &= \left(\frac{\partial s}{\partial q} \right)^\top \dot{q} + \left(\frac{\partial s}{\partial p} \right)^\top \dot{p} = \left(\frac{\partial s}{\partial q} \right)^\top \dot{q} + T \dot{p} \\ &= \left(\frac{\partial s}{\partial q} \right)^\top \left(\frac{\partial H}{\partial p} \right) - T \left(\frac{\partial H}{\partial q} + R \frac{\partial H}{\partial p} - Gu \right) \\ &= -T \left(\frac{\partial \mathcal{H}}{\partial q} \right) + \underbrace{\left(\left(\frac{\partial s}{\partial q} \right)^\top T^\top - T \left(\frac{\partial s}{\partial q} \right) \right)}_E \frac{\partial \mathcal{H}}{\partial s} - \underbrace{TRT^\top}_F \frac{\partial \mathcal{H}}{\partial s} + TGu, \end{aligned}$$

which expressed in a matrix notation results in (3.17). □

Using the same procedure as in the proof of *Lemma 3.1* we can demonstrate that the system

$$\begin{bmatrix} \dot{q} \\ \dot{p} \end{bmatrix} = \begin{bmatrix} 0 & M^{-1} M_d \\ -M_d M^{-1} & J_2 - R_2 \end{bmatrix} \begin{bmatrix} \frac{\partial \mathcal{H}_d}{\partial q} \\ \frac{\partial \mathcal{H}_d}{\partial p} \end{bmatrix}$$

can be transformed into

$$\begin{bmatrix} \dot{s} \\ \dot{q} \end{bmatrix} = \begin{bmatrix} C - D & -Q^\top \\ \hline Q & 0 \end{bmatrix} \begin{bmatrix} \frac{\partial \mathcal{H}_d}{\partial s} \\ \frac{\partial \mathcal{H}_d}{\partial q} \end{bmatrix}, \quad (3.18)$$

where

$$\begin{aligned}\mathcal{H}_d(q, s) &= \frac{1}{2}s^\top \mathcal{M}_d^{-1}(q)s + V_d(q), \\ \mathcal{M}_d^{-1}(q) &= T^{-\top} M_d^{-1} T^{-1}, \\ Q &= M^{-1} M_d T^\top, \\ C &= \left(\frac{\partial T p}{\partial q} \right)^\top Q - Q^\top \left(\frac{\partial T p}{\partial q} \right) + T J_2 T^\top, \\ D &= T R_2 T^\top.\end{aligned}$$

Lemma 3.2 *The control law resulting from the IDA-PBC technique is independent of the coordinate transformation considered in Lemma 3.1. Besides, the IDA-PBC control law expressed in the new coordinates is*

$$\bar{u}_{ida} = [I_m \quad 0_{m \times r}] \left(-Q^\top \frac{\partial \mathcal{H}_d}{\partial q} + (C - D) \frac{\partial \mathcal{H}_d}{\partial s} - E \frac{\partial \mathcal{H}}{\partial s} + T \frac{\partial \mathcal{H}}{\partial q} \right). \quad (3.19)$$

Proof The standard IDA-PBC control law expressed in the original coordinates is

$$u_{ida} = \left(G^\top G \right)^{-1} G^\top \left(\frac{\partial H}{\partial q} - M_d M^{-1} \frac{\partial H_d}{\partial q} + (J_2 - R_2) \frac{\partial H_d}{\partial p} \right). \quad (3.20)$$

Now, after transforming the nominal and desired systems to the new coordinates, the IDA-PBC methodology is applied and the following equation is obtained

$$T G \bar{u}_{ida} = -Q^\top \frac{\partial \mathcal{H}_d}{\partial q} + (C - D) \frac{\partial \mathcal{H}_d}{\partial s} - E \frac{\partial \mathcal{H}}{\partial s} + T \frac{\partial \mathcal{H}}{\partial q}.$$

Transforming back to the original coordinates we get

$$T G \bar{u}_{ida} = T \frac{\partial H}{\partial q} - T M_d M^{-1} \frac{\partial H_d}{\partial q} + T (J_2 - R_2) \frac{\partial H_d}{\partial p}. \quad (3.21)$$

From (3.20)-(3.21), it is clear that $\bar{u}_{ida} = u_{ida}$. The matching conditions are also equivalent in either coordinates, see Appendix A.1.

Assuming the matching conditions are fulfilled, the IDA-PBC control in the new coordinates is

$$\bar{u}_{ida} = \left(G^\top G \right)^{-1} G^\top T^{-1} \left(-Q^\top \frac{\partial \mathcal{H}_d}{\partial q} + (C - D) \frac{\partial \mathcal{H}_d}{\partial s} - E \frac{\partial \mathcal{H}}{\partial s} + T \frac{\partial \mathcal{H}}{\partial q} \right), \quad (3.22)$$

where the expression for T^{-1} is unknown. After a few calculations, see Appendix A.2, we get

$$T^{-1} = \begin{bmatrix} G & (G^\perp)^\top (G^\perp G^{\perp\top})^{-1} \\ (G^\top G)^{-1} G^\top T^{-1} & 0_{m \times r} \end{bmatrix},$$

which together with (3.22), results in (3.19). \square

Now, going back to the main point of this section, in order to compensate the parameter uncertainty in the system (3.14), the following control law is proposed

$$u = u_{ida} - \Phi(q, p)\hat{\theta}. \quad (3.23)$$

Proposition 3.2 *The system (3.14) with the control law (3.23) and the adaptation law*

$$\dot{\hat{\theta}} = K\Phi^\top G^\top \left(\frac{\partial H_d}{\partial p} \right), \quad (3.24)$$

with constant $\mathbb{R}^{l \times l} \ni K = K^\top \succ 0$, under the condition

$$[0_{r \times m} \ I_r](\varphi_1 - \varphi_2) = 0_r, \quad (3.25)$$

where

$$\begin{aligned} \varphi_1 &= TM_d \Delta_M \left(\frac{\partial H_d}{\partial q} - \left(\frac{\partial T p}{\partial q} \right) T^{-\top} \frac{\partial H_d}{\partial p} \right) + ET^{-\top} \left(\frac{\partial H_\Delta}{\partial p} \right), \\ \varphi_2 &= TR \left(\frac{\partial H}{\partial p} + \frac{\partial H_\Delta}{\partial p} \right) + T \left(\frac{\partial H_\Delta}{\partial q} - \left(\frac{\partial T p}{\partial q} \right) T^{-\top} \frac{\partial H_\Delta}{\partial p} \right), \end{aligned}$$

results in the system

$$\begin{bmatrix} \dot{q} \\ \dot{p} \end{bmatrix} = \begin{bmatrix} 0 & (M^{-1} + \Delta_M)M_d \\ -M_d(M^{-1} + \Delta_M) & L - L^\top + J_2 - R_2 \end{bmatrix} \begin{bmatrix} \frac{\partial H_d}{\partial q} \\ \frac{\partial H_d}{\partial p} \end{bmatrix} - \begin{bmatrix} 0 \\ G(q) \end{bmatrix} \Phi(q, p)\tilde{\theta}, \quad (3.26)$$

where $L = T^{-1}M_d \Delta_M T \left(\frac{\partial T p}{\partial q} \right) T^{-\top}$. The system (3.26) has a stable equilibrium point at $(q^*, 0)$. Additionally, if it is zero-state detectable from its output $y_d = G^\top \left(\frac{\partial H_d}{\partial p} \right)$, then the equilibrium is asymptotically stable.

The matrix of known functions $\Phi(q, p)$ is given by

$$\Phi\theta = [I_m \ 0_{m \times r}](\varphi_1 - \varphi_2) \quad (3.27)$$

where θ contains the true values of the uncertainties R , Δ_M and Δ_V as coefficients of (3.27).

Proof The mechanical system with parameter uncertainty (3.14) in the new coordinates using Lemma 3.1 is

$$\begin{bmatrix} \dot{s} \\ \dot{q} \end{bmatrix} = \begin{bmatrix} E - F & -T \\ T^\top & 0 \end{bmatrix} \begin{bmatrix} \frac{\partial \mathcal{H}}{\partial s} \\ \frac{\partial \mathcal{H}}{\partial q} \end{bmatrix} + \begin{bmatrix} E - F & -T \\ T^\top & 0 \end{bmatrix} \begin{bmatrix} \frac{\partial \mathcal{H}_\Delta}{\partial s} \\ \frac{\partial \mathcal{H}_\Delta}{\partial q} \end{bmatrix} + \begin{bmatrix} I_m \\ 0_{r \times m} \\ 0_{n \times m} \end{bmatrix} u.$$

Additionally, the system is decomposed as follows

$$\begin{bmatrix} \dot{s} \\ \dot{q} \end{bmatrix} = \overbrace{\begin{bmatrix} E & -T \\ T^\top & 0 \end{bmatrix} \begin{bmatrix} \frac{\partial \mathcal{H}}{\partial s} \\ \frac{\partial \mathcal{H}}{\partial q} \end{bmatrix}}^f + \overbrace{\begin{bmatrix} -F \frac{\partial \mathcal{H}}{\partial s} \\ 0_n \end{bmatrix}}^\delta + \overbrace{\begin{bmatrix} E - F & -T \\ T^\top & 0 \end{bmatrix} \begin{bmatrix} \frac{\partial \mathcal{H}_\Delta}{\partial s} \\ \frac{\partial \mathcal{H}_\Delta}{\partial q} \end{bmatrix}}^\delta + \begin{bmatrix} I_m \\ 0_{r \times m} \\ 0_{n \times m} \end{bmatrix} u, \quad (3.28)$$

where $f = [f_1, f_2]^\top$, $f_1 \in \mathbb{R}^m$, $f_2 \in \mathbb{R}^{2n-m}$, $\delta = [\delta_1, \delta_2]^\top$, $\delta_1 \in \mathbb{R}^m$, $\delta_2 \in \mathbb{R}^{2n-m}$ and the desired system is expressed as

$$\begin{bmatrix} \dot{s} \\ \dot{q} \end{bmatrix} = \overbrace{\begin{bmatrix} C - D & -Q^\top \\ Q & 0 \end{bmatrix} \begin{bmatrix} \frac{\partial \mathcal{H}_d}{\partial s} \\ \frac{\partial \mathcal{H}_d}{\partial q} \end{bmatrix}}^{\bar{f}}, \quad (3.29)$$

where $\bar{f} = [\bar{f}_1, \bar{f}_2]^\top$, $\bar{f}_1 \in \mathbb{R}^m$. The control law is designed so that the nominal system in (3.28) becomes (3.29), and the remaining part is compensated by the adaptive control law (3.24). Hence the chosen control law is

$$u = \bar{f}_1 - f_1 - \underbrace{\hat{\delta}_1}_{-\Phi \hat{\theta}} - \hat{\psi}_1, \quad (3.30)$$

where $\hat{\delta}_1$ and $\hat{\psi}_1$ are the estimates of δ_1 and $\psi_1 = [I_m \ 0_{m \times r}] T M_d \Delta_M \left(\frac{\partial \mathcal{H}_d}{\partial q} \right)$, respectively. Using Lemma 3.2, it can be shown that

$$\bar{f}_1 - f_1 = [I_m \ 0_{m \times r}] \left(-Q^\top \frac{\partial \mathcal{H}_d}{\partial q} + (C - D) \frac{\partial \mathcal{H}_d}{\partial s} - E \frac{\partial \mathcal{H}}{\partial s} + T \frac{\partial \mathcal{H}}{\partial q} \right) = u_{ida}.$$

Therefore (3.30) is equivalent to (3.23). The control law (3.30) transforms (3.28) into

$$\begin{aligned} \begin{bmatrix} \dot{s} \\ \dot{q} \end{bmatrix} &= \begin{bmatrix} f_1 \\ f_2 \end{bmatrix} + \begin{bmatrix} \delta_1 \\ \delta_2 \end{bmatrix} + \begin{bmatrix} \bar{f}_1 - f_1 - \hat{\delta}_1 - \hat{\psi}_1 \\ 0 \end{bmatrix} = \begin{bmatrix} \bar{f}_1 \\ f_2 \end{bmatrix} - \begin{bmatrix} \hat{\delta}_1 - \delta_1 + \hat{\psi}_1 \\ \delta_2 \end{bmatrix} \\ &= \begin{bmatrix} C - D & -Q^\top \\ Q & 0 \end{bmatrix} \begin{bmatrix} \frac{\partial \mathcal{H}_d}{\partial s} \\ \frac{\partial \mathcal{H}_d}{\partial q} \end{bmatrix} \\ &\quad + \begin{bmatrix} -F \frac{\partial \mathcal{H}}{\partial s} - F \frac{\partial \mathcal{H}_\Delta}{\partial s} + E \frac{\partial \mathcal{H}_\Delta}{\partial s} - T \frac{\partial \mathcal{H}_\Delta}{\partial q} \\ T^\top \left(\frac{\partial \mathcal{H}_\Delta}{\partial s} \right) \end{bmatrix} - \begin{bmatrix} \hat{\delta}_1 + \hat{\psi}_1 \\ 0_r \\ 0_n \end{bmatrix}. \end{aligned} \quad (3.31)$$

From (3.31), it is easy to note that, theoretically, the term $T^\top \left(\frac{\partial \mathcal{H}_\Delta}{\partial s} \right)$ should be imposed to be zero because it is not located in the channel of the adaptation (the first m rows of (3.31)). However, through the following manipulation

$$\begin{aligned} T^\top \left(\frac{\partial \mathcal{H}_\Delta}{\partial s} \right) &= T^\top \left(T^{-\top} \Delta_M T^{-1} s \right) = \Delta_M T^{-1} \mathcal{M}_d \mathcal{M}_d^{-1} s = \Delta_M T^{-1} \mathcal{M}_d \left(\frac{\partial \mathcal{H}_d}{\partial s} \right) \\ &= \Delta_M \mathcal{M}_d T^\top \left(\frac{\partial \mathcal{H}_d}{\partial s} \right), \end{aligned}$$

it can be inserted in the nominal desired system generating, once again, a port-Hamiltonian system

$$\begin{aligned} \begin{bmatrix} \dot{s} \\ \dot{q} \end{bmatrix} &= \begin{bmatrix} C - D & -Q^\top - T \mathcal{M}_d \Delta_M \\ Q + \Delta_M \mathcal{M}_d T^\top & 0 \end{bmatrix} \begin{bmatrix} \frac{\partial \mathcal{H}_d}{\partial s} \\ \frac{\partial \mathcal{H}_d}{\partial q} \end{bmatrix} \\ &\quad + \begin{bmatrix} T \mathcal{M}_d \Delta_M \frac{\partial \mathcal{H}_d}{\partial q} - F \frac{\partial \mathcal{H}}{\partial s} - F \frac{\partial \mathcal{H}_\Delta}{\partial s} + E \frac{\partial \mathcal{H}_\Delta}{\partial s} - T \frac{\partial \mathcal{H}_\Delta}{\partial q} \\ 0_n \end{bmatrix} - \begin{bmatrix} \hat{\delta}_1 + \hat{\psi}_1 \\ 0_r \\ 0_n \end{bmatrix}. \end{aligned} \quad (3.32)$$

Now, in order to adapt the closed-loop system (3.32), a condition that the uncertainties outside the PH system have to be located in the actuated channel is stated. This is

$$[0_{r \times m} \ I_r] \left(T \mathcal{M}_d \Delta_M \frac{\partial \mathcal{H}_d}{\partial q} - F \frac{\partial \mathcal{H}}{\partial s} - F \frac{\partial \mathcal{H}_\Delta}{\partial s} + E \frac{\partial \mathcal{H}_\Delta}{\partial s} - T \frac{\partial \mathcal{H}_\Delta}{\partial q} \right) = 0_r. \quad (3.33)$$

Once the condition (3.33) is satisfied, (3.32) becomes

$$\begin{bmatrix} \dot{s} \\ \dot{q} \end{bmatrix} = \begin{bmatrix} C - D & -Q^\top - T \mathcal{M}_d \Delta_M \\ Q + \Delta_M \mathcal{M}_d T^\top & 0 \end{bmatrix} \begin{bmatrix} \frac{\partial \mathcal{H}_d}{\partial s} \\ \frac{\partial \mathcal{H}_d}{\partial q} \end{bmatrix} - \begin{bmatrix} \hat{\delta}_1 + \hat{\psi}_1 - \delta_1 - \psi_1 \\ 0 \\ 0 \end{bmatrix},$$

which can equivalently be rewritten as

$$\begin{bmatrix} \dot{s} \\ \dot{q} \end{bmatrix} = \begin{bmatrix} C - D & -Q^\top - TM_d\Delta_M \\ Q + \Delta_M M_d T^\top & 0 \end{bmatrix} \begin{bmatrix} \frac{\partial H_d}{\partial s} \\ \frac{\partial H_d}{\partial q} \end{bmatrix} - \begin{bmatrix} TG \\ 0 \end{bmatrix} \Phi \tilde{\theta}. \quad (3.34)$$

Stability. Calculations to establish the stability of (3.34) can be performed in either pair of coordinates. In this case, they will be performed in the original coordinates. Transforming back (3.34) to the original coordinates yields the system (3.26). In this case, since the parameter uncertainties are considered to be time-independent, the system (3.26) is autonomous. Therefore, to prove stability, Theorem 2.1 is invoked.

A new total energy function is defined as

$$\bar{H}_d(q, p, \tilde{\theta}) = H_d(q, p) - H_d(q^*, 0) + \frac{1}{2} \tilde{\theta}^\top K^{-1} \tilde{\theta}.$$

Similar to Proposition 3.1, the addition of $H_d(q^*, 0)$ is made to ensure that $\bar{H}_d > 0$ and therefore be a suitable Lyapunov candidate. To demonstrate that \bar{H}_d is in fact a Lyapunov function, its time derivative is calculated

$$\begin{aligned} \dot{\bar{H}}_d &= \left(\frac{\partial H_d}{\partial q} \right)^\top \dot{q} + \left(\frac{\partial H_d}{\partial p} \right)^\top \dot{p} + \dot{\tilde{\theta}}^\top K^{-1} \tilde{\theta} \\ &= \left(\frac{\partial H_d}{\partial q} \right)^\top (M^{-1} + \Delta_M) M_d \left(\frac{\partial H_d}{\partial p} \right) \\ &\quad + \left(\frac{\partial H_d}{\partial p} \right)^\top \left(-M_d (M^{-1} + \Delta_M) \left(\frac{\partial H_d}{\partial q} \right) + (L - L^\top + J_2 - R_2) \left(\frac{\partial H_d}{\partial p} \right) \right) \\ &\quad - \left(\frac{\partial H_d}{\partial p} \right)^\top G \Phi \tilde{\theta} + \dot{\tilde{\theta}}^\top K^{-1} \tilde{\theta} \\ &= - \left(\frac{\partial H_d}{\partial p} \right)^\top R_2 \left(\frac{\partial H_d}{\partial p} \right) + \left(\dot{\tilde{\theta}}^\top K^{-1} - \left(\frac{\partial H_d}{\partial p} \right)^\top G \Phi \right) \tilde{\theta} \end{aligned} \quad (3.35)$$

$$= - \left(\frac{\partial H_d}{\partial p} \right)^\top G K_v G^\top \left(\frac{\partial H_d}{\partial p} \right) \leq -\lambda_{\min}\{K_v\} \|y_d(t)\|^2 \leq 0. \quad (3.36)$$

Since the value of θ is unknown, the term containing $\tilde{\theta}$ in (3.35) is required to be canceled, this is accomplished by selecting a suitable $\dot{\tilde{\theta}}$ and using the fact that $\dot{\tilde{\theta}} = \dot{\hat{\theta}}$, thus originating the adaptive law (3.24). From (3.36) it's clear that \bar{H}_d is a Lyapunov function, therefore $(q^*, 0)$ is a stable equilibrium of (3.26).

Asymptotic stability. Rearranging (3.34) together with (3.24) in order to obtain the following port-Hamiltonian system

$$\begin{bmatrix} \dot{q} \\ \dot{p} \\ \dot{\tilde{\theta}} \end{bmatrix} = \begin{bmatrix} 0 & (M^{-1} + \Delta_M)M_d & 0 \\ -M_d(M^{-1} + \Delta_M) & L - L^\top + J_2 - GK_vG^\top & -G\Phi K \\ 0 & K\Phi^\top G^\top & 0 \end{bmatrix} \begin{bmatrix} \frac{\partial \bar{H}_d}{\partial q} \\ \frac{\partial \bar{H}_d}{\partial p} \\ \frac{\partial \bar{H}_d}{\partial \tilde{\theta}} \end{bmatrix}. \quad (3.37)$$

The rearrangement yields a bigger system whose coordinates are now $(q, p, \tilde{\theta})$.

To prove asymptotic stability, the Barbashin-Krasovskii Theorem 2.3 is invoked and from it, the following is implied

$$\dot{\bar{H}}_d \leq -\lambda_{\min}\{K_v\}\|y_d(t)\|^2 = 0 \implies y_d = 0. \quad (3.38)$$

However, in order to satisfy the previous theorem it is required that $\dot{\bar{H}}_d = 0$ implies $(q, p, \tilde{\theta}) = (q^*, 0, \tilde{\theta}^*)$. To achieve that, the zero-state detectability condition is called upon, this is

$$y_d = 0 \implies \lim_{t \rightarrow \infty} (q, p, \tilde{\theta}) = (q^*, 0, \tilde{\theta}^*) \quad (3.39)$$

Now, combining (3.38)-(3.39) it is clear that $\dot{\bar{H}}_d = 0 \implies (q, p, \tilde{\theta}) = (q^*, 0, \tilde{\theta}^*)$. Therefore the Barbashin-Krasovskii Theorem 2.3 is applicable and the closed-loop system (3.37) is asymptotically stable. \square

Fulfilling the condition imposed in Proposition 3.2 as was stated can be tedious or even not possible. However, it can be relaxed by requiring each element of φ_1 and φ_2 to be 0_r . This leads to

$$[0_{r \times m} \quad I_r] T M_d \Delta_M \left(\frac{\partial H_d}{\partial q} - \left(\frac{\partial T p}{\partial q} \right) T^{-\top} \frac{\partial H_d}{\partial p} \right) = 0_r$$

$$[0_{r \times m} \quad I_r] T R \left(\frac{\partial H}{\partial p} \right) = 0_r$$

$$[0_{r \times m} \quad I_r] T R \left(\frac{\partial H_\Delta}{\partial p} \right) = 0_r$$

$$[0_{r \times m} \quad I_r] E T^{-\top} \left(\frac{\partial H_\Delta}{\partial p} \right) = 0_r$$

$$[0_{r \times m} \quad I_r] T \left(\frac{\partial H_\Delta}{\partial q} - \left(\frac{\partial T p}{\partial q} \right) T^{-\top} \frac{\partial H_\Delta}{\partial p} \right) = 0_r$$

Remark Proposition 3.2 does not guarantee that $\hat{\theta}$ reaches its true values.

Chapter 4

Adaptive IDA-PBC Application: Inertia Wheel Inverted Pendulum

In this chapter, the well-known IWIP system will be used to study its response against the uncertainties addressed in Chapter 3. The IWIP system will be subject to the control law resulting from the standard IDA-PBC technique, namely (2.20), plus the adaptive IDA-PBC control law resulting from Propositions 3.1 to 3.2, and then the response to each control law will be analyzed to verify the validity of the propositions. Before reaching the simulations stage, some previous calculations have to be performed. These calculations will be presented in the following subsections.

4.1 IWIP Model

Figure 4.1 shows a schematic of the IWIP system.

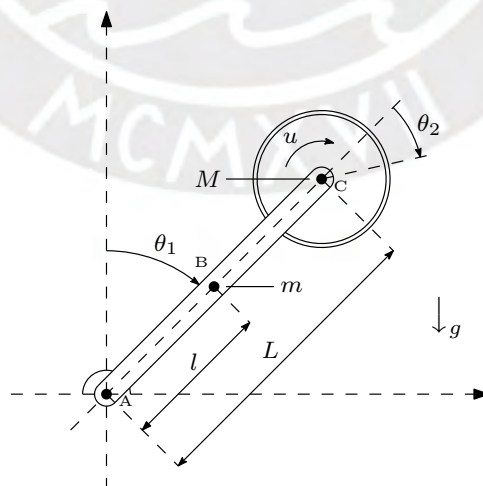


Figure 4.1. – IWIP system.

4. Adaptive IDA-PBC Application: Inertia Wheel Inverted Pendulum

Table 4.1 shows the IWIP system's parameters. The IWIP's dynamics are obtained

Parameter	Description	Units
θ_1	Pendulum angle with respect to the vertical axis	rad
θ_2	Wheel angle with respect to the pendulum axis	rad
m	Pendulum mass	kg
M	Wheel mass	kg
l	Length from pendulum base (A) to its center of mass (B)	m
L	Pendulum length: (A) to (C)	m
I_A	Pendulum moment of inertia around (A)	kg · m ²
I_2	Wheel moment of inertia around (C)	kg · m ²
g	Gravity constant	m/s ²

Table 4.1. – IWIP system's parameters.

using Newton's second law of motion (derived from [33])

$$u = I_2(\ddot{\theta}_1 + \ddot{\theta}_2) + r_2\dot{\theta}_2,$$

$$MgL \sin(\theta_1) + mgl \sin(\theta_1) - u = I_A\ddot{\theta}_1 + ML^2\ddot{\theta}_1 + r_1\dot{\theta}_1.$$

Equivalently, the motion equations can be expressed as

$$\begin{bmatrix} I_1 + I_2 & I_2 \\ I_2 & I_2 \end{bmatrix} \begin{bmatrix} \ddot{\theta}_1 \\ \ddot{\theta}_2 \end{bmatrix} - \begin{bmatrix} bg \sin(\theta_1) \\ 0 \end{bmatrix} + \overbrace{\begin{bmatrix} r_1 & 0 \\ 0 & r_2 \end{bmatrix}}^{\bar{R}} \begin{bmatrix} \dot{\theta}_1 \\ \dot{\theta}_2 \end{bmatrix} = \begin{bmatrix} 0 \\ 1 \end{bmatrix} u, \quad (4.1)$$

$$I_1 = I_A + ML^2, \quad b = ML + ml.$$

A coordinate transformation is done to obtain a simple representation of (4.1), that is

$$q = T_1\theta, \quad T_1 = \begin{bmatrix} 1 & 0 \\ 1 & 1 \end{bmatrix}.$$

Additionally, the system (4.1) is pre-multiplied by $T_1^{-\top}$ to achieve a symmetric inertia matrix. The resulting system is

$$\overbrace{\begin{bmatrix} I_1 & 0 \\ 0 & I_2 \end{bmatrix}}^M \begin{bmatrix} \ddot{q}_1 \\ \ddot{q}_2 \end{bmatrix} - \begin{bmatrix} bg \sin(q_1) \\ 0 \end{bmatrix} + \overbrace{\begin{bmatrix} r_1 + r_2 & -r_2 \\ -r_2 & r_2 \end{bmatrix}}^R \begin{bmatrix} \dot{q}_1 \\ \dot{q}_2 \end{bmatrix} = \overbrace{\begin{bmatrix} -1 \\ 1 \end{bmatrix}}^G u. \quad (4.2)$$

4. Adaptive IDA-PBC Application: Inertia Wheel Inverted Pendulum

Expressing (4.2) in Port-Hamiltonian representation yields

$$\begin{bmatrix} \dot{q} \\ \dot{p} \end{bmatrix} = \begin{bmatrix} 0 & I_n \\ -I_n & -R \end{bmatrix} \begin{bmatrix} \frac{\partial H}{\partial q} \\ \frac{\partial H}{\partial p} \end{bmatrix} + \begin{bmatrix} 0 \\ G \end{bmatrix} u, \quad (4.3)$$

where

$$\begin{aligned} H &= \frac{1}{2} p^\top M^{-1} p + V(q), \\ &= \frac{1}{2} p^\top M^{-1} p + bg(\cos(q_1) + 1). \end{aligned}$$

4.2 Standard IDA- PBC

In this section, it is considered that the nominal system (4.3) has no friction, i.e., $R = 0$. The target PH system is

$$\begin{aligned} \begin{bmatrix} \dot{q} \\ \dot{p} \end{bmatrix} &= \begin{bmatrix} 0 & M^{-1} M_d \\ -M_d M^{-1} & J_2 - G K_v G^\top \end{bmatrix} \begin{bmatrix} \frac{\partial H_d}{\partial q} \\ \frac{\partial H_d}{\partial p} \end{bmatrix}, \\ y_d &= G^\top \frac{\partial H_d}{\partial p}, \end{aligned} \quad (4.4)$$

where $M_d = M_d^\top \succ \rho I$ for some $\rho \in \mathbb{R}^+$, $J_2 = -J_2^\top$, $K_v = K_v^\top \succ 0$ and

$$H_d = \frac{1}{2} p^\top M_d^{-1} p + V_d(q).$$

The desired equilibrium is the pendulum upward position ($q_1^* = 0$). Moreover, just as mentioned in [33], since the disk is symmetric there is no particular reason to choose q_2^* aligned with q_1^* . However, it is chosen $q_2^* = 0$ to prove the generality of the IDA-PBC technique.

As described in Chapter 2, there are two main steps to carry out in order to obtain the IDA-PBC controller. These steps will be developed in the next subsections.

4.2.1 Energy Shaping

Since the inertia matrix M is constant we choose M_d to be constant as well, that is

$$M_d = \begin{bmatrix} m_1 & m_2 \\ m_2 & m_3 \end{bmatrix}.$$

The desired inertia matrix M_d has to fulfill a positive definiteness condition. Hence, the following inequalities must hold: $m_1 > 0$, $m_1 m_3 - m_2^2 > 0$. From the PDE

4. Adaptive IDA-PBC Application: Inertia Wheel Inverted Pendulum

corresponding to the kinetic energy

$$G^\perp \left\{ \frac{\partial p^\top M^{-1} p}{\partial q} - M_d M^{-1} \left(\frac{\partial p^\top M_d^{-1} p}{\partial q} \right) + 2J_2 \frac{\partial H_d}{\partial p} \right\} = 0,$$

it is concluded that $J_2 = 0$. The remaining PDE is the only one that needs to be solved, this is

$$G^\perp \left\{ \frac{\partial V}{\partial q} - M_d M^{-1} \frac{\partial V_d}{\partial q} \right\} = 0.$$

For the IWIP system we have

$$G^\perp = \begin{bmatrix} 1 & 1 \end{bmatrix}, \quad \frac{\partial V}{\partial q} = \begin{bmatrix} -bg \sin(q_1) \\ 0 \end{bmatrix}.$$

The PDE to be solved is

$$\left(\frac{m_1 + m_2}{I_1} \right) \frac{\partial V_d}{\partial q_1} + \left(\frac{m_2 + m_3}{I_2} \right) \frac{\partial V_d}{\partial q_2} = -bg \sin(q_1),$$

which is computed in MAPLE to get the following solution

$$V_d = \frac{bg \cos(q_1) I_1}{m_1 + m_2} + \alpha(\beta(q)),$$

$$\beta(q) = \frac{(m_1 + m_2) I_2 q_2 - (m_2 + m_3) I_1 q_1}{(m_1 + m_2) I_2} = q_2 - \overbrace{\frac{I_1 (m_2 + m_3)}{I_2 (m_1 + m_2)}}^{\gamma_2} q_1,$$

where $\alpha(\beta(q))$ is an arbitrary function that has to be chosen such that the condition $q^* = \arg \min V_d(q)$ is fulfilled. The necessary conditions to verify that $V_d(q)$ has an isolated minimum at q^* are

$$\left. \frac{\partial V_d}{\partial q} \right|_{q^*} = 0, \quad \left. \frac{\partial^2 V_d}{\partial q^2} \right|_{q^*} > 0.$$

The first condition yields

$$\left. \frac{\partial V_d}{\partial q} \right|_{q^*} = \left[-\frac{abg \sin(q_1)}{m_1 + m_2} + \frac{\partial \alpha}{\partial \beta} \frac{\partial \beta}{\partial q_1} \quad \frac{\partial \alpha}{\partial \beta} \frac{\partial \beta}{\partial q_2} \right]^\top \Big|_{q^*} = \left[\frac{\partial \alpha}{\partial \beta} \gamma_2 \quad \frac{\partial \alpha}{\partial \beta} \right]^\top = 0. \quad (4.5)$$

4. Adaptive IDA-PBC Application: Inertia Wheel Inverted Pendulum

From (4.5), in order to fulfill the first condition then $\frac{\partial \alpha}{\partial \beta} \Big|_{q^*} = 0$. For the second condition the following is obtained

$$\frac{\partial^2 V_d}{\partial q^2} \Big|_{q^*} = \left[\begin{array}{cc} -\frac{abg \cos(q_1)}{m_1+m_2} + \frac{\partial^2 \alpha}{\partial \beta^2} \left(\frac{\partial \beta}{\partial q_1} \right)^2 & \frac{\partial^2 \alpha}{\partial \beta^2} \frac{\partial \beta}{\partial q_2} \frac{\partial \beta}{\partial q_1} \\ \frac{\partial^2 \alpha}{\partial \beta^2} \frac{\partial \beta}{\partial q_2} \frac{\partial \beta}{\partial q_1} & \frac{\partial^2 \alpha}{\partial \beta^2} \end{array} \right] \Big|_{q^*} > 0. \quad (4.6)$$

From (4.6), $\frac{\partial^2 \alpha}{\partial \beta^2} \Big|_{q^*} > 0$ and $m_1 < -m_2$ must be satisfied. A possible choice of the arbitrary function that satisfies those conditions is $\alpha = \frac{K_1}{2} \beta^2$ [33], where $K_1 > 0$ is an adjustable gain.

At this point, the energy shaping control law u_{es} can be calculated

$$\begin{aligned} u_{es} &= \left(G^\top G \right)^{-1} G^\top \left(\frac{\partial V}{\partial q} - M_d M^{-1} \frac{\partial V_d}{\partial q} \right) \\ &= \underbrace{\frac{m_2 b g}{m_1 + m_2}}_{\gamma_1} \sin(q_1) - \underbrace{\frac{K_1 (m_1 m_3 - m_2^2)}{I_2 (m_1 + m_2)}}_{K_p} (q_2 + \gamma_2 q_1). \end{aligned}$$

After a few calculations and using the previous conditions, it is possible to show the permissible region of the gains in u_{es} , that is

$$\gamma_1 > b g, \quad K_p > 0, \quad \gamma_2 > 0.$$

4.2.2 Damping Injection

The damping injection term is

$$u_{di} = -K_v G^\top \frac{\partial H_d}{\partial p},$$

where $K_v > 0$ is a gain. The passive output, which is a part of u_{di} , expressed in terms of the desired inertia matrix elements is

$$G^\top \frac{\partial H_d}{\partial p} = \frac{1}{m_1 m_3 - m_2^2} ((m_1 + m_2) p_2 - (m_2 + m_3) p_1) = \underbrace{\frac{I_2 (m_1 + m_2)}{m_1 m_3 - m_2^2}}_{K_2} (\dot{q}_2 + \gamma_2 \dot{q}_1),$$

where $K_2 = -\frac{K_1}{K_p} < 0$.

In order to guarantee the asymptotic stability of the system, it is required to prove at least that the system (4.4) is zero-state detectable from the output y_d .

4.2.3 Zero-State Detectability

The zero-state detectability condition initially assumes that the output is zero, that is

$$y_d = G^\top \frac{\partial H_d}{\partial p} \equiv 0 \implies K_2(\dot{q}_2 + \dot{q}_1 \gamma_2) \equiv 0 \implies \dot{q}_2 = -\dot{q}_1 \gamma_2 \quad (4.7)$$

The desired system is represented by (4.4). From (4.4) together with (4.7), it is known that

$$\begin{aligned} \dot{p} &= -M_d M^{-1} \frac{\partial H_d}{\partial q} - GK_v \overbrace{G^\top \frac{\partial H_d}{\partial p}}^0 = -M_d M^{-1} \frac{\partial H_d}{\partial q} \\ &= \begin{bmatrix} -m_1 f(q) - m_2 g(q) \\ -m_2 f(q) - m_3 g(q) \end{bmatrix}, \end{aligned} \quad (4.8)$$

where

$$f(q) = \frac{1}{I_1} \left(-\frac{I_1 b g \sin(q_1)}{m_1 + m_2} + K_1 (q_1 \gamma_2 + q_2) \gamma_2 \right), \quad g(q) = \frac{K_1 (q_1 \gamma_2 + q_2)}{I_2}. \quad (4.9)$$

From (4.7), we know that $\dot{q}_2 = -\dot{q}_1 \gamma_2$, $\ddot{q}_2 = -\ddot{q}_1 \gamma_2$ and $q_2 + q_1 \gamma_2 = \text{const.}$ We now perform algebraic operations to the elements of \dot{p} in order to achieve $\ddot{q}_2 + \ddot{q}_1 \gamma_2 = 0$, that is

$$\ddot{q}_2 + \ddot{q}_1 \gamma_2 = \frac{\dot{p}_2}{I_2} + \frac{\dot{p}_1 \gamma_2}{I_1} = Z_1 \sin(q_1) + \overbrace{Z_2 (q_2 + q_1 \gamma_2)}^{\text{const.}} = 0, \quad (4.10)$$

where

$$\begin{aligned} Z_1 &= \frac{b g (I_2 m_1 \gamma_2 + I_1 m_2)}{I_1 (m_1 + m_2) I_2} = \text{const.} \\ Z_2 &= -\frac{K_1 (I_2^2 m_2 \gamma_2^2 + 2 I_2 I_1 m_2 \gamma_2 + I_1^2 m_3)}{I_1^2 I_2^2} = \text{const.} \end{aligned} \quad (4.11)$$

From (4.10), we know that $Z_1 \sin(q_1)$ has to be also constant, thus:

$$\sin(q_1) = \text{const.} \implies q_1 = \text{const.} \implies q_2 = \text{const.} \implies \dot{q}_1 = \dot{q}_2 = 0 \implies \dot{p} = 0. \quad (4.12)$$

From (4.8) and (4.12), we get

$$f(q) = -\frac{m_2}{m_1} g(q) = -\frac{m_3}{m_2} g(q). \quad (4.13)$$

The only solution for (4.13) is

$$f(q) = g(q) = 0 \implies q_2 + q_1 \gamma_2 = 0 \implies \sin(q_1) = 0 \implies q_1 = q_2 = 0 \quad \forall q_1 \in \langle -\pi, \pi \rangle.$$

4. Adaptive IDA-PBC Application: Inertia Wheel Inverted Pendulum

Based on all the performed calculations, it has been proven that the target PH system (4.4) satisfies the stronger condition for asymptotic stability, that is, zero-state observability instead of zero-state detectability.

All the terms required in the design of the IDA-PBC controller have been calculated and now it can be presented

$$u_{ida} = \gamma_1 \sin(q_1) + K_p(q_2 + \gamma_2 q_1) - K_v K_2(\dot{q}_2 + \gamma_2 \dot{q}_1). \quad (4.14)$$

Alternatively, (4.14) can be rewritten in terms of q and p

$$u_{ida} = \gamma_1 \sin(q_1) + k_1 q_1 + k_2 q_2 + k_3 p_1 + k_4 p_2, \quad (4.15)$$

where

$$k_1 = K_p \gamma_2, \quad k_2 = K_p, \quad k_3 = -\frac{K_v K_2 \gamma_2}{I_1}, \quad k_4 = -\frac{K_v K_2}{I_2}. \quad (4.16)$$

The basic values for this gains together with IWIP system's parameters values were taken from [50]. Some of the gains were slightly modified because they do not exactly satisfy the relationships between (4.14) and (4.15). The main values used in this work are

$$\begin{aligned} \gamma_1 &= 6.1284, & \gamma_2 &= 542.447, & K_p &= 0.0011, \\ K_v &= 1.98, & K_1 &= 10^{-6}, & K_2 &= -9.0909 \times 10^{-4}, \end{aligned}$$

which together with the IWIP's parameters stated in Table 4.2 lead to the controller

Parameter	Value
m	3.228 kg
M	330.81×10^{-3} kg
l	60×10^{-3} m
L	44×10^{-3} m
I_A	43.0×10^{-3} kg · m ²
I_2	417.6×10^{-6} kg · m ²
g	9.81 m/s ²

Table 4.2. – IWIP system's parameters values.

gains

$$\begin{aligned} k_1 &= 0.5967, & k_2 &= 0.0011, \\ k_3 &= 22.3632, & k_4 &= 4.3103. \end{aligned}$$

4. Adaptive IDA-PBC Application: Inertia Wheel Inverted Pendulum

Below are shown the simulations for the IWIP's system response subject to the standard IDA-PBC control law (4.15) starting at the initial coordinates $[q^\top(0), p^\top(0)]^\top = [0.2 \ 0 \ 0 \ 0]^\top$. It is clear from Figures 4.2 to 4.4, that the IDA-PBC control law u_{ida} asymptotically stabilizes the IWIP system.

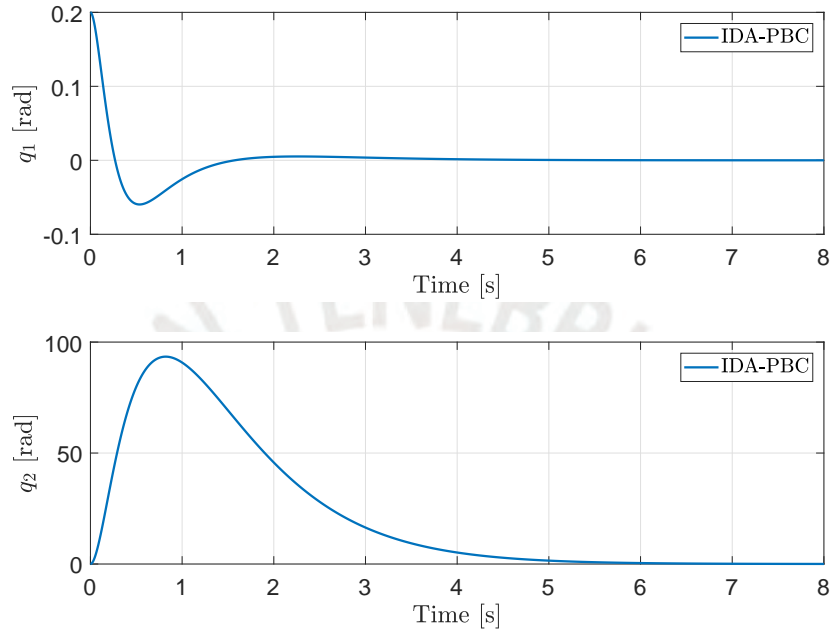


Figure 4.2. – Simulation 1: Evolution of q over time.

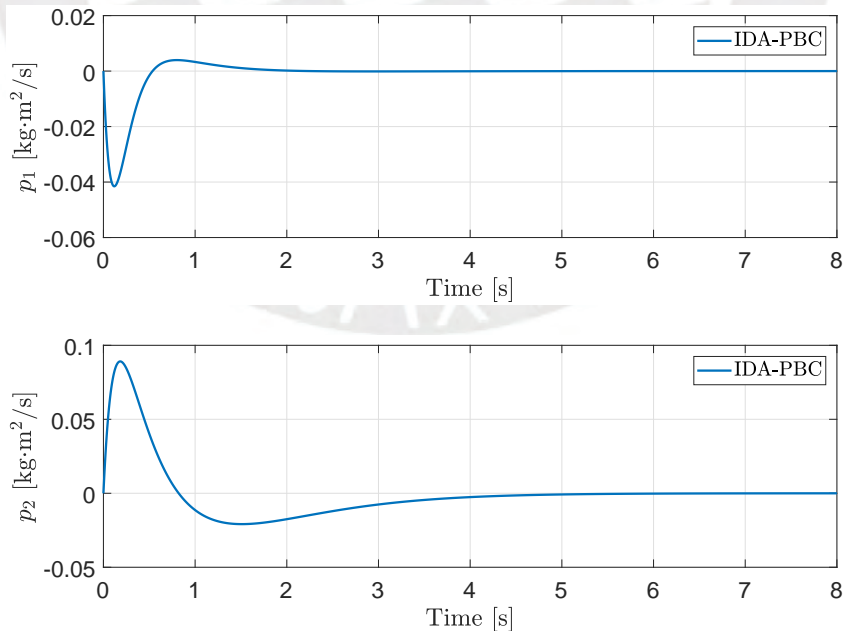


Figure 4.3. – Simulation 1: Evolution of p over time.

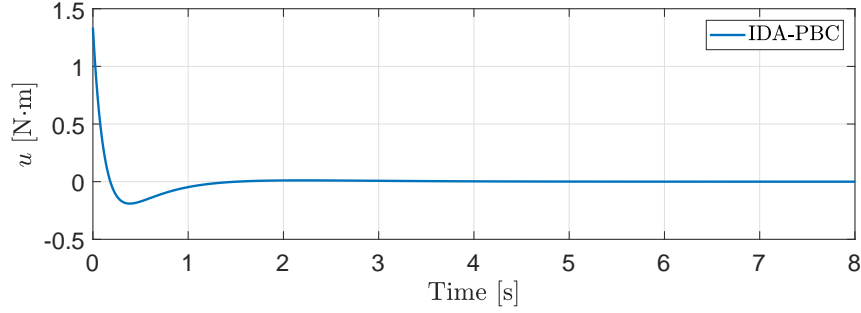


Figure 4.4. – Simulation 1: Evolution of u over time.

4.3 Simulation for Input Uncertainty

In this section, an input uncertainty will be considered to analyze the system response using the adaptive control law stated in Proposition 3.1 and then compare it to the response produced by the standard IDA-PBC control law. For this simulation, assuming $R = 0$, the input control uncertainty is expressed as follows

$$\begin{bmatrix} \dot{q} \\ \dot{p} \end{bmatrix} = \begin{bmatrix} 0 & I_n \\ -I_n & 0 \end{bmatrix} \begin{bmatrix} \frac{\partial H}{\partial q} \\ \frac{\partial H}{\partial p} \end{bmatrix} + \begin{bmatrix} 0 \\ G(q) \end{bmatrix} (u + A \sin(t)). \quad (4.17)$$

From (4.17), it is easy to note that

$$\Phi = \sin(t), \quad \theta = A.$$

Let us recall that to prove asymptotic stability of the system (4.17) using the Proposition 3.1 with the control law (3.2), it is required to prove zero-state detectability.

4.3.1 Zero-State Detectability

The assumption (4.7) keeps applying to this case. The target PH system (3.3) together with the adaptive law (3.4) is represented by

$$\begin{bmatrix} \dot{q} \\ \dot{p} \\ \dot{\tilde{\theta}} \end{bmatrix} = \begin{bmatrix} 0 & M^{-1}M_d & 0 \\ -M_dM^{-1} & -GK_vG^\top & -G\Phi K \\ 0 & K\Phi^\top G^\top & 0 \end{bmatrix} \begin{bmatrix} \frac{\partial \bar{H}_d}{\partial q} \\ \frac{\partial \bar{H}_d}{\partial p} \\ \frac{\partial \bar{H}_d}{\partial \tilde{\theta}} \end{bmatrix}, \quad (4.18)$$

where

$$\bar{H}_d = H_d + \frac{1}{2} \tilde{\theta}^\top K^{-1} \tilde{\theta}. \quad (4.19)$$

4. Adaptive IDA-PBC Application: Inertia Wheel Inverted Pendulum

It is clear that there is no need to include in \bar{H}_d the term that was previously included in the proof of Proposition 3.1 to ensure that $\bar{H}_d > 0$, since it was just a formalism to be able to apply Lyapunov's stability theory, plus, it makes no difference when calculating the partial derivatives of \bar{H}_d . From (4.18), the following is obtained

$$\begin{aligned}\dot{\tilde{\theta}} &= K\Phi^\top \overbrace{G^\top \frac{\partial H_d}{\partial p}}^0 = 0 \rightarrow \tilde{\theta} = \text{const.}, \\ \dot{p} &= -M_d M^{-1} \frac{\partial H_d}{\partial q} - GK_v \overbrace{G^\top \frac{\partial H_d}{\partial p}}^0 - G\Phi\tilde{\theta} = -M_d M^{-1} \frac{\partial H_d}{\partial q} - G\Phi\tilde{\theta} \\ &= \begin{bmatrix} -m_1 f(q) - m_2 g(q) + \Phi\tilde{\theta} \\ -m_2 f(q) - m_3 g(q) - \Phi\tilde{\theta} \end{bmatrix},\end{aligned}\tag{4.20}$$

where $f(q)$ and $g(q)$ are the same as in (4.9).

Applying the same approach as in (4.10), we get

$$\ddot{q}_2 + \ddot{q}_1 \gamma_2 = \frac{\dot{p}_2}{I_2} + \frac{\dot{p}_1 \gamma_2}{I_1} = Z_1 \sin(q_1) + \overbrace{Z_2(q_2 + q_1 \gamma_2)}^{\text{const.}} + Z_3 \Phi\tilde{\theta} = 0, \quad \Phi = \sin(t),\tag{4.21}$$

where Z_1 and Z_2 are the same as stated in (4.11), and

$$Z_3 = \frac{I_2 \gamma_2 - I_1}{I_2 I_1} = \text{const.}\tag{4.22}$$

Isolating $\sin(q_1)$ in (4.21) and replacing it in \dot{p}_1 in order to obtain \ddot{q}_1 , we get

$$\ddot{q}_1 = D_1 \sin(t) + D_2,\tag{4.23}$$

where

$$\begin{aligned}D_1 &= \frac{(m_1 + m_2)\tilde{\theta}}{I_1 m_2 + I_2 m_1 \gamma_2} = \text{const.}, \\ D_2 &= \frac{K_1(m_1 m_3 - m_2^2)(q_1 \gamma_2 + q_2)}{I_2(I_1 m_2 + I_2 m_1 \gamma_2)} = \text{const.}\end{aligned}$$

The solution of (4.23) is

$$q_1(t) = -D_1 \sin(t) + \frac{1}{2} D_2 t^2 + (\dot{q}_1(0) + D_1)t + q_1(0).\tag{4.24}$$

Since it is known that the system (4.18) is stable, the admissible values of the coefficients in (4.24) are: $D_1 = -\dot{q}_1(0)$ and $D_2 = 0$. The latter implies that $q_1 \gamma_2 + q_2 = 0$. Therefore,

4. Adaptive IDA-PBC Application: Inertia Wheel Inverted Pendulum

(4.24) and (4.21) respectively become

$$q_1(t) = \dot{q}_1(0) \sin(t) + q_1(0), \quad (4.25)$$

$$\sin(\dot{q}_1(0) \sin(t) + q_1(0)) = -\frac{Z_1 \tilde{\theta}}{Z_3} \sin(t). \quad (4.26)$$

The solution to (4.26) is given by

$$\tilde{\theta} = 0, \quad \dot{q}_1(0) = 0, \quad q_1(0) = k\pi, \quad \forall k \in \mathbb{Z}. \quad (4.27)$$

Combining (4.27) with (4.25) yields

$$q_1(t) = q_2(t) = 0, \quad \forall q_1 \in \langle -\pi, \pi \rangle. \quad (4.28)$$

In this case the stronger property zero-state observability is proven. Moreover, the estimated parameter reaches its true value. Summarizing $\lim_{t \rightarrow \infty} (q, p, \tilde{\theta}) = (0, 0, 0)$.

4.3.2 Simulation Results

For these simulations, the control law (3.2) and the adaptive law (3.4) are employed, considering Table 4.3.

Parameter	Φ	K	$\hat{\theta}(0)$	$[q^\top(0), p^\top(0)]^\top$
Value	$\sin(t)$	1.08	0	$[0.2 \ 0 \ 0 \ 0]^\top$

Table 4.3. – Controller Parameters: Input Uncertainty.

Figures 4.5 to 4.8 show the system response with respect to $A = 0.8$. From Figure 4.5, it is easy to note that the adaptive IDA-PBC control law (3.2) manages to compensate the input uncertainty $A \sin(t)$, while the standard IDA-PBC yields a continuous oscillatory response, which is, obviously, not a desired response.

4. Adaptive IDA-PBC Application: Inertia Wheel Inverted Pendulum

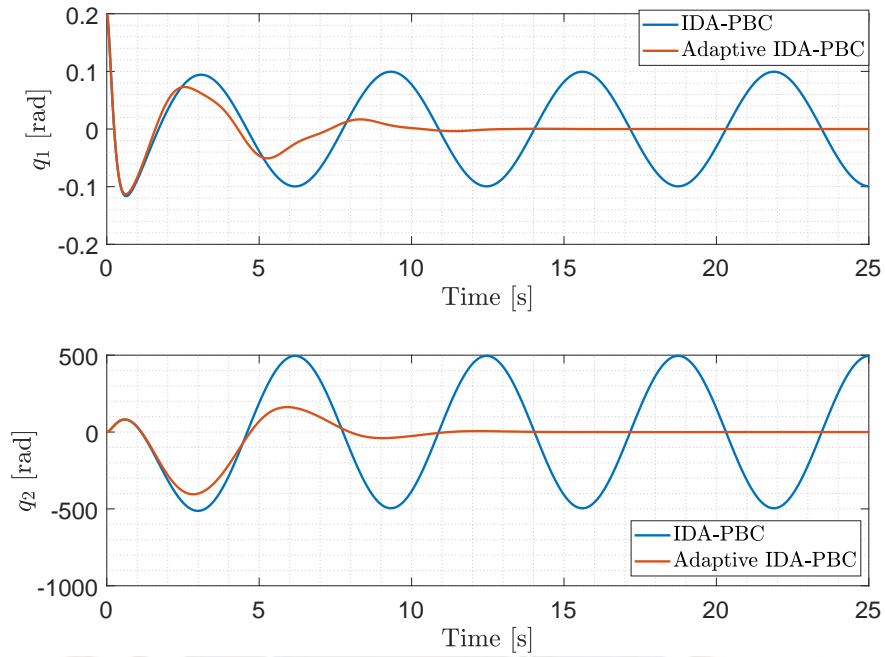


Figure 4.5. – Simulation 2: Evolution of q over time ($A = 0.8$).

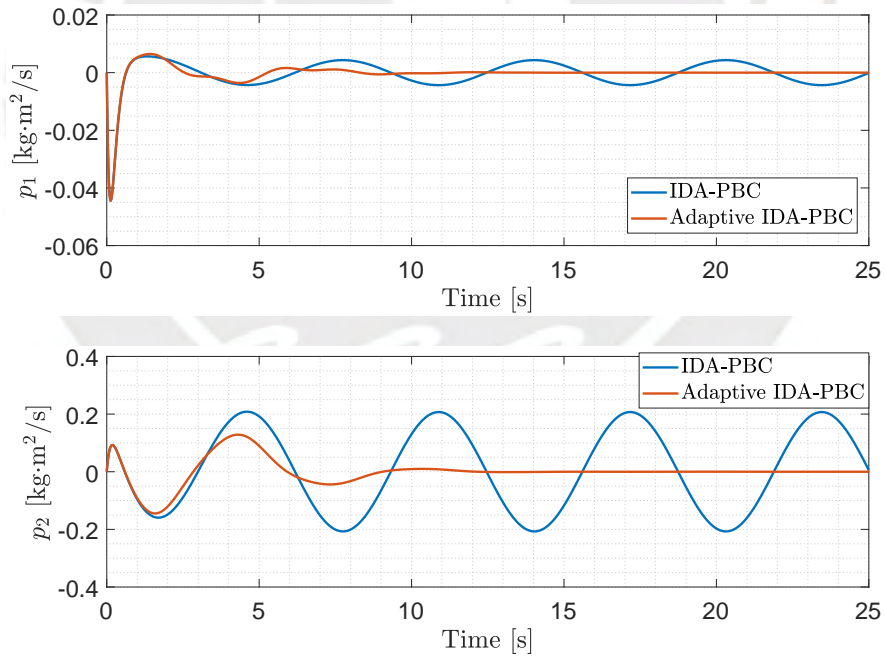


Figure 4.6. – Simulation 2: Evolution of p over time ($A = 0.8$).

From the zero-state detectability calculations, it is known that $\lim_{t \rightarrow \infty} (q, p, \tilde{\theta}) = (0, 0, 0)$, which means that the parameter estimation has to reach its true value. This can be verified in Figure 4.7.

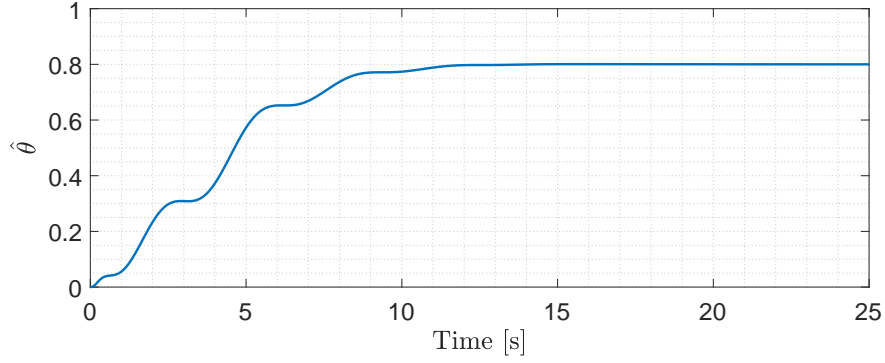


Figure 4.7. – Simulation 2: Evolution of $\hat{\theta}$ over time ($A = 0.8$).

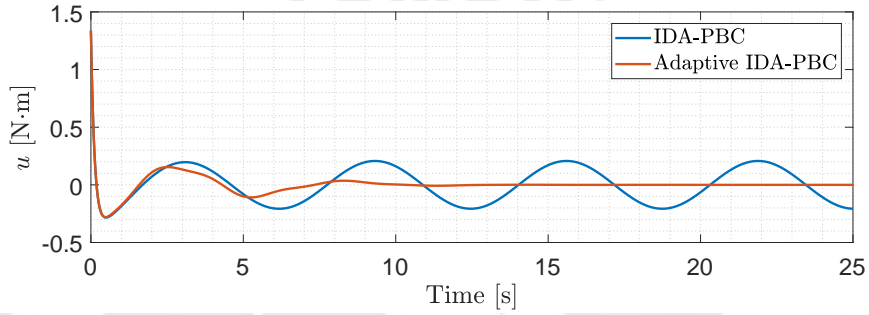


Figure 4.8. – Simulation 2: Evolution of u over time ($A = 0.8$).

4.4 Simulation for Friction Compensation

The control law resulting from the IDA-PBC technique did not take into consideration the effect of the friction, which may lead to a closed-loop instability. This issue is addressed in [45], where some conditions are given to ensure the stability of the resulting system. In this section, the adaptive control law from Proposition 3.2 will be used to compensate for the effect of the friction. The IWIP dynamical system with friction is described by (4.3).

From the Proposition 3.2, the stated conditions have to be satisfied. However, only the relaxed version of those conditions are fulfilled, that is

$$[0_{r \times m} \quad I_r] T M_d \Delta_M \left(\frac{\partial H_d}{\partial q} - \left(\frac{\partial T p}{\partial q} \right) T^{-\top} \frac{\partial H_d}{\partial p} \right) = 0_r \rightarrow \text{Satisfied because } \Delta_M = 0$$

$$[0_{r \times m} \quad I_r] T R \left(\frac{\partial H_\Delta}{\partial p} \right) = 0_r \rightarrow \text{Satisfied because } H_\Delta = 0$$

$$[0_{r \times m} \quad I_r] E T^{-\top} \left(\frac{\partial H_\Delta}{\partial p} \right) = 0_r \rightarrow \text{Satisfied because } H_\Delta = E = 0$$

$$[0_{r \times m} \quad I_r] T \left(\frac{\partial H_\Delta}{\partial q} - \left(\frac{\partial T p}{\partial q} \right) T^{-\top} \frac{\partial H_\Delta}{\partial p} \right) = 0_r \rightarrow \text{Satisfied because } H_\Delta = 0$$

4. Adaptive IDA-PBC Application: Inertia Wheel Inverted Pendulum

The only condition that needs calculations is

$$[0_{r \times m} \quad I_r]TR\left(\frac{\partial H}{\partial p}\right) = -[0 \quad 1]\begin{bmatrix} -\frac{1}{2}(\dot{q}_1(r_1 + 2r_2) - 2r_2\dot{q}_2) \\ r_1\dot{q}_1 \end{bmatrix} = -r_1\dot{q}_1 = 0. \quad (4.29)$$

From (4.29), it is clear that only friction in the actuated coordinate can be compensated. The functions involved in $\Phi(q, p)$, considering $r_1 = 0$, are

$$[I_m \quad 0_{m \times r}]TR\left(\frac{\partial H}{\partial p}\right) = -[1 \quad 0]\begin{bmatrix} -\frac{1}{2}(\dot{q}_1(r_1 + 2r_2) - 2r_2\dot{q}_2) \\ r_1\dot{q}_1 \end{bmatrix} = r_2(\dot{q}_1 - \dot{q}_2). \quad (4.30)$$

Then it is clear that

$$\Phi(q, p) = \dot{q}_1 - \dot{q}_2, \quad \theta = r_2.$$

4.4.1 Zero-State Detectability

Here, the assumption (4.7) still holds. The target PH system (3.26) together with the adaptive law (3.24), taking into account that $\Delta_M = J_2 = 0$, is represented by (4.18). Therefore, (4.20) is still valid.

Applying the same approach as in (4.21), we get

$$\ddot{q}_2 + \ddot{q}_1\gamma_2 = \frac{\dot{p}_2}{I_2} + \frac{\dot{p}_1\gamma_2}{I_1} = Z_1 \sin(q_1) + \overbrace{Z_2(q_2 + q_1\gamma_2)}^{const.} + Z_3\Phi\tilde{\theta} = 0, \quad \Phi = \dot{q}_1 - \dot{q}_2, \quad (4.31)$$

where Z_1 , Z_2 and Z_3 are the same as (4.22).

Isolating $\sin(q_1)$ in (4.31), using the relationship $\dot{q}_1 - \dot{q}_2 = \dot{q}_1(1 + \gamma_2)$ and replacing it in \dot{p}_1 in order to obtain \ddot{q}_1

$$\ddot{q}_1 = D_1\dot{q}_1 + D_2, \quad (4.32)$$

where

$$D_1 = \frac{1}{I_1} \left(\tilde{\theta} - \frac{m_1(I_2\gamma_2 - I_1)(1 + \gamma_2)\tilde{\theta}}{I_2m_1\gamma_2 + I_1m_2} \right) = const.,$$

$$D_2 = \left(\frac{m_1K_1(I_2^2m_1\gamma_2^2 + 2I_2I_1m_2\gamma_2 + I_1^2m_3)}{I_1^2I_2(I_2m_1\gamma_2 + I_1m_2)} - \frac{m_1K_1\gamma_2}{I_1^2} - \frac{m_2K_1}{I_1I_2} \right) (q_1\gamma_2 + q_2),$$

with $D_2 = const.$ The solution of (4.32) is

$$q_1(t) = \frac{e^{D_1 t}(D_1\dot{q}_1(0) + D_2)}{D_1^2} - \frac{D_2 t}{D_1} + \frac{D_1^2 q_1(0) - D_1\dot{q}_1(0) - D_2}{D_1^2}, \quad (4.33)$$

4. Adaptive IDA-PBC Application: Inertia Wheel Inverted Pendulum

Since the system (4.18) is stable, the following must hold with respect to (4.33)

$$\begin{aligned} D_1 \leq 0 &\implies \tilde{\theta} \leq 0, \\ D_2 = 0 &\implies q_1 \gamma_2 + q_2 = 0. \end{aligned} \quad (4.34)$$

Combining (4.34) with (4.31) yields

$$\dot{q}_1 = \zeta \sin(q_1), \quad \zeta = -\frac{Z_1}{Z_3(1 + \gamma_2)\tilde{\theta}} < 0, \quad \forall \tilde{\theta} \neq 0. \quad (4.35)$$

The solution of (4.35) is

$$\left| \tan \frac{q_1}{2} \right| = e^{\zeta t}. \quad (4.36)$$

From (4.36), it is clear that

$$\lim_{t \rightarrow \infty} q_1(t) = q_2(t) = 0, \quad \forall q_1 \in \langle -\pi, \pi \rangle. \quad (4.37)$$

In this case zero-state detectability condition is verified. Summarizing $\lim_{t \rightarrow \infty} (q, p, \tilde{\theta}) = (0, 0, \tilde{\theta}^*)$.

4.4.2 Simulation Results

For these simulations, the control law (3.23) and the adaptation law (3.24) are employed, considering Table 4.4.

Parameter	Φ	K	$\hat{\theta}(0)$	$[q^\top(0), p^\top(0)]^\top$
Value	$\dot{q}_1 - \dot{q}_2$	2.08×10^{-5}	0	$[0.2 \ 0 \ 0 \ 0]^\top$

Table 4.4. – Controller Parameters: Friction Uncertainty.

Figures 4.9 to 4.12 show the IWIP's system response to $r_2 = 0.0012$. From Figures 4.9 to 4.10, it's clear that both control laws have a similar response. Even though the convergence time of the response from the adaptive IDA-PBC technique is slightly faster than the one from the IDA-PBC, both responses achieve asymptotic stability.

4. Adaptive IDA-PBC Application: Inertia Wheel Inverted Pendulum

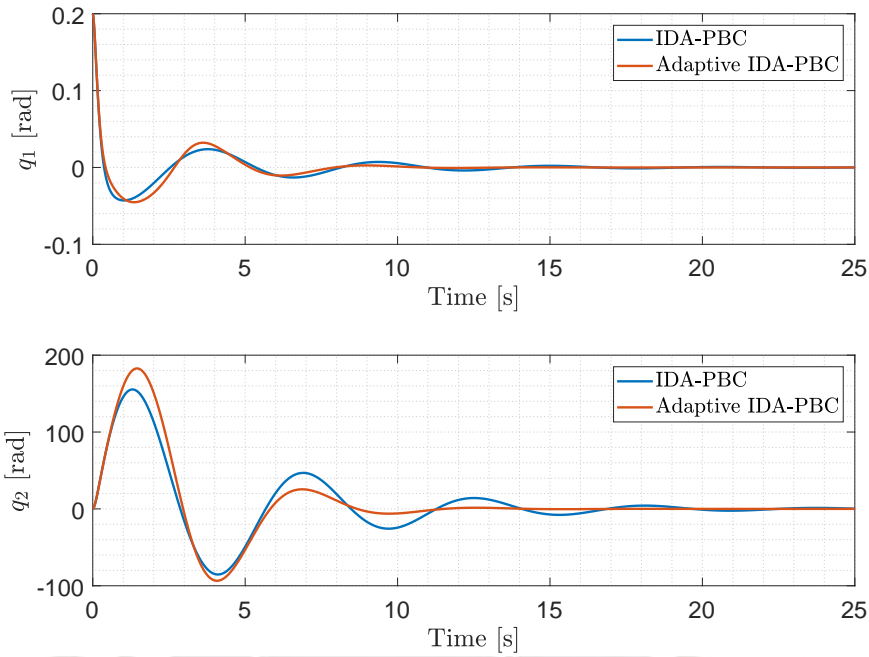


Figure 4.9. – Simulation 3: Evolution of q over time ($r_2 = 0.0012$).

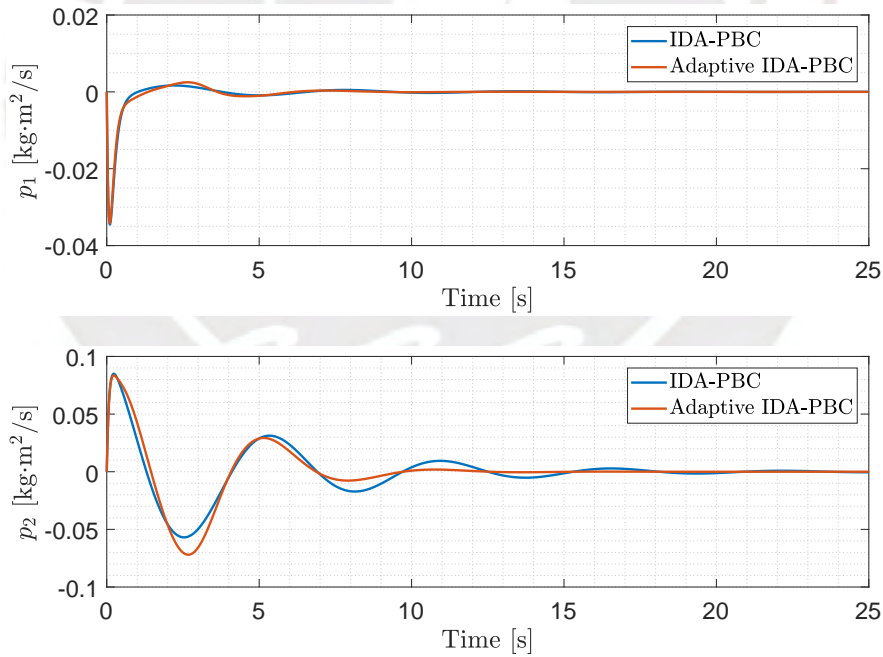


Figure 4.10. – Simulation 3: Evolution of p over time ($r_2 = 0.0012$).

From the zero-state detectability calculations, it is known that $\lim_{t \rightarrow \infty} (q, p, \tilde{\theta}) = (0, 0, \tilde{\theta}^*)$, which means that the parameter estimation does not necessarily reach its true value, this complies with what is shown in Figure 4.11.

4. Adaptive IDA-PBC Application: Inertia Wheel Inverted Pendulum

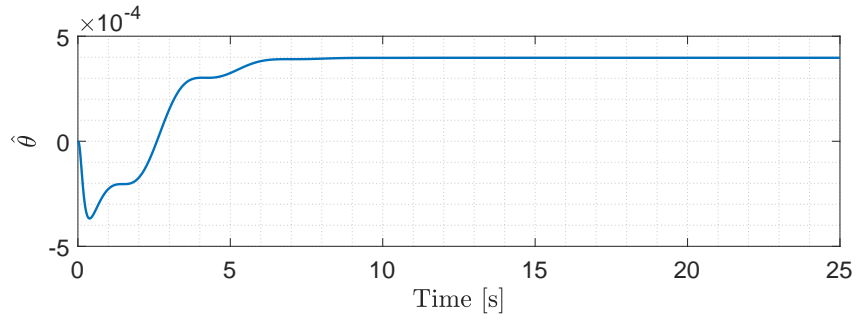


Figure 4.11. – Simulation 3: Evolution of $\hat{\theta}$ over time ($r_2 = 0.0012$).

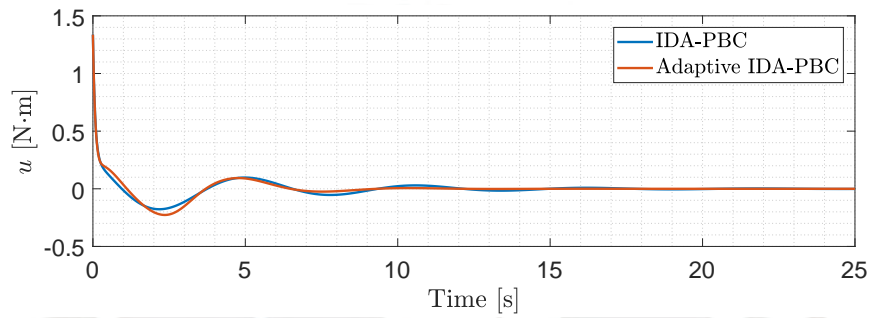


Figure 4.12. – Simulation 3: Evolution of u over time ($r_2 = 0.0012$).

Figures 4.13 to 4.16 show the IWIP's system response to $r_2 = 0.0017$.

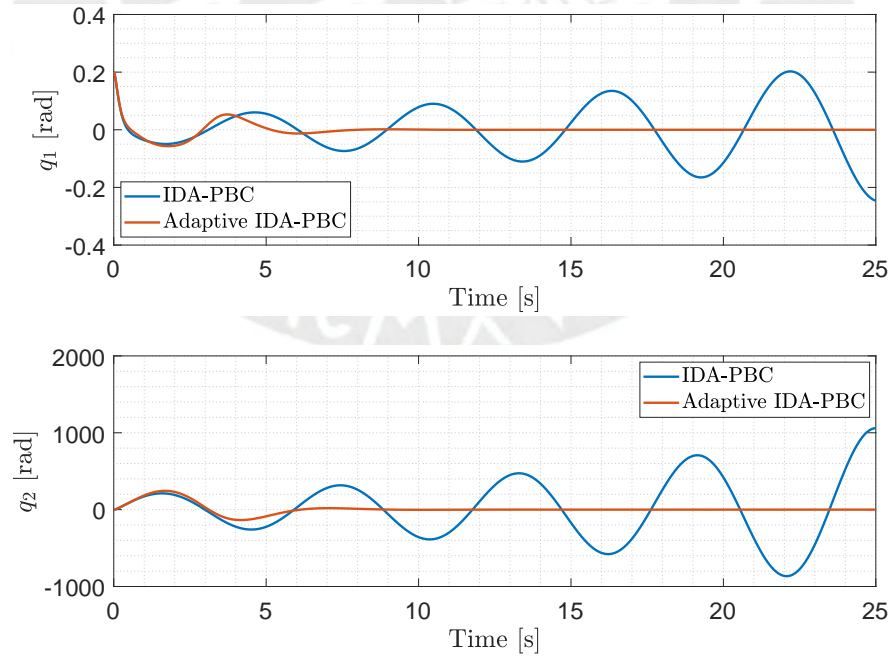


Figure 4.13. – Simulation 4: Evolution of q over time ($r_2 = 0.0017$).

4. Adaptive IDA-PBC Application: Inertia Wheel Inverted Pendulum

In Figure 4.13, it's noted that the IDA-PBC technique does not asymptotically stabilize the system anymore. In fact, it seems to start to become unstable. However, as it is shown in Figure 4.17, it does not become unstable, at least up to where it was simulated. Adaptive IDA-PBC proves to asymptotically stabilize the IWIP system despite the effect of friction that was not considered in the standard IDA-PBC technique.

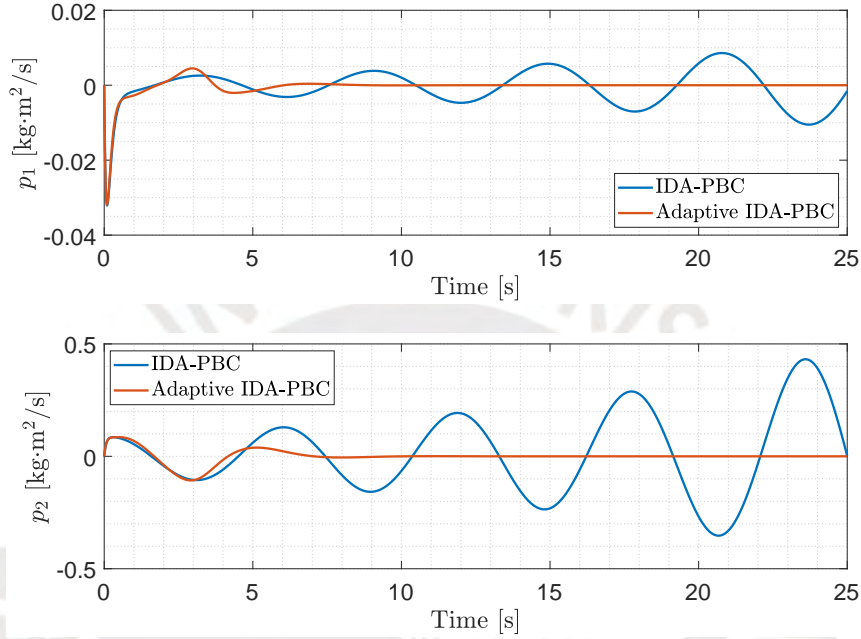


Figure 4.14. – Simulation 4: Evolution of p over time ($r_2 = 0.0017$).

For this simulation, it remains valid the fact that the parameter estimation does not necessarily reach its true value, this is verified in Figure 4.15.

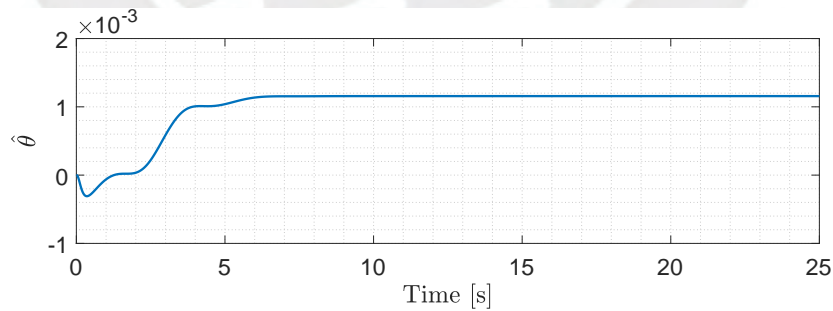


Figure 4.15. – Simulation 4: Evolution of $\hat{\theta}$ over time ($r_2 = 0.0017$).

4. Adaptive IDA-PBC Application: Inertia Wheel Inverted Pendulum

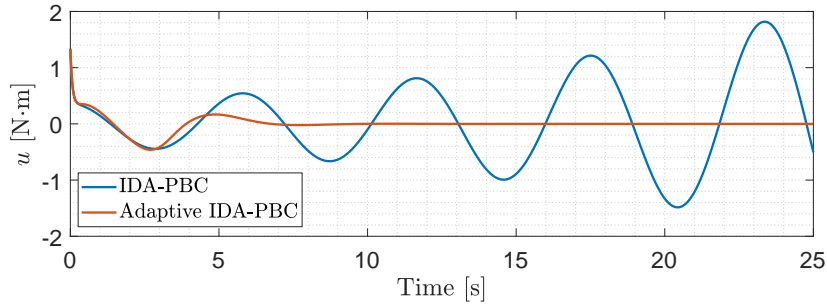


Figure 4.16. – Simulation 4: Evolution of u over time ($r_2 = 0.0017$).

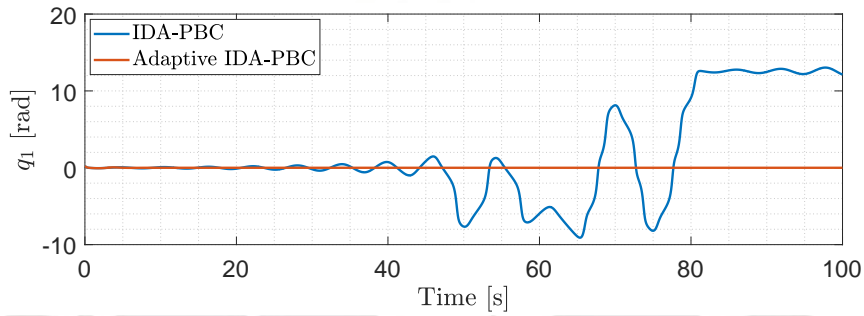


Figure 4.17. – Simulation 4: Wider view of the evolution of q_1 ($r_2 = 0.0017$).

From the simulations, with the previous values of r_2 , it is seen that a slightly increment in r_2 resulted in a drastic change in the system's response under the IDA-PBC technique. In contrast, the adaptive IDA-PBC technique can manage bigger increments and still be able to asymptotically stabilize the IWIP system. Figure 4.18 shows the system's response to $r_2 = 0.02$ under the adaptive IDA-PBC technique and Figure 4.19 shows the response to both controllers where it is easy to note that the IDA-PBC technique is not enough to guarantee asymptotic stability.

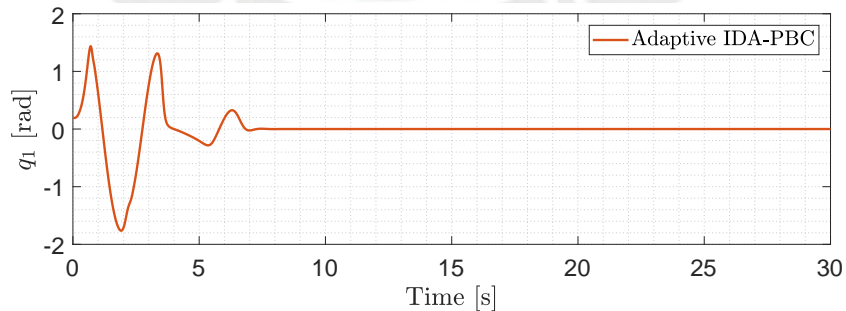


Figure 4.18. – Simulation 5: Evolution of q_1 (adaptive only) over time ($r_2 = 0.02$).

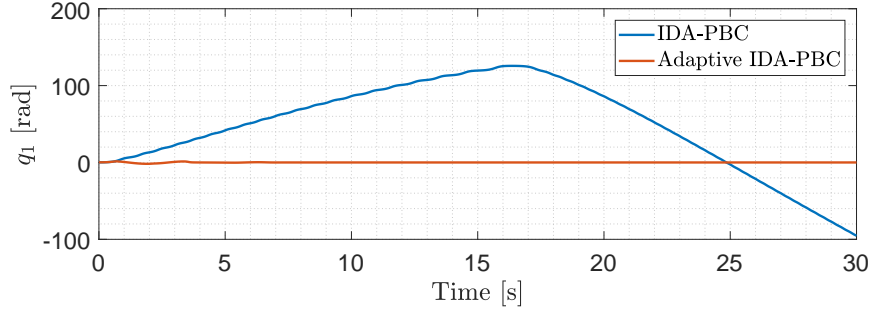


Figure 4.19. – Simulation 5: Evolution of q_1 over time ($r_2 = 0.02$).

4.5 Simulation Subject to Parameter Uncertainty

Usually, when working with mechanical systems the values assigned to variables like inertia are just a close approximation. Hence, the system response to the designed controller could be slightly different from what the simulations showed or even worse, the system could become unstable depending on the system dynamics and how far away are the approximations from the real values of the previously mentioned variables. In this section, the adaptive control law stated in Proposition 3.2 will be used and then compared to the standard IDA-PBC. The parameter uncertainty is reflected in total energy of the system, this is

$$\begin{aligned} H_R &= \frac{1}{2} p^\top \overbrace{(M^{-1} + \Delta_M)}^{\tilde{M}^{-1}} p + (V + \Delta_V) \\ &= \underbrace{\frac{1}{2} p^\top M^{-1} p + V}_H + \underbrace{\frac{1}{2} p^\top \Delta_M p + \Delta_V}_{H_\Delta}. \end{aligned}$$

We choose Δ_M and Δ_V such that they have the same structure as M and V respectively

$$\begin{aligned} \Delta_M &= \Delta_M^\top = \begin{bmatrix} \Delta_{11} & \Delta_{12} \\ \Delta_{12} & \Delta_{13} \end{bmatrix}, \\ \Delta_V &= B(\cos(q_1) + 1). \end{aligned}$$

The following step is to fulfill the conditions stated in Proposition 3.2. In this case the relaxed version of those conditions is employed, that is

$$[0_{r \times m} \quad I_r] TR \left(\frac{\partial H}{\partial p} \right) = 0_r \rightarrow \text{Satisfied because } R = 0.$$

$$[0_{r \times m} \quad I_r] TR \left(\frac{\partial H_\Delta}{\partial p} \right) = 0_r \rightarrow \text{Satisfied because } R = 0.$$

4. Adaptive IDA-PBC Application: Inertia Wheel Inverted Pendulum

$$[0_{r \times m} \quad I_r]ET^{-\top} \left(\frac{\partial H_{\Delta}}{\partial p} \right) = 0_r \rightarrow \text{Satisfied because } E = 0.$$

Performing calculations for the condition

$$\begin{aligned} [0_{r \times m} \quad I_r]T \left(\frac{\partial H_{\Delta}}{\partial q} - \left(\frac{\partial T p}{\partial q} \right) T^{-\top} \frac{\partial H_{\Delta}}{\partial p} \right) &= [0 \quad 1] \begin{bmatrix} -\frac{1}{2} & \frac{1}{2} \\ 1 & 1 \end{bmatrix} \begin{bmatrix} -B \sin(q_1) \\ 0 \end{bmatrix} \\ &= -B \sin(q_1) = 0. \end{aligned} \quad (4.38)$$

It is clear that stability of the target PH system (3.26), using Proposition 3.2, cannot be ensured under an uncertainty in the potential energy. For the remaining condition we have

$$[0_{r \times m} \quad I_r]TM_d \Delta_M \left(\frac{\partial H_d}{\partial q} - \left(\frac{\partial T p}{\partial q} \right) T^{-\top} \frac{\partial H_d}{\partial p} \right) = 0_r,$$

which leads to the following inertia uncertainty matrix

$$\Delta_M = \begin{bmatrix} \Delta_{11} & -\frac{(m_1 + m_2)}{(m_2 + m_3)} \Delta_{11} \\ -\frac{(m_1 + m_2)}{(m_2 + m_3)} \Delta_{11} & \frac{(m_1 + m_2)^2}{(m_2 + m_3)^2} \Delta_{11} \end{bmatrix},$$

and so, the matrix of known functions $\Phi(q, p)$ derives from

$$[I_m \quad 0_{m \times r}]TM_d \Delta_M \left(\frac{\partial H_d}{\partial q} - \left(\frac{\partial T p}{\partial q} \right) T^{-\top} \frac{\partial H_d}{\partial p} \right) = \Delta_{11} N_1 (N_2 \sin(q_1) - N_3 (q_1 \gamma_2 + q_2)),$$

where

$$N_1 = \frac{m_1 m_3 - m_2^2}{(m_2 + m_3)^2 (m_1 + m_2)} = \text{const.},$$

$$N_2 = I_1 b g (m_2 + m_3) = \text{const.},$$

$$N_3 = K_1 (m_1 + m_2) (\gamma_2 (m_2 + m_3) - (m_1 + m_2)) = \text{const.}$$

Then it is clear that

$$\Phi(q, p) = N_1 (N_2 \sin(q_1) - N_3 (q_1 \gamma_2 + q_2)), \quad \theta = \Delta_{11}.$$

Now, the effect of Δ_M on the system's inertia matrix is calculated as follows

$$\begin{aligned} \tilde{M} &= (M^{-1} + \Delta_M)^{-1} \\ &= \frac{1}{Z} \begin{bmatrix} (Z - \Delta_{11} I_1) I_1 & \frac{(m_1 + m_2) \Delta_{11} I_1 I_2}{m_2 + m_3} \\ \frac{(m_1 + m_2) \Delta_{11} I_1 I_2}{m_2 + m_3} & (I_1 \Delta_{11} + 1) I_2 \end{bmatrix}, \end{aligned}$$

4. Adaptive IDA-PBC Application: Inertia Wheel Inverted Pendulum

where

$$Z = \frac{(m_1 + m_2)^2 \Delta_{11} I_2}{(m_2 + m_3)^2} + \Delta_{11} I_1 + 1.$$

4.5.1 Zero-State Detectability

The assumption in (4.7) still holds. The target PH system (3.26) together with the adaptive law (3.24), taking into account that $\frac{\partial T_p}{\partial q} = J_2 = 0$, is represented by

$$\begin{bmatrix} \dot{q} \\ \dot{p} \\ \dot{\theta} \end{bmatrix} = \begin{bmatrix} 0 & (M^{-1} + \Delta_M)M_d & 0 \\ -M_d(M^{-1} + \Delta_M) & -GK_v G^\top & -G\Phi K \\ 0 & K\Phi^\top G^\top & 0 \end{bmatrix} \begin{bmatrix} \frac{\partial \bar{H}_d}{\partial q} \\ \frac{\partial \bar{H}_d}{\partial p} \\ \frac{\partial \bar{H}_d}{\partial \theta} \end{bmatrix}, \quad (4.39)$$

where \bar{H}_d is the same as in (4.19). From (4.39), the following is obtained

$$\begin{aligned} \dot{\theta} &= K\Phi^\top G^\top \overbrace{\frac{\partial \bar{H}_d}{\partial p}}^0 = 0 \rightarrow \tilde{\theta} = \text{const.}, \\ \dot{p} &= -M_d(M^{-1} + \Delta_M) \frac{\partial \bar{H}_d}{\partial q} - G\Phi\tilde{\theta} \\ &= \begin{bmatrix} -\bar{m}_1 f(q) - \bar{m}_2 g(q) + \Phi\tilde{\theta} \\ -\bar{m}_3 f(q) - \bar{m}_4 g(q) - \Phi\tilde{\theta} \end{bmatrix}, \end{aligned} \quad (4.40)$$

where

$$\begin{aligned} \bar{m}_1 &= m_1 \left(\frac{1}{I_1} + \Delta_{11} \right) - \frac{m_2 \Delta_{11} (m_1 + m_2)}{m_2 + m_3} = \text{const.}, \\ \bar{m}_2 &= m_2 \left(\frac{1}{I_2} + \frac{\Delta_{11} (m_1 + m_2)^2}{(m_2 + m_3)^2} \right) - \frac{m_1 \Delta_{11} (m_1 + m_2)}{m_2 + m_3} = \text{const.}, \\ \bar{m}_3 &= m_2 \left(\frac{1}{I_1} + \Delta_{11} \right) - \frac{m_3 \Delta_{11} (m_1 + m_2)}{m_2 + m_3} = \text{const.}, \\ \bar{m}_4 &= m_3 \left(\frac{1}{I_2} + \frac{\Delta_{11} (m_1 + m_2)^2}{(m_2 + m_3)^2} \right) - \frac{m_2 \Delta_{11} (m_1 + m_2)}{m_2 + m_3} = \text{const.}, \\ f(q) &= -\frac{I_1 b g \sin(q_1)}{m_1 + m_2} + K_1 (q_1 \gamma_2 + q_2) \gamma_2, \\ g(q) &= K_1 (q_1 \gamma_2 + q_2). \end{aligned}$$

Applying the same approach as in (4.10), we get

$$\ddot{q}_2 + \ddot{q}_1 \gamma_2 = \frac{\dot{p}_2}{I_2} + \frac{\dot{p}_1 \gamma_2}{I_1} = Z_1 \sin(q_1) + \overbrace{Z_2 (q_2 + q_1 \gamma_2)}^{\text{const.}} + Z_3 \Phi \tilde{\theta} = 0, \quad (4.41)$$

4. Adaptive IDA-PBC Application: Inertia Wheel Inverted Pendulum

$$\Phi = Z_4 \sin(q_1) + Z_5(q_2 + q_1\gamma_2),$$

where

$$\begin{aligned} Z_1 &= \frac{bg(I_2\bar{m}_1\gamma_2 + I_1\bar{m}_3)}{I_2(m_1 + m_2)}, \\ Z_2 &= -\frac{K_1(\gamma^2 I_2\bar{m}_1 + (I_2\bar{m}_2 + I_1\bar{m}_3)\gamma_2 + I_1\bar{m}_4)}{I_1 I_2}, \\ Z_3 &= \frac{I_2\gamma_2 - I_1}{I_1 I_2}, \quad Z_4 = N_1 N_2, \quad Z_5 = N_1 N_3. \end{aligned}$$

Equation (4.41) can be rewritten as

$$\bar{Z}_1 \sin(q_1) + \overbrace{\bar{Z}_2(q_2 + q_1\gamma_2)}^{const.} = 0, \quad (4.42)$$

where

$$\begin{aligned} \bar{Z}_1 &= Z_1 + Z_3 Z_4 \tilde{\theta}, \\ \bar{Z}_2 &= Z_2 + Z_3 Z_5 \tilde{\theta}. \end{aligned}$$

From (4.42), we know that $\bar{Z}_1 \sin(q_1)$ has to also be constant, thus:

$$\sin(q_1) = const. \implies q_1 = const. \implies q_2 = const. \implies \dot{q}_1 = \dot{q}_2 = 0 \implies \dot{p} = 0. \quad (4.43)$$

From (4.43) and (4.40), we get

$$f(q) = -\frac{m_2}{m_1} g(q) = -\frac{m_3}{m_2} g(q). \quad (4.44)$$

The only solution for (4.44) is

$$f(q) = g(q) = 0 \implies q_2 + q_1\gamma_2 = 0 \implies \sin(q_1) = 0 \implies q_1 = q_2 = 0 \quad \forall q_1 \in \langle -\pi, \pi \rangle.$$

From all the operations that were carried out in this subsection, it is clear that the target PH system (4.39) is zero-state observable, thus asymptotic stability is proved. Summarizing $\lim_{t \rightarrow \infty} (q, p, \tilde{\theta}) = (0, 0, \tilde{\theta}^*)$.

4.5.2 Simulation Results

For these simulations, the control law (3.23) and the adaptive law (3.24) are employed, considering Table 4.5.

4. Adaptive IDA-PBC Application: Inertia Wheel Inverted Pendulum

Parameter	Φ	K	$\hat{\theta}(0)$	$[q^\top(0), p^\top(0)]^\top$
Value	$N_1(N_2 \sin(q_1) - N_3(q_1\gamma_2 + q_2))$	7.08×10^3	0	$[0.2 \ 0 \ 0 \ 0]^\top$

Table 4.5. – Controller Parameters: Parameter Uncertainty.

Figures 4.20 to 4.23 show the IWIP's system response with respect to $\Delta_{11} = 15$. For such choice of Δ_{11} , the inertia matrix changes as follows

$$\begin{bmatrix} 0.0437 & 0 \\ 0 & 0.0004 \end{bmatrix} \rightarrow \begin{bmatrix} 0.0264 & -1.8 \times 10^{-5} \\ -1.8 \times 10^{-5} & 0.0004 \end{bmatrix}.$$

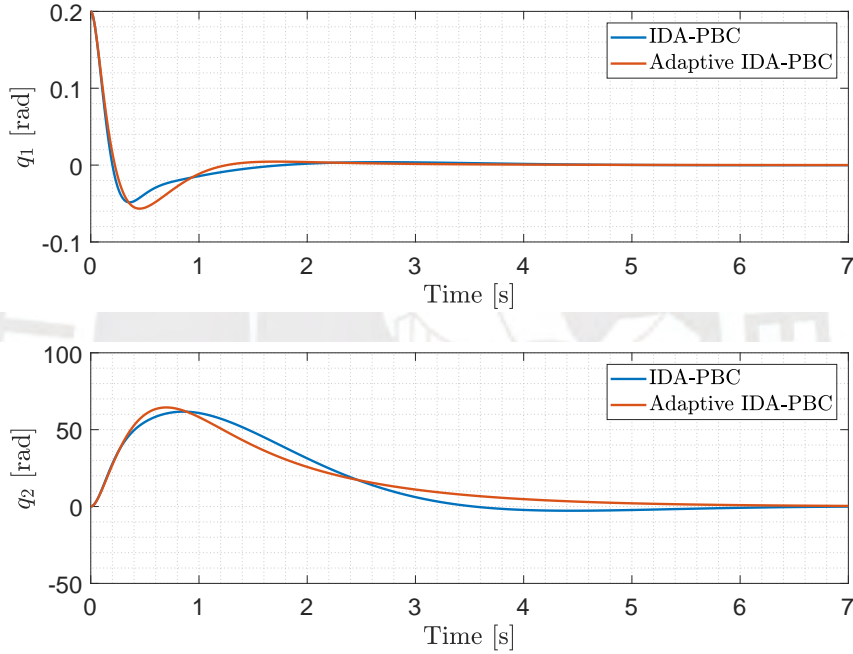


Figure 4.20. – Simulation 6: Evolution of q over time ($\Delta_{11} = 15$).

It is clear from Figure 4.20, that decreasing the values of the inertia matrix leads to a smoother response of the system compared to the standard IDA-PBC without uncertainties. Additionally, the adaptive IDA-PBC technique yields a slightly faster response compared to the standard IDA-PBC.

4. Adaptive IDA-PBC Application: Inertia Wheel Inverted Pendulum

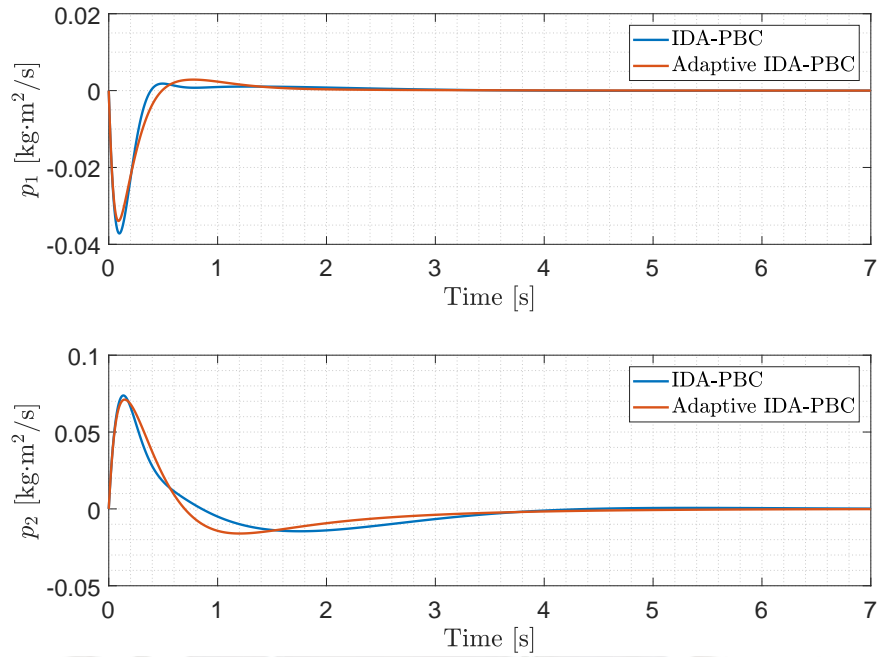


Figure 4.21. – Simulation 6: Evolution of p over time ($\Delta_{11} = 15$).

From the zero-state detectability calculations, it is known that $\lim_{t \rightarrow \infty} (q, p, \tilde{\theta}) = (0, 0, \tilde{\theta}^*)$, which means that the parameter estimation does not necessarily reach its true value. This matches with what is shown in Figure 4.22.

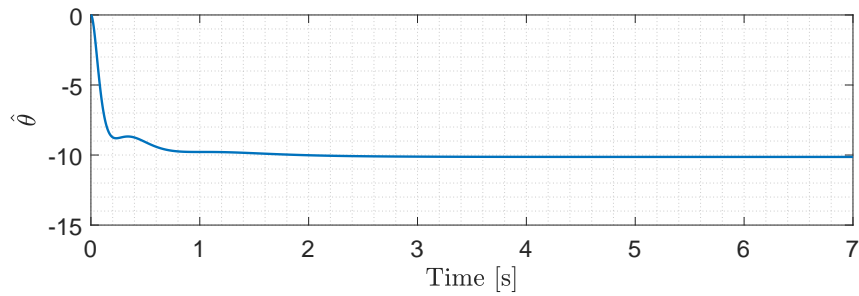


Figure 4.22. – Simulation 6: Evolution of $\hat{\theta}$ over time. ($\Delta_{11} = 15$).

4. Adaptive IDA-PBC Application: Inertia Wheel Inverted Pendulum

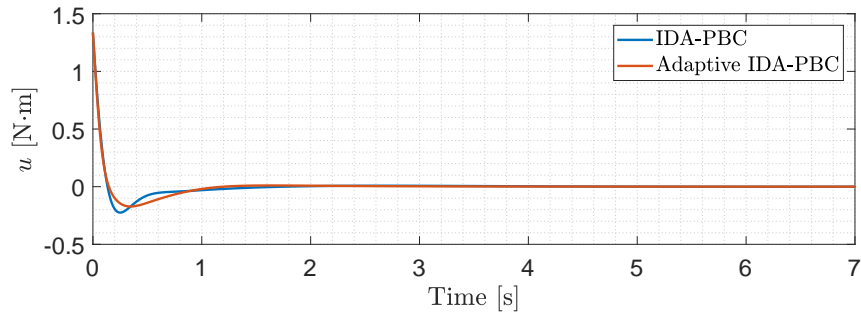


Figure 4.23. – Simulation 6: Evolution of u over time ($\Delta_{11} = 15$).

Figures 4.24 to 4.27 show the IWIP's system response with respect to $\Delta_{11} = -22$. For such choice of Δ_{11} , the inertia matrix changes as follows

$$\begin{bmatrix} 0.0437 & 0 \\ 0 & 0.0004 \end{bmatrix} \rightarrow \begin{bmatrix} 1.1097 & 0.0011 \\ 0.0011 & 0.0004 \end{bmatrix}.$$

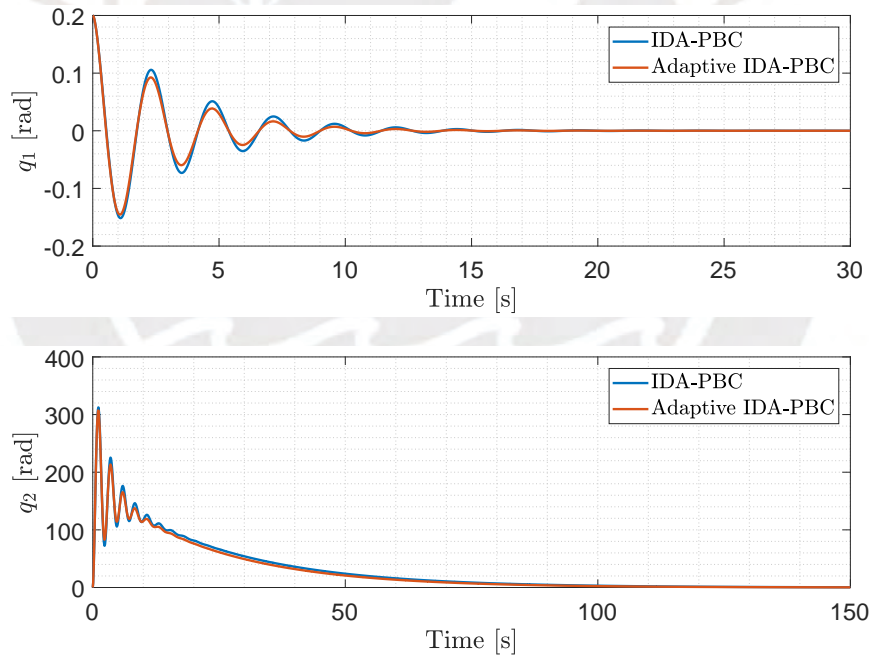


Figure 4.24. – Simulation 7: Evolution of q over time ($\Delta_{11} = -22$).⁹

From Figure 4.24, it is noted that, as the inertia values increase, the response of the system becomes more oscillating, plus, stabilization time increases considerably. The

⁹For this simulation, a wider time range is used to depict the asymptotic stabilization.

4. Adaptive IDA-PBC Application: Inertia Wheel Inverted Pendulum

system's response subject to adaptive IDA-PBC has a slightly better performance (less overshoot and convergence time) compared to the standard IDA-PBC.

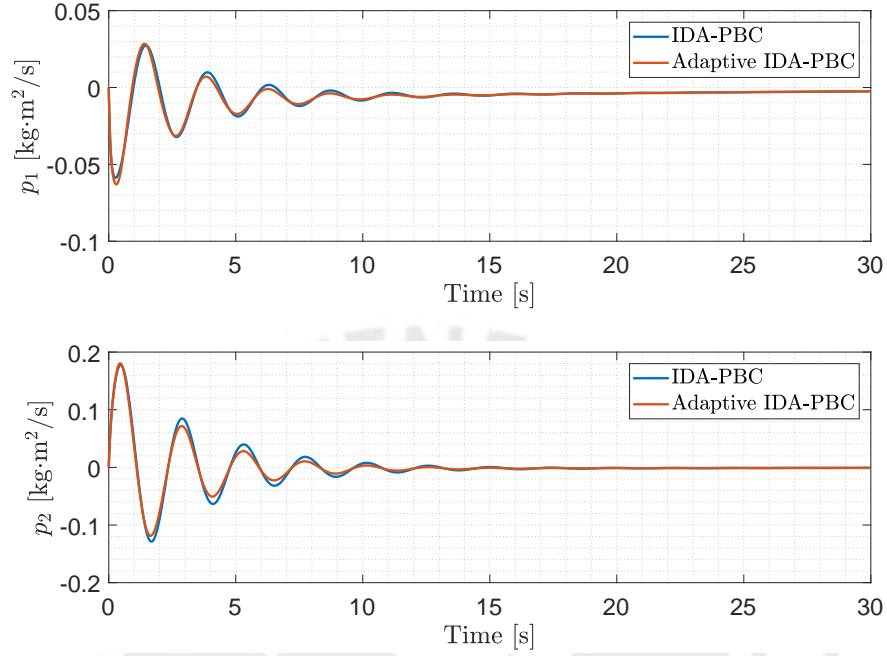


Figure 4.25. – Simulation 7: Evolution of p over time ($\Delta_{11} = -22$).

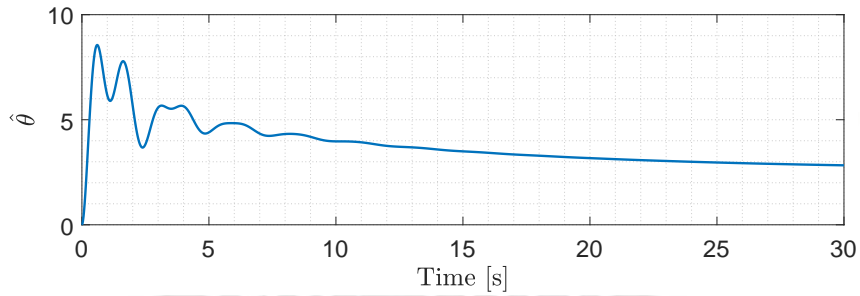


Figure 4.26. – Simulation 7: Evolution of $\hat{\theta}$ over time ($\Delta_{11} = -22$).

4. Adaptive IDA-PBC Application: Inertia Wheel Inverted Pendulum

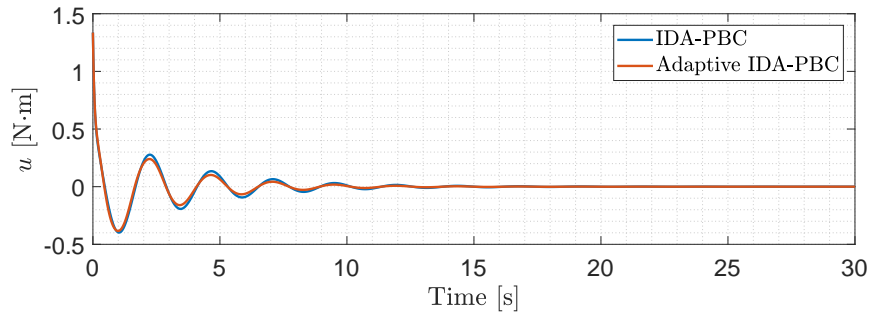


Figure 4.27. – Simulation 7: Evolution of u over time ($\Delta_{11} = -22$).

As it has been seen, for the simulations with $\Delta_{11} = -22$ considering Table 4.5, the system responses for both controllers are very similar to each other, and not very desirable. To improve this behavior, there are two main ways. The first one, motivated by a physical knowledge, is to set the initial estimation value to a non-zero value. However, there is a problem with this approach: Since the propositions stated in this work do not guarantee the estimation parameter convergence, the choice of this initial estimation may turn out not intuitive at all. This fact can be noticed in Figures 4.28 to 4.33, where it can be seen that for a choice of $\hat{\theta}(0) = -25$ (Figures 4.28 to 4.30), which is close to the true value of Δ_{11} , the system response has worse performance compared to the response resulting from the choice of $\hat{\theta}(0) = 0$. However, the choice of $\hat{\theta}(0) = 25$ (Figures 4.31 to 4.33), which is not relatively close to the true value of Δ_{11} , yields a better behavior.

4. Adaptive IDA-PBC Application: Inertia Wheel Inverted Pendulum

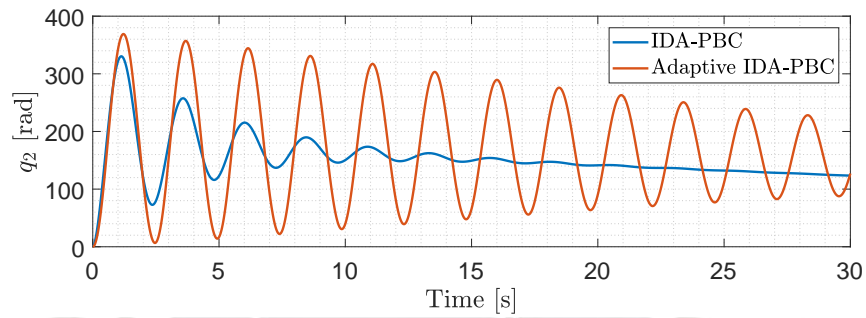
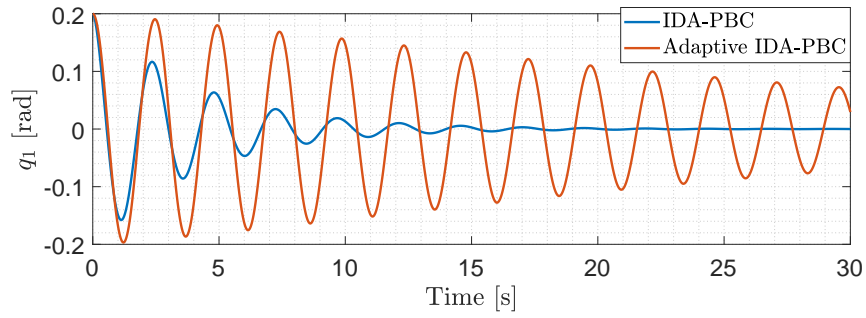


Figure 4.28. – Simulation 8: Evolution of q over time ($\hat{\theta}(0) = -25$).

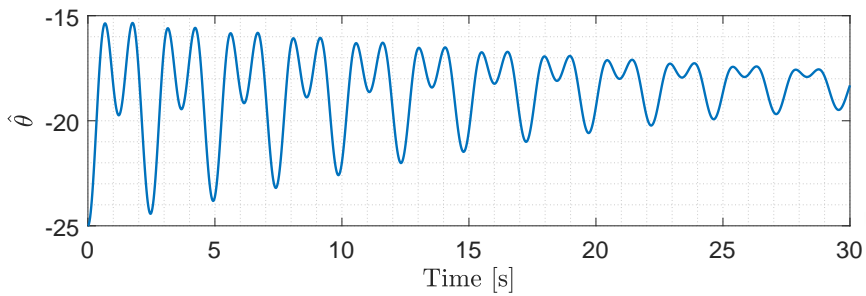


Figure 4.29. – Simulation 8: Evolution of $\hat{\theta}$ over time ($\hat{\theta}(0) = -25$).

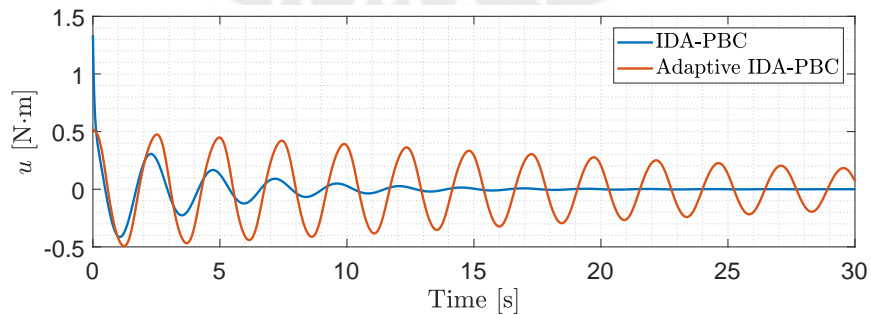


Figure 4.30. – Simulation 8: Evolution of u over time ($\hat{\theta}(0) = -25$).

4. Adaptive IDA-PBC Application: Inertia Wheel Inverted Pendulum

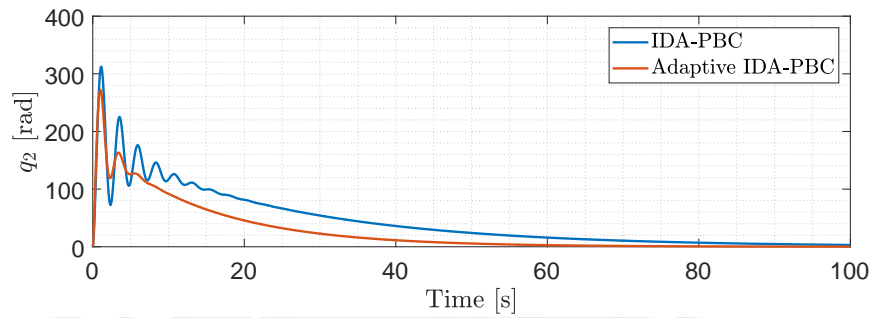
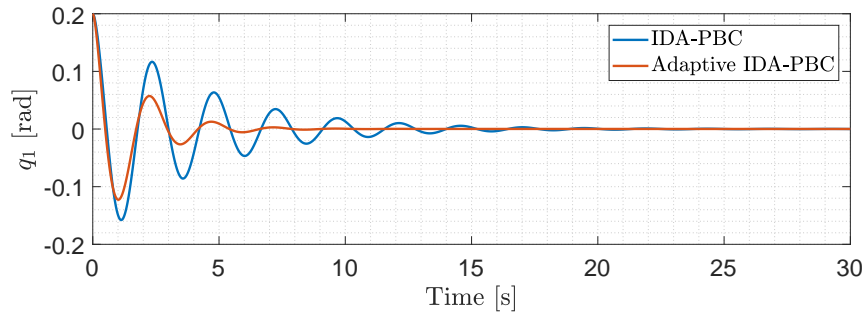


Figure 4.31. – Simulation 9: Evolution of q over time ($\hat{\theta}(0) = 25$).

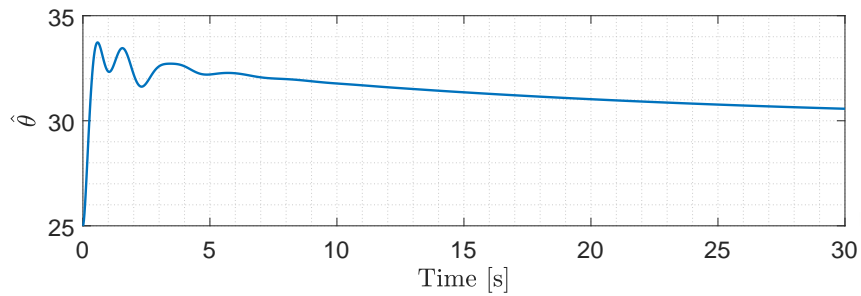


Figure 4.32. – Simulation 9: Evolution of $\hat{\theta}$ over time ($\hat{\theta}(0) = 25$).

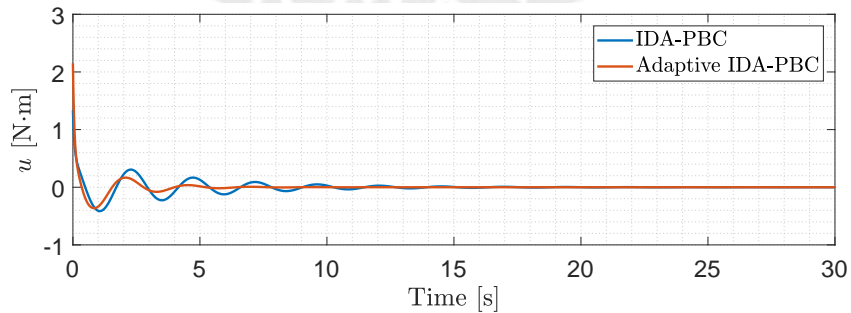


Figure 4.33. – Simulation 9: Evolution of u over time ($\hat{\theta}(0) = 25$).

4. Adaptive IDA-PBC Application: Inertia Wheel Inverted Pendulum

From Figure 4.30 and Figure 4.33, it is clear that the choice of a non-zero $\hat{\theta}(0)$ affects directly the control input peak magnitude. For instance, the control input peak to improve the system's behavior (Figure 4.33) is considerably higher than the one resulting from the standard IDA-PBC.

The second and more suitable way, at least for this system, is to adjust the adaptation rate gain, i.e., K , leaving the initial estimation to be zero. In this case, physical considerations have also to be taken into account. The original choice of $K = 7.08 \times 10^3$, for this system, is suitable when the inertia matrix elements have smaller magnitudes than those considered in the dynamic modeling. However, as it has been seen, as the inertia matrix's elements increase in magnitude (e.g., $\Delta_{11} = -22$), this value of K is not good enough to compensate for such uncertainties. This issue is solved, in this case, by increasing the value of K . The choice of $K = 7.08 \times 10^4$, considering $\Delta_{11} = -22$, yields the system's behavior showed in Figures 4.34 to 4.36.

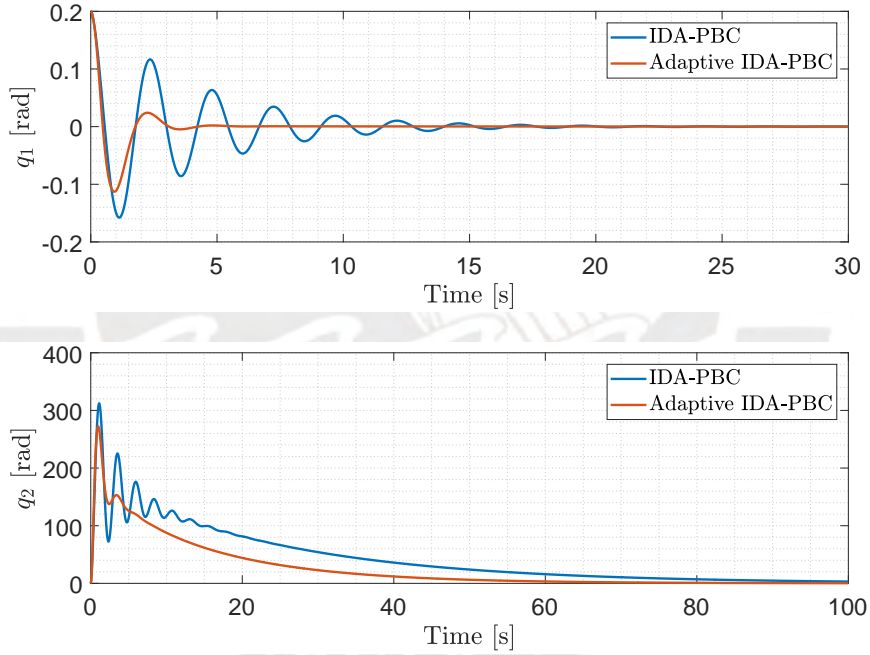


Figure 4.34. – Simulation 10: Evolution of q over time ($K = 7.08 \times 10^4$).

4. Adaptive IDA-PBC Application: Inertia Wheel Inverted Pendulum

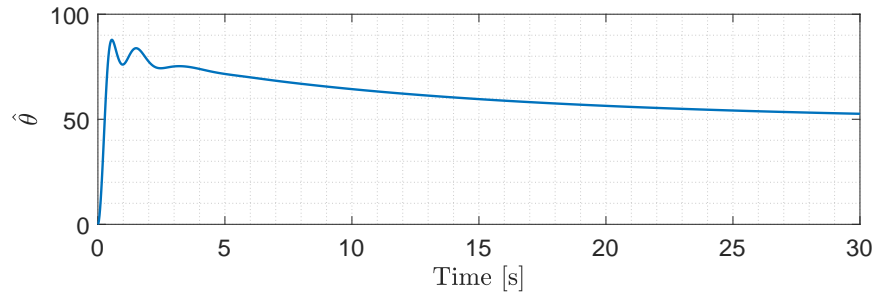


Figure 4.35. – Simulation 10: Evolution of $\hat{\theta}$ over time ($K = 7.08 \times 10^4$).

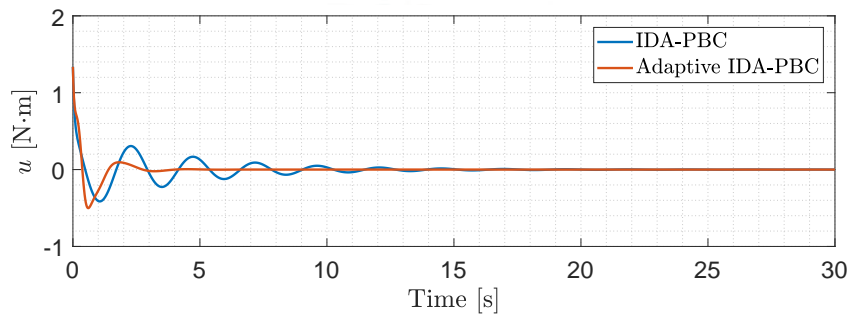


Figure 4.36. – Simulation 10: Evolution of u over time ($K = 7.08 \times 10^4$).

It is easy to see from Figures 4.34 to 4.36, that, for this considered value of Δ_{11} , the system response subject to adaptive IDA-PBC has a remarkably better performance (less overshoot and convergence time) compared to the standard IDA-PBC. However, the increment on the value of K is not suitable if we are in the case that the inertia matrix elements have smaller magnitudes than those considered in the dynamic modeling (e.g., $\Delta_{11} = 15$). This fact can be seen in Figures 4.37 to 4.39, where we simulate with $\Delta_{11} = 15$.

4. Adaptive IDA-PBC Application: Inertia Wheel Inverted Pendulum

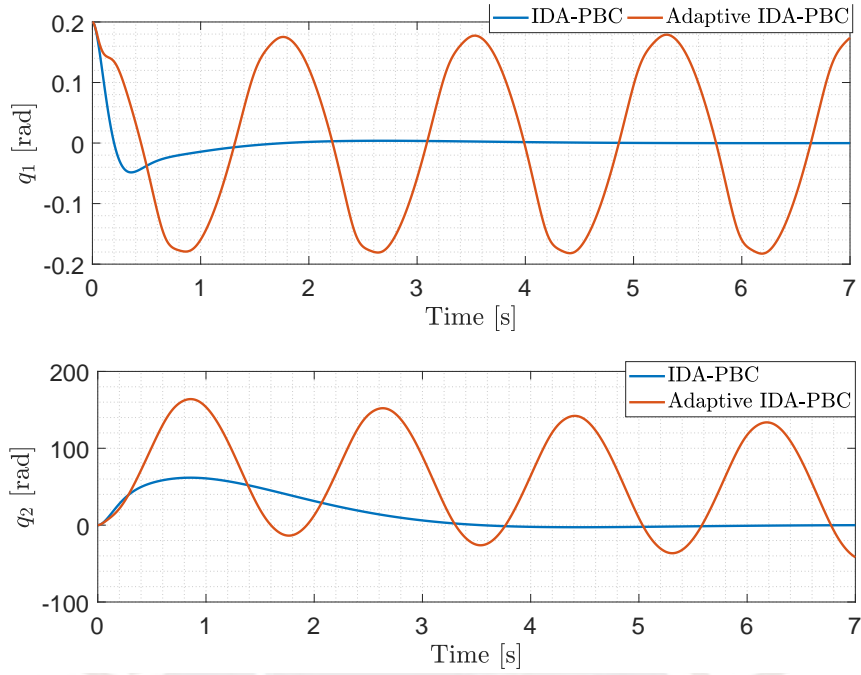


Figure 4.37. – Simulation 11: Evolution of q over time ($K = 7.08 \times 10^4$)

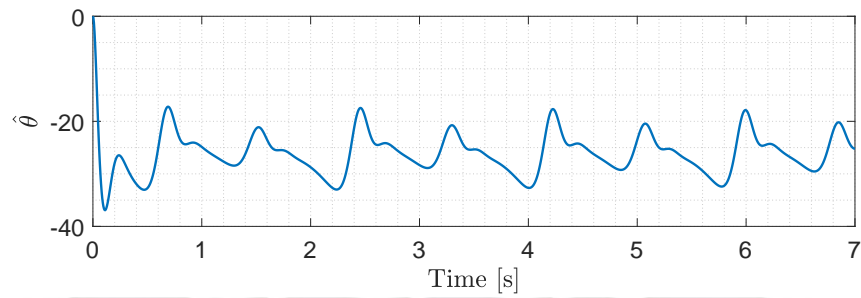


Figure 4.38. – Simulation 11: Evolution of $\hat{\theta}$ over time ($K = 7.08 \times 10^4$)

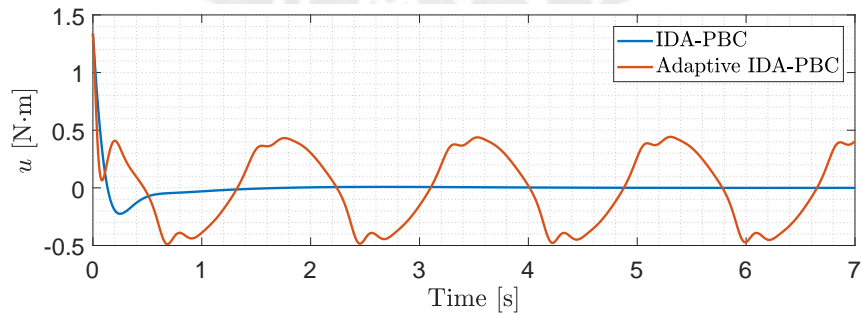


Figure 4.39. – Simulation 11: Evolution of u over time ($K = 7.08 \times 10^4$)

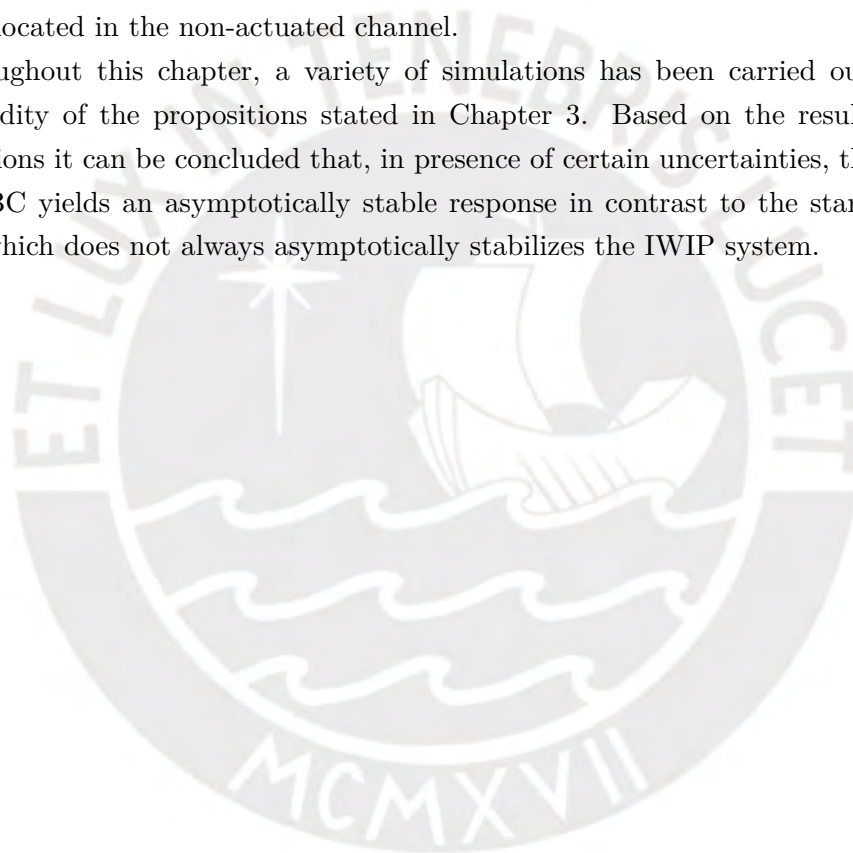
4. Adaptive IDA-PBC Application: Inertia Wheel Inverted Pendulum

Therefore, the use of the adaptive IDA-PBC requires, aside from the standard IDA-PBC calculation, a good tuning of the adaptive gain rate K , taking into account physical considerations.

It was mentioned that when a non-zero initial parameter estimation was selected, the control input peak varies depending on the value of $\hat{\theta}(0)$. However, it is clear from Figure 4.36 and Figure 4.39, that just adjusting K does not have an impact in the control input peak. Therefore, we obtain a better performance (with a suitable K) with the same control input peak.

One remark regarding these set of simulations performed to compensate for parameter uncertainties is that most of the variation in the inertia occurs in the inertial element that is located in the non-actuated channel.

Throughout this chapter, a variety of simulations has been carried out to verify the validity of the propositions stated in Chapter 3. Based on the results of those simulations it can be concluded that, in presence of certain uncertainties, the adaptive IDA-PBC yields an asymptotically stable response in contrast to the standard IDA-PBC, which does not always asymptotically stabilizes the IWIP system.



Chapter 5

Conclusion and Future Work

In this work, an adaptive control scheme is proposed for a class of mechanical systems, namely, the class of UMSs characterized in [33]. This adaptive control scheme is combined with the IDA-PBC technique. The goal of the adaptive IDA-PBC is to asymptotically stabilize such class of UMSs undergoing the effect of uncertainties (not necessarily matched). The propositions stated in Chapter 3 define the structure of the matrix of known basis functions. The adaptive IDA-PBC technique does guarantee the parameter estimation convergence.

To illustrate the validity of the adaptive IDA-PBC technique, a variety of simulations were carried out on the IWIP system, subject to different types of uncertainties. The first set of simulations was performed assuming that the control input was affected by a time-dependent input disturbance. For this case, asymptotic stability of the system was demonstrated as well as parameter estimation convergence, while the standard IDA-PBC could only achieve stability. The following set of simulations were performed considering friction (only in the matched channel), which is obviated in the calculation of the standard IDA-PBC. The results show clearly that the standard IDA-PBC, at least for this system, can only asymptotically stabilize within a limited range of friction coefficient values, while the adaptive IDA-PBC can asymptotically stabilize the system within a much greater range. The last set of simulations deals with parameter uncertainties in the system's total energy. From the result of these simulations, it is concluded that both the standard and adaptive IDA-PBC yield an asymptotically stable response. For the specific case of the IWIP system, the right choice of the adaptive rate gain can lead to a better performance of the adaptive IDA-PBC (less overshoot and convergence time). Additionally, the asymptotic stabilization occurs in the presence of an unmatched inertia-uncertainty.

The application realm of this work can be expanded by further investigating the following topics. First, apply the adaptive IDA-PBC to the more general SIDA-PBC

using generalized forces [43]. Additionally, in the last set of simulations (inertia uncertainties) the actuated and non-actuated terms in the inertia matrix are coupled. Therefore, some calculations and simulations were performed to decouple these uncertainties. Even though these simulations showed an outstanding behavior compared to the standard IDA-PBC, no analytic proof was found to corroborate these results.





Appendices

Appendix A

Additional Calculations

A.1 Matching Condition and Equivalent Formulation

The matching condition in the original coordinates is

$$G^\perp \left(\frac{\partial H}{\partial q} - M_d M^{-1} \frac{\partial H_d}{\partial q} + J_2 \frac{\partial H_d}{\partial p} \right) = 0. \quad (\text{A.1})$$

From the new coordinates we get

$$TGu_{es} = T \frac{\partial \mathcal{H}}{\partial q} - E \frac{\partial \mathcal{H}}{\partial s} - Q^\top \frac{\partial \mathcal{H}_d}{\partial q} + C \frac{\partial \mathcal{H}_d}{\partial s}. \quad (\text{A.2})$$

Transforming back (A.2) to the original coordinates the following is obtained

$$TGu_{es} = T \frac{\partial H}{\partial q} - TM_d M^{-1} \frac{\partial H_d}{\partial q} + TJ_2 \frac{\partial H_d}{\partial p},$$

which is equivalent to (A.1).

A.2 Calculation of the Inverse Transformation Matrix

To obtain the term T^{-1} , considering that T is a non-singular square matrix, we can apply the following relationship

$$TT^{-1} = I, \quad \begin{bmatrix} (G^\top G)^{-1} G^\top \\ G^\perp \end{bmatrix} \begin{bmatrix} a & b \end{bmatrix} = \begin{bmatrix} (G^\top G)^{-1} G^\top a & (G^\top G)^{-1} G^\top b \\ G^\perp a & G^\perp b \end{bmatrix} = \begin{bmatrix} I & 0 \\ 0 & I \end{bmatrix}, \quad (\text{A.3})$$

where $a \in \mathbb{R}^{n \times m}$ and $b \in \mathbb{R}^{n \times r}$. From (A.3) it's clear that

$$\begin{aligned} a &= G, \\ b &= (G^\perp)^\top (G^\perp G^\perp{}^\top)^{-1}, \end{aligned}$$

then

$$T^{-1} = \begin{bmatrix} G & (G^\perp)^\top (G^\perp G^\perp{}^\top)^{-1} \end{bmatrix}.$$



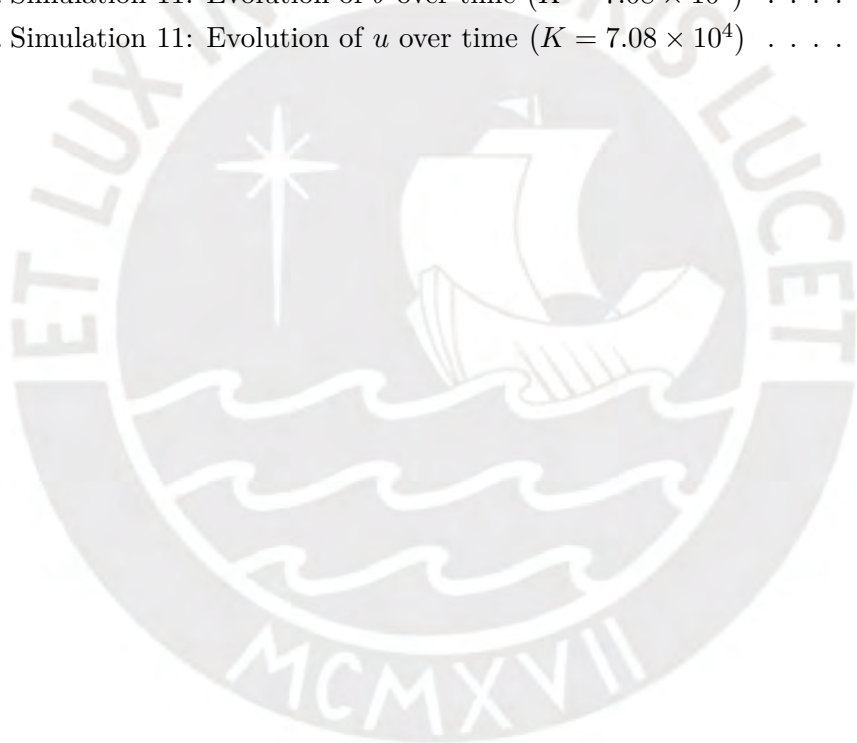
Abbreviations

UMS	Underactuated Mechanical System
DOF	Degrees of Freedom
TORA	Translational Oscillator Rotational Actuator
IWIP	Inertia Wheel Inverted Pendulum
PH	Port-Hamiltonian
PCH	Port-Controlled Hamiltonian
PFL	Partial Feedback Linearization
SMC	Sliding Mode Control
IDA	Interconnection and Damping Assignment
SIDA	Simultaneous Interconnection and Damping Assignment
PBC	Passivity-Based Control
EL	Euler-Lagrange
CL	Controlled Lagrangian
PDE	Partial Differential Equation
ODE	Ordinary Differential Equation
ES	Energy Shaping
ADI	Adaptive Dynamic Inversion
VTOL	Vertical Take-Off and Landing
UAV	Unmanned Aerial Vehicle
ZSD	Zero-State detectable

List of Figures

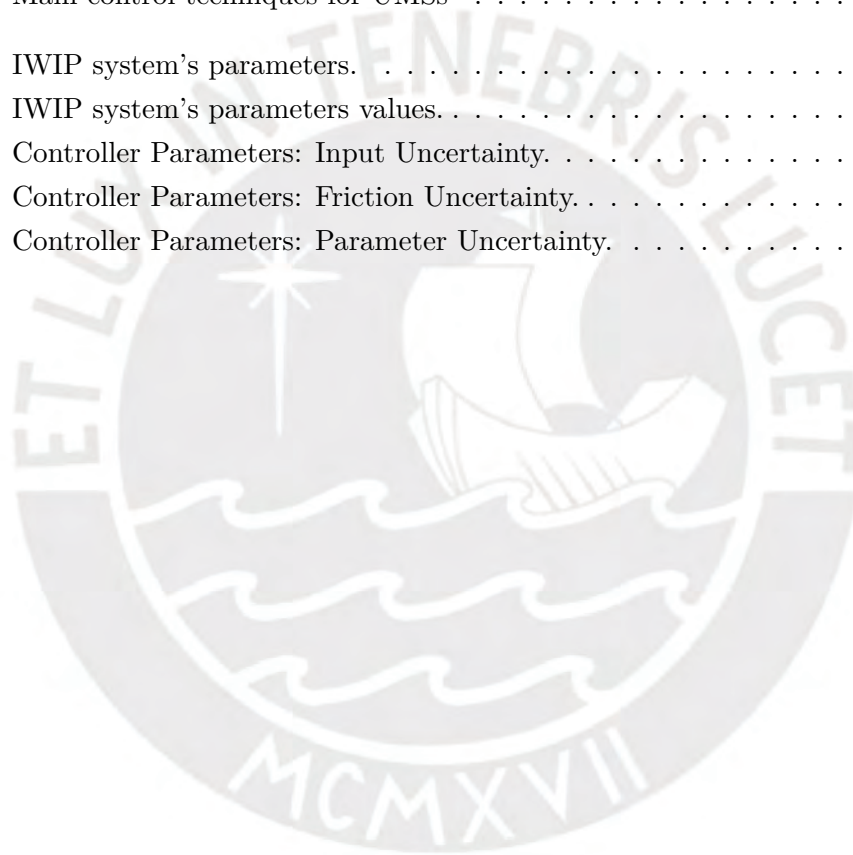
2.1. Adaptive control diagram	26
4.1. IWIP system.	38
4.2. Simulation 1: Evolution of q over time.	45
4.3. Simulation 1: Evolution of p over time.	45
4.4. Simulation 1: Evolution of u over time.	46
4.5. Simulation 2: Evolution of q over time ($A = 0.8$).	49
4.6. Simulation 2: Evolution of p over time ($A = 0.8$).	49
4.7. Simulation 2: Evolution of $\hat{\theta}$ over time ($A = 0.8$).	50
4.8. Simulation 2: Evolution of u over time ($A = 0.8$).	50
4.9. Simulation 3: Evolution of q over time ($r_2 = 0.0012$).	53
4.10. Simulation 3: Evolution of p over time ($r_2 = 0.0012$).	53
4.11. Simulation 3: Evolution of $\hat{\theta}$ over time ($r_2 = 0.0012$).	54
4.12. Simulation 3: Evolution of u over time ($r_2 = 0.0012$).	54
4.13. Simulation 4: Evolution of q over time ($r_2 = 0.0017$).	54
4.14. Simulation 4: Evolution of p over time ($r_2 = 0.0017$).	55
4.15. Simulation 4: Evolution of $\hat{\theta}$ over time ($r_2 = 0.0017$).	55
4.16. Simulation 4: Evolution of u over time ($r_2 = 0.0017$).	56
4.17. Simulation 4: Wider view of the evolution of q_1 ($r_2 = 0.0017$).	56
4.18. Simulation 5: Evolution of q_1 (adaptive only) over time ($r_2 = 0.02$).	56
4.19. Simulation 5: Evolution of q_1 over time ($r_2 = 0.02$).	57
4.20. Simulation 6: Evolution of q over time ($\Delta_{11} = 15$).	61
4.21. Simulation 6: Evolution of p over time ($\Delta_{11} = 15$).	62
4.22. Simulation 6: Evolution of $\hat{\theta}$ over time. ($\Delta_{11} = 15$).	62
4.23. Simulation 6: Evolution of u over time ($\Delta_{11} = 15$).	63
4.24. Simulation 7: Evolution of q over time ($\Delta_{11} = -22$). ¹⁰	63
4.25. Simulation 7: Evolution of p over time ($\Delta_{11} = -22$).	64
4.26. Simulation 7: Evolution of $\hat{\theta}$ over time ($\Delta_{11} = -22$).	64

4.27. Simulation 7: Evolution of u over time ($\Delta_{11} = -22$).	65
4.28. Simulation 8: Evolution of q over time ($\hat{\theta}(0) = -25$).	66
4.29. Simulation 8: Evolution of $\hat{\theta}$ over time ($\hat{\theta}(0) = -25$).	66
4.30. Simulation 8: Evolution of u over time ($\hat{\theta}(0) = -25$).	66
4.31. Simulation 9: Evolution of q over time ($\hat{\theta}(0) = 25$).	67
4.32. Simulation 9: Evolution of $\hat{\theta}$ over time ($\hat{\theta}(0) = 25$).	67
4.33. Simulation 9: Evolution of u over time ($\hat{\theta}(0) = 25$).	67
4.34. Simulation 10: Evolution of q over time ($K = 7.08 \times 10^4$).	68
4.35. Simulation 10: Evolution of $\hat{\theta}$ over time ($K = 7.08 \times 10^4$).	69
4.36. Simulation 10: Evolution of u over time ($K = 7.08 \times 10^4$).	69
4.37. Simulation 11: Evolution of q over time ($K = 7.08 \times 10^4$).	70
4.38. Simulation 11: Evolution of $\hat{\theta}$ over time ($K = 7.08 \times 10^4$).	70
4.39. Simulation 11: Evolution of u over time ($K = 7.08 \times 10^4$).	70



List of Tables

1.1. Main control techniques for UMSs	4
4.1. IWIP system's parameters.	39
4.2. IWIP system's parameters values.	44
4.3. Controller Parameters: Input Uncertainty.	48
4.4. Controller Parameters: Friction Uncertainty.	52
4.5. Controller Parameters: Parameter Uncertainty.	61



References

- [1] A. Choukchou-Braham, B. Cherki, M. Djemaï, and K. Busawon, *Analysis and Control of Underactuated Mechanical Systems*. Springer, 2013.
- [2] R. Tedrake, “Underactuated Robotics: Learning, Planning, and Control for Efficient and Agile Machines: Course Notes for MIT 6.832,” 2009. [Online]. Available: https://ocw.mit.edu/courses/electrical-engineering-and-computer-science/6-832-underactuated-robotics-spring-2009/readings/MIT6_832s09_read_preface.pdf
- [3] R. Ortega and M. W. Spong, “Adaptive motion control of rigid robots: A tutorial,” in *Proceedings of the 27th IEEE Conference on Decision and Control*, 1988, pp. 1575–1584.
- [4] R. Ortega, J. A. L. Pérez, P. J. Nicklasson, and H. Sira-Ramírez, *Passivity-based Control of Euler-Lagrange Systems: Mechanical, Electrical and Electromechanical Applications*. Springer, 1998.
- [5] R. Ortega, A. Van Der Schaft, B. Maschke, and G. Escobar, “Interconnection and damping assignment passivity-based control of port-controlled hamiltonian systems,” *Automatica*, vol. 38, no. 4, pp. 585–596, 2002.
- [6] F. Gómez-Estern, R. Ortega, F. R. Rubio, and J. Aracil, “Stabilization of a class of underactuated mechanical systems via total energy shaping,” in *IEEE Conference on Decision and Control*, vol. 2, 2001, pp. 1137–1143.
- [7] E. Lavretsky, “Adaptive control: Introduction, overview, and applications,” in *Lecture notes from IEEE Robust and Adaptive Control Workshop*, 2008.
- [8] D. A. Dirks and J. M. Scherpen, “Structure preserving adaptive control of port-Hamiltonian systems,” *IEEE Transactions on Automatic Control*, vol. 57, no. 11, pp. 2880–2885, 2012.

-
- [9] N. K. Haddad, A. Chemori, and S. Belghith, “External disturbance rejection in IDA-PBC controller for underactuated mechanical systems: From theory to real time experiments,” in *IEEE Conference on Control Applications (CCA)*, 2014, pp. 1747–1752.
- [10] R. Olfati-Saber, “Nonlinear control of underactuated mechanical systems with application to robotics and aerospace vehicles,” Ph.D. dissertation, Massachusetts Institute of Technology, 2001.
- [11] Y. Liu and H. Yu, “A survey of underactuated mechanical systems,” *IET Control Theory & Applications*, vol. 7, no. 7, pp. 921–935, 2013.
- [12] N. P. I. Aneke, “Control of underactuated mechanical systems,” Ph.D. dissertation, Technische Universiteit Eindhoven, 2003.
- [13] A. Bloch, J. Baillieul, P. Crouch, J. E. Marsden, D. Zenkov, P. S. Krishnaprasad, and R. M. Murray, *Nonholonomic mechanics and control*. Springer, 2003, vol. 24.
- [14] M. W. Spong, “Underactuated mechanical systems,” in *Control problems in robotics and automation*. Springer, 1998, pp. 135–150.
- [15] —, “Partial feedback linearization of underactuated mechanical systems,” in *Proceedings of the IEEE/RSJ/GI International Conference on Intelligent Robots and Systems’ 94. Advanced Robotic Systems and the Real World’, IROS’94*, vol. 1, 1994, pp. 314–321.
- [16] —, “Energy based control of a class of underactuated mechanical systems,” in *IFAC World Congress*, 1996, pp. 431–435.
- [17] —, “The swing up control problem for the acrobot,” *IEEE control systems*, vol. 15, no. 1, pp. 49–55, 1995.
- [18] W.-S. Man and J.-S. Lin, “Nonlinear control design for a class of underactuated systems,” in *IEEE International Conference on Control Applications (CCA)*, 2010, pp. 1439–1444.
- [19] K. Pettersen and H. Nijmeijer, “Tracking control of an underactuated surface vessel,” in *IEEE Conference on Decision and Control*, vol. 4, 1998, pp. 4561–4566.
- [20] M. Zhang and T.-J. Tarn, “Hybrid control of the Pendubot,” *IEEE/ASME transactions on mechatronics*, vol. 7, no. 1, pp. 79–86, 2002.

-
- [21] P. Kokotović, M. Krstić, and I. Kanellakopoulos, “Backstepping to passivity: recursive design of adaptive systems,” in *Proceedings of the 31st IEEE Conference on Decision and Control*, 1992, pp. 3276–3280.
- [22] M. Krstić, I. Kanellakopoulos, P. V. Kokotović *et al.*, *Nonlinear and adaptive control design*. Wiley, 1995, vol. 222.
- [23] X.-m. Yuan, K.-c. Cao, T. Zhang, and H.-s. Hu, “Trajectory tracking control for a quad-rotor UAV based on integrator backstepping,” in *27th Chinese Control and Decision Conference (CCDC)*, 2015, pp. 1790–1795.
- [24] A. Abdessameud and A. Tayebi, “Global trajectory tracking control of VTOL-UAVs without linear velocity measurements,” *Automatica*, vol. 46, no. 6, pp. 1053–1059, 2010.
- [25] R. Olfati-Saber, “Global configuration stabilization for the VTOL aircraft with strong input coupling,” *IEEE transactions on Automatic Control*, vol. 47, no. 11, pp. 1949–1952, 2002.
- [26] J. Ghommam, F. Mnif, and N. Derbel, “Global stabilisation and tracking control of underactuated surface vessels,” *IET control theory & applications*, vol. 4, no. 1, pp. 71–88, 2010.
- [27] W. Perruquetti and J.-P. Barbot, *Sliding mode control in engineering*. CRC press, 2002.
- [28] J. Huang, Z.-H. Guan, T. Matsuno, T. Fukuda, and K. Sekiyama, “Sliding-mode velocity control of mobile-wheeled inverted-pendulum systems,” *IEEE Transactions on robotics*, vol. 26, no. 4, pp. 750–758, 2010.
- [29] N. B. Almutairi and M. Zribi, “On the sliding mode control of a ball on a beam system,” *Nonlinear dynamics*, vol. 59, no. 1-2, p. 221, 2010.
- [30] H. Ashrafiuon and R. S. Erwin, “Shape change maneuvers for attitude control of underactuated satellites,” in *Proceedings of the 2005 American Control Conference*, 2005, pp. 895–900.
- [31] G. Blankenstein, R. Ortega, and A. J. van der Schaft, “The matching conditions of controlled Lagrangians and IDA-passivity based control,” *International Journal of Control*, vol. 75, no. 9, pp. 645–665, 2002.
- [32] R. Ortega and E. García-Canseco, “Interconnection and damping assignment passivity-based control: A survey,” *European Journal of control*, vol. 10, no. 5, pp. 432–450, 2004.

-
- [33] R. Ortega, M. Spong, F. Gómez-Estern, and G. Blankenstein, “Stabilization of a class of underactuated mechanical systems via interconnection and damping assignment,” *IEEE Transactions on Automatic Control*, vol. 47, no. 8, pp. 1218–1233, 2002.
- [34] M. Ryalat and D. S. Laila, “IDA-PBC for a class of underactuated mechanical systems with application to a rotary inverted pendulum,” in *IEEE 52nd Annual Conference on Decision and Control (CDC)*, 2013, pp. 5240–5245.
- [35] S. Prajna, A. van der Schaft, and G. Meinsma, “An LMI approach to stabilization of linear port-controlled Hamiltonian systems,” *Systems & control letters*, vol. 45, no. 5, pp. 371–385, 2002.
- [36] R. Ortega, I. Mareels, A. van der Schaft, and B. Maschke, “Energy shaping revisited,” in *Proceedings of the 2000 IEEE International Conference on Control Applications*, 2000, pp. 121–126.
- [37] P. Borja, R. Cisneros, and R. Ortega, “A constructive procedure for energy shaping of port—Hamiltonian systems,” *Automatica*, vol. 72, pp. 230–234, 2016.
- [38] A. Donaire, R. Mehra, R. Ortega, S. Satpute, J. G. Romero, F. Kazi, and N. M. Singh, “Shaping the energy of mechanical systems without solving partial differential equations,” in *American Control Conference (ACC)*, 2015, pp. 1351–1356.
- [39] D. E. Chang, “Generalization of the IDA-PBC method for stabilization of mechanical systems,” in *18th Mediterranean Conference on Control & Automation (MED)*, 2010, pp. 226–230.
- [40] N. Crasta, R. Ortega, H. Pillai, and J. G. Velazquez, “The matching equations of energy shaping controllers for mechanical systems are not simplified with generalized forces,” *4th IFAC Workshop on Lagrangian and Hamiltonian Methods for Non Linear Control*, vol. 45, no. 19, pp. 48–53, 2012.
- [41] C. Batlle, A. Dòria-Cerezo, G. Espinosa-Pérez, and R. Ortega, “Simultaneous interconnection and damping assignment passivity-based control: the induction machine case study,” *International Journal of control*, vol. 82, no. 2, pp. 241–255, 2009.
- [42] A. Donaire, R. Ortega, and J. G. Romero, “Simultaneous interconnection and damping assignment passivity-based control of mechanical systems using dissipative forces,” *Systems & Control Letters*, vol. 94, pp. 118–126, 2016.

-
- [43] —, “Simultaneous interconnection and damping assignment passivity-based control of mechanical systems using generalized forces,” *Systems & Control Letters*, 2015. [Online]. Available: <https://arxiv.org/pdf/1506.07679v1.pdf>
- [44] S. D. Londoño, “Total Energy Shaping for Underactuated Mechanical Systems: Dissipation and Nonholonomic Constraints,” Ph.D. dissertation, Technische Universität München, 2016.
- [45] F. Gómez-Estern and A. van der Schaft, “Physical Damping in IDA-PBC Controlled Underactuated Mechanical Systems.” *European Journal of control*, vol. 10, no. 5, pp. 451–468, 2004.
- [46] P. Ioannou and J. Sun, *Robust Adaptive Control*. Prentice Hall, 1996.
- [47] D. Pucci, F. Romano, and F. Nori, “Collocated adaptive control of underactuated mechanical systems,” *IEEE Transactions on Robotics*, vol. 31, no. 6, pp. 1527–1536, 2015.
- [48] D. Dirksz and J. Scherpen, “Adaptive control of port-Hamiltonian systems,” in *Proceedings of the 19th International Symposium on Mathematical Theory of Networks and Systems (MTNS)*, vol. 5, no. 9, 2010.
- [49] S. P. Nagesh Rao, G. A. Lopes, D. Jeltsema, R. Babuska *et al.*, “Port-hamiltonian systems in adaptive and learning control: A survey.” *IEEE Transactions on Automatic Control*, vol. 61, no. 5, pp. 1223–1238, 2016.
- [50] N. K. Haddad, A. Chemori, J. Pena, and S. Belghith, “Stabilization of inertia wheel inverted pendulum by model reference adaptive IDA-PBC: From simulation to real-time experiments,” in *3rd International Conference on Control, Engineering & Information Technology (CEIT)*, 2015, pp. 1–6.
- [51] Y. Wang, G. Feng, and D. Cheng, “Simultaneous stabilization of a set of nonlinear port-controlled hamiltonian systems,” *Automatica*, vol. 43, no. 3, pp. 403–415, 2007.
- [52] H. K. Khalil, *Nonlinear systems*, 3rd ed. Prentice-Hall, 2002.
- [53] J.-J. E. Slotine, W. Li *et al.*, *Applied nonlinear control*. Prentice-Hall, 1991.
- [54] A. van der Schaft, *L2-gain and passivity techniques in nonlinear control*, 2nd ed. Springer, 2000.

- [55] C. I. Byrnes, A. Isidori, and J. C. Willems, “Passivity, feedback equivalence, and the global stabilization of minimum phase nonlinear systems,” *IEEE Transactions on Automatic Control*, vol. 36, no. 11, pp. 1228–1240, 1991.
- [56] A. Astolfi, R. Ortega, and R. Sepulchre, “Stabilization and disturbance attenuation of nonlinear systems using dissipativity theory,” *European journal of control*, vol. 8, no. 5, pp. 408–431, 2002.
- [57] R. Sepulchre, M. Janković, and P. V. Kokotović, *Constructive nonlinear control*. Springer, 2012.
- [58] A. van der Schaft, “Port-Hamiltonian systems: an introductory survey,” in *Proceedings of the international congress of mathematicians*, vol. 3, 2006, pp. 1339–1365.
- [59] A. van der Schaft, D. Jeltsema *et al.*, “Port-Hamiltonian systems theory: An introductory overview,” *Foundations and Trends in Systems and Control*, vol. 1, no. 2-3, pp. 173–378, 2014.
- [60] R. Ortega, A. van der Schaft, F. Castaños, and A. Astolfi, “Control by Interconnection and Standard Passivity-Based Control of Port-Hamiltonian Systems,” *IEEE Transactions on Automatic Control*, vol. 53, no. 11, pp. 2527–2542, 2008.
- [61] J. Ferguson, A. Donaire, R. Ortega, and R. H. Middleton, “New results on disturbance rejection for energy-shaping controlled port-Hamiltonian systems,” 2017. [Online]. Available: <http://arxiv.org/abs/1710.06070>